To what extent are temperature levels changing due to greenhouse gas emissions?

John K. Dagsvik and Sigmund H. Moen

Abstract

Weather and temperatures vary in ways that are difficult to explain and predict precisely. In this article we review data on temperature variations in the past as well possible reasons for these variations. Subsequently, we review key properties of global climate models and statistical analyses conducted by others on the ability of the global climate models to track historical temperatures. These tests show that standard climate models are rejected by time series data on global temperatures. Finally, we update and extend previous statistical analysis of temperature data (Dagsvik et al., 2020). Using theoretical arguments and statistical tests we find, as in Dagsvik et al. (2020), that the effect of man-made CO_2 emissions does not appear to be strong enough to cause systematic changes in the temperature fluctuations during the last 200 years.

Address: John K. Dagsvik, Statistics Norway, PO Box 2633, St Hanshaugen, 0131 Oslo, Norway. Email: john.dagsvik@ssb.no

Sigmund H. Moen, Retired Civil Engineer

Sammendrag

Et typisk trekk ved observerte temperaturserier over de siste 200 årene er at de gjennomgående viser lange sykler og en økende trend. Et sentralt spørsmål er om denne utviklingen er en del av en syklus som er analog til tidligere temperaturvariasjoner, eller om en systematisk endring av temperaturnivået har funnet sted i løpet av denne perioden, som et resultat av menneskeskapte utslipp av CO_2. Selv om temperaturene i de senere årene skulle vise seg å avvike systematisk fra variasjonene i tidligere tider, er det likevel en komplisert utfordring å tallfeste hvor mye av denne endringen som skyldes utslipp av CO_2.

Formålet med denne artikkelen er å drøfte dette spørsmålet nærmere, nemlig om det kan sies å være bevist om deler av temperaturøkningen i løpet av de siste 200 år skyldes utslipp av klimagasser.

I denne artikkelen beskrives først hvilke data som er tilgjengelige for analyse av variasjonene i klimatiske forhold.

Dernest diskuteres mulige kilder til temperaturvariasjon i kapittel 3. Her har skydannelse, strømninger i havene samt havenes kapasitet til å lagre CO_2 vesentlig betydning. Nyere forsking tyder på at variasjoner i solas magnetiske felt har stor betydning for langsiktige svingninger i solaktiviteten. Ifølge teori og rekonstruerte temperaturdata påvirkes klima av sykliske variasjonene i jordbanen, jordaksen samt planetbanene til Jupiter, Saturn, Neptun og Uranus.

I kapittel 4 gis det en oversikt over sentrale egenskaper til de globale klimamodellene basert på eksisterende litteratur. I kapittel 5 diskuteres statistiske tester av de globale klimamodellene. Disse viser at det er manglende konsistens mellom variasjonene i temperaturprediksjonene fra de globale klimamodellene og variasjonene i de konstruerte globale temperatureriene. Med andre ord sår disse resultatene tvil om klimamodellene er i stand til å skille mellom naturlige temperatur-variasjoner versus variasjoner som skyldes menneskeskapte CO_2 i løpet av de siste 150 år.

Endelig rapporteres resultater fra en statistisk analyse av observerte tidsserier av temperaturdata fra ulike deler av jordkloden i kapitlene 6 og 7. Denne analysen benytter den samme tilnærmingen som Dagsvik mfl. (2020). Mens Dagsvik mfl. (2020) ikke hadde temperaturdata for de seneste årene, benytter vi temperaturserier i denne artikkelen som er ajourførte inntil 2021. Vi finner, i likhet med Dagsvik mfl. (2020), at hypotesen om at temperaturprosessen varierer tilfeldig rundt et konstant nivå (stasjonaritet) ikke blir forkastet. Dette kan tyde på at effekten av CO2 utslipp de siste 200 årene ikke er sterk nok til å forårsake systematiske endringer i temperatursvingningene.

1. Introduction

A typical feature of observed temperature series over the last two centuries is that they show, more or less, an increasing trend, see Appendix D and Figures B1, B6 and B7 in Appendix B. A key question is whether this tendency is part of a cycle, or whether the temperature pattern during this period deviates systematically from previous variations. Even if recent recorded temperature variations should turn out to deviate from previous variation patterns in a systematic way it is still a difficult challenge to establish how much of this change is due to increasing man-made emissions of carbon dioxide (CO_2) and other greenhouse gases.

At present, there is apparently a high degree of consensus among many climate researchers that the temperature increase of the last decades is systematic (and partly man-made). This is certainly the impression conveyed by the mass media. For non-experts, it is very difficult to obtain a comprehensive picture of the research in this field, and it is almost impossible to obtain an overview and understanding of the scientific basis for such a consensus (Koonin, 2021, Curry, 2023). By looking at these issues in more detail, this article reviews past observed and reconstructed temperature data as well as properties and tests of the global climate models (GCMs). Moreover, we conduct statistical analyses of observed and reconstructed temperature series and test whether the recent fluctuation in temperatures differs systematically from previous temperature cycles, due possibly to emission of greenhouse gases.[1]

In the global climate models (GCMs) most of the warming that has taken place since 1950 is attributed to human activity. Historically, however, there have been large climatic variations. Temperature reconstructions indicate that there is a 'warming' trend that seems to have been going on for as long as approximately 400 years. Prior to the last 250 years or so, such a trend could only be due to natural causes. The length of the observed time series is consequently of crucial importance for analyzing empirically the pattern of temperature fluctuations and to have any hope of distinguishing natural variations in temperatures from man-made ones. Fortunately, many observed temperature series are significantly longer than 100 years and in addition, as mentioned above, there are reconstructed temperature series that are much longer.

After the thermometer was invented in the 17th century, systematic temperature measurements were undertaken in many cities. This was the case, for example, in Uppsala with measurements from 1722, Berlin from 1756 and Paris from 1757, to name but a few. The longest

---

[1] Even if it cannot be proved in a rigorous sense that there is a systematic change in the temperature, it may still be rational to advocate a green environmental and economic policy globally, based on the precautionary principle.

available instrumental record of monthly temperatures in the world is from central England and begins in 1659.[2]

One way to distinguish the effect of man-made emissions of greenhouse gases on temperatures from the effect of natural causes, is to check if temperature variations can be explained using GCMs. For this to be possible, a minimum requirement must be that GCMs are able to reproduce historically observed temperatures. Several researchers have applied advanced statistical methods to investigate the ability of GCMs to track global temperature series, and we review results from their analysis.

Since the total impact on climate from various sources is not well understood the fluctuations in observed and reconstructed time series temperature data may be hard to explain. They may therefore to some extent appear unsystematic (stochastic). An alternative research approach is therefore to investigate whether the temperature series are consistent with a statistical model, and what the features of such a model might be. This was the approach taken by Dagsvik et al. (2020) and several of the references therein. A rigorous statistical analysis of the temperature phenomenon is, however, more complicated than might be expected. There are several reasons for this. First, it turns out that temperature, as a temporal process, appears to have cycles that can last for decades (long memory), if not hundreds of years. It is for precisely this reason that even such a prolonged increase in recent observed temperature series should not simply be interpreted as a trend leading to permanent climate change.

The paper is organized as follows. In Section 2 we describe data and discuss some stylized facts about climate variations in prehistoric times. Moreover, we describe various observed and reconstructed data sets that are available, and we give a summary of climate variations in the past. In Section 3 we discuss some sources of temperature variations. Section 4 contains a summary description of some key features of the GCMs based mainly on Curry (2017) and Voosen (2016) and in Section 5 we review analyses in the literature on the ability of GCMs to track global temperature series. Section 6 discusses and motivates the specific statistical modelling approach we have applied in this paper and in Section 7 the resulting empirical results are discussed. This analysis extends and updates the study of Dagsvik et al. (2020) based on the same methodology as in Dagsvik et al. (2020). Whereas the analysis of Dagsvik et al. (2020) did not use data for the

---

[2] Thermoscopes were the earliest types of thermometers and they only showed changes in temperature but did not show numerical values. One of the first thermoscopes was developed by Galeleo Galilei in 1593. It used water as the liquid and glass bulbs inside an open tube. The glass bulbs rose and fell with the changes in temperature. In 1612, Santorio Santorio, used a numerical scale on the thermoscope but it was very rudimentary. In 1654 the first sealed glass tube was developed by Ferdinand II, the Grand Duke of Tuscany. It contained alcohol and had a numerical scale, but was not very accurate. The more modern thermometer was invented in 1709 by Daniel Fahrenheit. It was an enclosed glass tube that had a numerical scale, called the Fahrenheit scale. The early version of this thermometer contained alcohol and in 1714 Fahrenheit developed a mercury thermometer using the same scale.

most recent years the current study is based on data up to 2021, and the empirical results confirm the results obtained by Dagsvik et al. (2020). One key result is that the hypothesis of the temperature process being stationary is not rejected. Finally, in Section 8 we provide bounds on maximum temperature values under specific assumptions about the temperature process. Most of the results from the statistical analysis are reported in online appendices (Appendices C and D).[3]

2. The available data

This section gives a brief description of the data that are reviewed or analyzed in this paper. Apart from the last 250 years, data are based on reconstructions from several sources such as ice cores, tree rings and lake sediments (see for example Varenholt and Lüning, 2015, ch. 4). An ice core is a core sample that is obtained from an ice sheet or a glacier. Since the ice forms from the incremental buildup of annual layers of snow, lower layers are older than upper, and an ice core contains ice formed over a range of years. Cores can contain ice more than two million years old (Yan et al., 2019). The physical properties of the ice and of material trapped in it can be used to reconstruct the climate over the age range of the core. The proportions of different oxygen and hydrogen isotopes provide information about ancient temperatures, and the air trapped in tiny bubbles can be analyzed to determine the level of atmospheric gases such as CO_2. Since 1979 satellite observations in the troposphere have been used to estimate temperature.

2.1. Temperature variations in the past

Ice cores from Greenland and Antarctica provide unique archives of past climate and environmental changes based only on natural physical processes. Figure B2 in Appendix B shows reconstructed temperatures over the past 420,000 years obtained at the Vostok station, Antarctica (Petit et al., 1999, 2001). The record spans over four glacial periods and five interglacial periods, including the present.

The preceding four interglacial periods are seen at about 125,000, 280,000, 325,000 and 415,000 years before now, with much longer glacial periods in between. All four previous interglacial periods are seen to be warmer than the present. The typical length of a glacial period is about 100,000 years, while an interglacial period typically lasts for about 10-15,000 years. The present inter-glacial period has now lasted about 11,600 years.

---

[3] The online Appendix 4 of Dagsvik et al. (2020) contains all the R codes used for the statistical analysis of the temperature data developed by Mariachiara Fortuna (mariachiara.fortuna1@gmail.com).

Figure B3 shows the cyclical and parallel fluctuations of reconstructed temperatures and CO_2 during the last 420,000 years according to results from the Vostok ice core record. By analysing Antarctic blue ice Yan et al. (2019) have found that the high correlation between temperature and CO_2 also occurs up to 2 million years ago during the time when the glacial period appeared to be only 40,000 years. Moberg et al. (2005) and Lundqvist (2010), among others, have reconstructed temperatures for the northern hemisphere from AD 1 to 1979 (Figure B6 in Appendix B) by using data from borehole drillings, tree rings and lake sediments. These data show considerable variation in temperatures during the last two millennia, such as during the little ice age.

Kobashi et al. (2011) have reconstructed Greenland surface snow temperature variability over the past 4,000 years (until 1993) at the GISP2 site (near the Summit of the Greenland ice sheet) with a new method that utilizes argon and nitrogen isotopic ratios from occluded air bubbles (Figure B4, Appendix B). These data indicate that warmer temperatures were the norm in the earlier part of the past 4,000 years, including century-long intervals nearly 1°C warmer than the decade (2001-2010). Therefore, it appears that the current decadal mean temperature in Greenland has not exceeded the envelope of natural variability over the past 4,000 years. Schönwiese (1995) has reconstructed temperatures from ice cores in Greenland for the last 11,000 years (Figure B5, Appendix B). These reconstructions show that during the past 10,000 years temperatures over long periods were higher than they are today. The warmest phase occurred 4,000 to 8,000 years ago and is known as the Holocene Climate Optimum or the Atlantic Period.

There are other reconstructed temperature and CO_2 measurements for the last few millennia not reviewed here. Some of them have similar patterns as the ones reviewed here whereas others (based on ice cores from different locations) show a different picture. Thus, similarly to the observed data displayed in Appendix D there appears to be considerable regional variations in the samples of reconstructed temperature data. Furthermore, there may be substantial measurement errors in the reconstructed data which contribute to the variation across different reconstructed data sets.

2.2. Observed temperature records

Data on observed temperatures stem from several sources. The sources are the National Aeronautics and Space Administration (NASA), the Goddard Institute for Space Studies (GISS), the European Climate Assessment & Data and national meteorological institutes, such as the Swedish Meteorological and Hydrological Institute and the Norwegian Meteorological Institute, the Hadley Centre Central England Temperature (HadCET dataset, starting in 1659) and the

University of Alabama at Huntsville (UHA) (Satellite data). The data, certified by NASA, comprise a large number of series of temperatures from more than 100 countries. The temperature data (observed) we have used in the statistical analysis in this paper were collected by Hov Moen (2020) from NASA. The time series are available as annual and monthly figures. These data are far from perfect since most of the series contain one or several periods of missing observations.

Most of the series are corrected for environmental change in the surroundings of the measuring instrument and for errors arising at the point of measurement, such as known equipment or procedural faults, change of measuring site, change of surroundings, change of averaging method, etc. Presumably some of the data series may still be affected by a local urban heat island (UHI) effect larger than assumed by standard UHI correction techniques, or by temporal, local temperature inversions prevailing during winter periods with calm conditions in cold regions (O'Neill et al., 2022).

By using several selection criteria, 75 time series from 32 countries were included in the statistical analysis in this paper. Most of these time series are updates of the series used by Dagsvik et al. (2020) in their analysis. The criteria were based on the quality of the data, such as length and number of missing observations. Note that the data are based solely on observed air temperatures. Thus, no sea surface temperatures are used in this study, in contrast to the global temperature series produced (constructed) by several climate research centers. The reason for not using sea surface temperature observations is that they are, apart from recent decades, not observed at given observation sites. Appendix C (online) contains more information about the temperature series used in this study.

2.3. Global temperature construction

Estimates of global temperatures are produced and maintained by the Met Office Hadley Centre (UK) (HadCRUT), the US National Oceanic and Atmospheric Administration, the National Climatic Data Center (USA) (NCDC), NASA Goddard Institute for Space Studies (USA) (NASA GISS) and UAH. Global surface temperatures are typically constructed as simple or weighted averages of observed local temperature anomalies. A temperature anomaly is the difference between the long-term average temperature (sometimes called a reference value) and the actual temperature.[4]

---

[4] Global Temperature Record, Climatic Research Unit web site http://www.cru.uea.ac.uk/cru/info/warming/, Global Temperature (Meteorological Stations), Goddard Institute of Space Studies web site http://data.giss.nasa.gov/gistemp/graphs/

The surface records represent a blend of sea surface data collected by moving ships, drifting and tethered buoys, satellite measurements from the troposphere (UAH), plus data from land stations of partly unknown quality and unknown degree of representativeness for their region. Specifically, values for each hemisphere are the simple or weighted average of all the non-missing, grid-box anomalies in the hemisphere. The weights used are the areas of the grid boxes or cosines of the central latitudes of each grid box. For the three global surface air temperature estimates, HadCRUT, NCDC and GISS, the reference period differs. HadCRUT refers to the period 1961-1990, while NCDC and GISS as reference instead use 1901-2000 and 1951-1980, respectively, which results in higher positive temperature anomalies. For all three surface air temperature records, but especially NCDC and GISS, administrative changes to anomaly values are quite often introduced, even for observations several years back in time. Some changes may be due to the delayed reductions of stations or addition of new station data, while others probably have their origin in a change of technique to calculate average values. It is impossible to evaluate the validity of such administrative changes for an outside user of these records. In addition, throughout the 19th century and early 20th century, sea surface measurements were typically obtained by drawing buckets of water onto a ship's deck.

During the 20th century the makeup of the measurement network shifted towards engine room intake water temperature measurements, special insulated buckets, and the use of hull contact sensors. The end of the 20th century saw the deployment of large networks of drifting buoys and other platforms, which continue to provide more comprehensive temperature measurement coverage than was previously possible using purely ship based measurements. Many of the land stations have also moved geographically during their existence, and their instrumentation changed. See Brohan et al. (2006) and O'Neill et al. (2022) for more evidence and discussion about the uncertainties and homogenization adjustments of the European temperature records.

The satellite temperature records also have their problems, but these are generally of a more technical nature and therefore correctable. In addition, the temperature sampling by satellites is more regular and complete on a global basis than that represented by the surface records.

It therefore appears that the different temperature records might not be of equal scientific quality. While both NCDC and GISS seem to have undergone quite large administrative changes, and therefore might be considered unstable, the changes introduced to HadCRUT3 are fewer and smaller (Figure 1B in Appendix B). It is apparent that the degree of uncertainty (measurement errors) in these global temperature series have changed over time. Also, the number of weather stations and sea observation sites have increased over time. As a result, the variance of the measurement errors has probably decreased over time. These features represent a serious obstacle

for conducting rigorous statistical time series analysis based on the (constructed) global temperature series. Even if the underlying true temperature series for each weather station were stationary, the corresponding (constructed) global temperature series therefore might be non-stationary.

Essex et al. (2006) question the whole concept of global temperature. In summary, their argument goes as follows: There are an infinite number of ways one can construct weighted averages for any given set of local temperature data, since physical principles provide no explicit basis for choosing among them. Distinct and equally valid statistical rules can and do show opposite trends when applied to the results of computations from physical models and real data in the atmosphere. A given set of local temperature measurements distributed across the world can be interpreted as there are both a "warming" and a "cooling" tendency going on simultaneously, making the notion of global warming physically ill-posed.

3. What are key sources of temperature variations?

The sun is the main source of energy for the Earth. This energy is delivered in a form of solar radiation in different wavelengths, called total solar irradiance. Variations of solar irradiance lead to heating of the upper planetary atmosphere and complex processes of solar energy transport towards a planetary surface.

As reviewed above, reconstructed temperature records obtained from ice core drillings show that there have been more or less regular glacial periods (Petit et al., 2001, see Figure B2 in Appendix B). The glacial periods appear to be roughly consistent with the Milankovitch cycles. Milankovitch cycles describe the collective effects of changes in the Earth's movements on its climate over thousands of years. The term is named after the Serbian mathematician and astronomer Milutin Milankovitch. Milankovitch (1879-1958) hypothesized that variations in eccentricity, axial tilt, and precession of the Earth's elliptical orbit resulted in cyclical variation in the solar radiation reaching the Earth, and that this orbital forcing strongly influenced the Earth's climatic patterns.

It is known that the oceans have an enormous capacity to store CO_2, depending on the sea temperature. When the sea temperature rises, this capacity decreases. In contrast, it follows from Henry's law that when the CO_2 level increases in the atmosphere, a corresponding proportionate

increase occurs in the oceans as well.[5] What is observed is thus the net effect. Accordingly, one explanation of the graphs in Figure B3 in Appendix B is that the variation of the storage capacity of the oceans, due to fluctuating temperatures, is the dominating effect.

In addition to seasonal variations and glacial periods, observed temperatures seem to vary for reasons that are only partly understood. Some of the variations are due to solar radiation, cloud formations and greenhouse gases (water vapor, argon, CO_2, aerosols,[6] methane, nitrous oxide and ozone).

Recently, Zharkova (2020) and Zharkova et al. (2015) have studied the role of the solar background magnetic field in defining solar activity. By applying principal component analysis, they were able to quantify the observed magnitudes of magnetic field at different times and consequently make long-term prediction of solar activity on a millennium timescale. Their approach revealed a presence of not only 11-year solar cycles but also of grand solar cycles with duration of 350–400 years. They demonstrated that these grand cycles are formed by the interferences of two magnetic waves with close but not equal frequencies produced by the double solar dynamo action at different depths of the solar interior. These grand cycles are always separated by grand solar minima of Maunder minimum type, which regularly occurred in the past.[7] During these grand solar minima, there is a significant reduction of solar magnetic field and solar irradiance, which yields a reduction of terrestrial temperatures derived for these periods from the analysis of terrestrial biomass during the past 12,000 or more years. The most recent grand solar minimum occurred during the little ice age (Maunder Minimum) (1645–1710), which led to reduction of solar irradiance by 0.22 percent from the modern one and a decrease of the average terrestrial temperature by 1.0–1.5°C. According to the research by these authors there will be an upcoming grand solar minimum, when solar magnetic field and its magnetic activity will be reduced by 70 per cent. During this grand minimum, one would expect a reduction of the average terrestrial temperature, ceteris paribus, by up to 1.0°C in the decade 2031–2043.

In other recent studies (Scafetta and Bianchini, 2022, and Yndestad, 2022) it is suggested that Earth's global temperature variabilities have solar-lunar forced stationary temperature cycles of up to 4450 years. The primary causes of the identified multidecadal temperature variation is the stationary orbital cycles produced by the Jovian planets (Jupiter, Saturn, Uranus and Neptune) and

---

[5] Hendry's law states that the mass of a dissolved gas in a given volume of solvent at equilibrium is proportional to the partial pressure of the gas.

[6] Areosols are liquid or solid particles (from volcanos for examples) that are small enough to be suspended in the air.

[7] Maunder minimum stands for prolonged sunspot minimum.

the 18.6-year lunar nodal cycle resulting from the Earth's axis nutation. According to this theory the sea surface temperature will have a deep minimum in 2070.

The clouds are known to affect global temperatures on longer timescales. Solar variations and water vapor affect the abundance of clouds in our atmosphere according to research at the National Space Institute at the Technical University of Denmark and the Racah Institute of Physics at the Hebrew University of Jerusalem (Svensmark et al., 2016). Large eruptions on the surface of the Sun can temporarily shield Earth from so-called cosmic rays which appear to affect cloud formation.

The most important greenhouse gas is water vapor which varies greatly at any given place and time. About 66-85 per cent of the natural greenhouse effect can be traced back to water vapor and small droplets in clouds (Varenholt and Lüning, 2015, ch. 6). The next most significant greenhouse gas is CO_2, which is different from water vapor in that its concentration in the atmosphere is pretty much the same all over the Earth. The amount of CO_2 and other gases that humans have added to the atmosphere over the past 250 years increases the ability of the atmosphere to impede heat from diffusing into space.

But other variations may be the result of the climate system itself (chaotic behavior). In fact, there is no need for "external" influences to produce periodic and seemingly stochastic variations in processes governed by deterministic non-linear dynamic systems, such as GCMs. See for example May (1976) who demonstrates that a simple non-linear dynamic model exhibits chaotic behavior. A phenomenon such as El Niño may be the result of the climate system itself.

El Niño Southern Oscillation (ENSO) is an oceanic-atmospheric circulation system in the Pacific region involving the El Niño phenomenon and the Southern Oscillation. The latter describes a pressure shift between the South Asian low pressure zone and the South Pacific high pressure zone. El Niño occurs in the tropical Pacific every 2-7 years, typically around Christmas time. The event is characterized by a strong warming of the upper layer in this oceanic region. When this happens, high pressure and low pressure atmospheric systems trade places, and this leads to a partial reversal in air and ocean currents. El Niño has profound impacts on the climate, which not only have consequences for the Pacific region but for the entire globe. For example, during warm El Niño years, Southern Asia, Australia and the Amazon area are plagued with drought, whereas other parts of South America are inundated by heavy rain. (Varenholt and Lüning, 2015, pp. 122−124).

4. Review of the Global climate models

GCMs are representations of the Earth's climate system that can be used to analyze and simulate variations in the climate under different conditions, including the development of global temperature. Existing GCMs are comprehensive and complex, and it is almost impossible for non-specialists to acquire more than a superficial understanding of them. Here, we shall only give a brief description of their key properties, based to a large extent on Curry (2011, 2017, 2023) and Voosen (2016). We refer to these authors and Bader et al. (2008) for more detailed descriptions and discussions.

GCMs consist of a number of modules that represent the contributions to climate variations made by the atmosphere, ocean, land surface, sea ice and glaciers. The atmospheric module simulates the evolution of wind, temperature, humidity and atmospheric pressure using complex mathematical equations that can be solved only by using computers. GCMs also use equations that describe how heat is transported in the ocean and how the ocean exchanges heat and moisture with the atmosphere. GCMs have a sub-model for the land surface that describes how vegetation, soil and snow or ice cover exchange energy and moisture with the atmosphere. Finally, GCMs have sub-models that represent ocean ice and glaciers. While some of the relations in GCMs are based on well-established theory from physics, such as the Navier-Stokes equations, there are representations that are only approximations and not based on physical laws. Unfortunately, no analytic solution of the Navier-Stokes equations has so far been obtained.[8] To solve all these equations approximately using computers, the atmosphere, oceans and land are divided into a three-dimensional grid (space and time resolution). Common resolutions for GCMs are about 100-200km in the horizontal direction and about one km vertically, and a time-stepping resolution of about 30 minutes. Due to the relatively coarse resolutions of the models, there are many important processes that take place within the cells determined by the model resolution, such as clouds and precipitation. These 'subscale' processes are modelled using ad hoc parametric relations that are intended to be approximate representations of the actual processes, based on observations or derivations from more detailed models. The parameters in these relationships are calibrated so that the model fits the weather and climate observations in a selected period. The parameter choices associated with the ad hoc subscale models that represent clouds and precipitation are among the most demanding, and they are the reason for the largest differences between the simulations from different climate models.

---

[8] The Clay Mathematics Institute has declared the existence and analytic solution of the Navier-Stokes equations to be one of the top seven problems in all of mathematics and is offering a million $ prize for its solution.

The GCMs have various limitations. First, the effect of increasing CO_2 emissions on the climate cannot be evaluated precisely on time scales that are of the order of less than or equal to 100 years. Second, there is a lack of knowledge of the uncertainty which is partly due to the choice of the subscale models and the parameterization and calibration of these, as well as insufficient data. Third, according to some evaluations, GCMs are not sufficiently reliable to distinguish between natural and man-made causes of the temperature increase in the 20th century. Some of the predictions from GCMs are accompanied by standard errors, as in statistical analysis. But since the GCMs are deterministic models one cannot interpret these standard errors in the same way as in statistics.[9] Fourth, GCMs are typically evaluated applying the same observations used to calibrate the model parameters. In an article in *Science*, Voosen (2016) writes; *"Indeed, whether climate scientists like to admit it or not, nearly every model has been calibrated precisely to the 20th century climate records – otherwise it would have ended up in the trash".* Unfortunately, models that match 20th century data as a result of calibration using the same 20th century data are of dubious quality for determining the causes of the 20th century temperature variability. The problem is that some of the variables representing sources of climate variability other than greenhouse gases are not properly controlled for during the calibrations. The resulting calibration of the climate sensitivity may therefore be biased. Further critical evaluations are given by several authors, such as Essex (2022).

As mentioned in the previous section climate can also change owing to internal processes within the climate system even without any variations in external forcings (chaos). In the GCMs the source of chaos is the nonlinearity of the Navier-Stokes equations. If the initial conditions are not known exactly for a dynamic model based on the Navier-Stokes relations the forecast trajectory will diverge from the actual one, and it is not necessarily the case that small perturbations have small effects.[10] In fact, slightly different initial conditions can yield wildly different outputs.[11] In order to assess the uncertainty due to internal variability, researchers use so-called ICE (Initial Condition Ensembles) simulations. This means that outputs of GCMs are simulated starting from

---

[9]The reference to probability distributions in the context of GCMs can be somewhat misleading since climate models are not stochastic models according to common terminology. It simply refers to the distribution of results generated by simulations of different calibrated versions and scenarios. See Stephenson et al. (2012) for a discussion of this issue. See also Curry (2011) for a discussion of climate uncertainty.

[10] "Since the climate system is complex, occasionally chaotic, dominated by abrupt changes and driven by competing feedbacks with large unknown thresholds, climate prediction is difficult, if not impracticable." (Rial et al., 2004).

[11] In 2001 IPCC researchers wrote: *...in sum, a strategy must recognize what is possible. In climate research and modelling, we should recognize that we are dealing with a coupled non-linear chaotic system, and therefore that the long-term prediction of future climate states is not possible. The most we can expect to achieve is the prediction of the probability distribution of the system's future possible states by the generation of ensembles of model solutions.* Intergovernmental panel on climate change. synthesis Report, section 14.2.2.2, p. 774.

slightly different initial conditions. As the climate system is chaotic, slightly different initial conditions lead to different trajectories.

5. How well do climate models predict past temperatures?

The problem with assessing the effect on the climate from man-made increase of CO_2 is that all else is not necessarily equal because other factors are at work that influence climate, such as important amplifiers and feedback mechanisms which are poorly understood, see Varenholt and Lüning (2015) and the references therein.[12] One way of assessing the effect of CO_2 emissions on the temperature is to apply the GCMs. A key question is therefore whether the GCMs can be trusted to provide reliable predictions. One way of examining the quality of the GCMs is to check if the temperature predictions (hindcasts) from the GCMs are able to track the global temperature time series. Several researchers have investigated the ability of GCMs to track temperature over time, as well as their ability to track the precipitation and sea level pressure in specific locations such as the Arctic and North America (Beenstock et al., 2016, McKitrick and Christy, 2020, Fildes and Kourentzes, 2011, and Koonin, 2021, pp. 86–96). At the outset, it is not entirely clear what it means to track global temperatures over time since global temperatures are not observed, they are constructs. Unfortunately, there is, as mentioned above, no obvious way of how global temperatures should be constructed, as it is not clear how the temperature output from GCMs should be interpreted. But it may seem reasonable to assume that even if the temperature output from the GCMs does not predict the same levels as the constructed global temperatures one should still expect that the pattern of variations of the two series are similar.

Prior to Beenstock et al. (2016) the ability of GCMs to track global temperature series has not, to the best of our knowledge, been subjected to rigorous empirical testing by means of advanced statistical methods such as cointegration tests.[13] In this section we summarize some results obtained by Beenstock et al. (2016), and McKitrick and Christy (2020).

Let $X(t)$ denote global air temperature at time t and let X be the corresponding time series (temperature process). Let $Z(t)$ be a set (vector) of input variables that enters the GCMs at time t and let Z be the corresponding time series. As mentioned above, significant drivers of the temperature process included in Z are factors such as solar radiation, aerosols and greenhouse

---

[12] It has been well established that the forests of the Earth absorb a considerable amount of CO_2.

[13] Kaufman and Stern (2004) have applied cointegration tests to annual forecasts for three GCMs and concluded that two of the three were cointegrated. Unfortunately, the critical values they used were too lenient because they did not correct for degrees of freedom, see Beenstock et al. (2016).

gases. Reconstructions of past values of these variables have been made by means of ice core samples. Let $\hat{X}(t) = g(Z(t); \hat{b})$ be the (predicted) temperature at time t produced by the GCMs, where $g(Z(t);b)$, as a function of $Z(t)$, represents the relation between temperature at time t and $Z(t)$ and $\hat{b}$ is an estimate of b, which is a vector of unknown coefficients. The estimate $\hat{b}$ is determined so that the GCM temperature output is close to parts of the global temperature records (calibration). As discussed above, some elements of the function g are derived from physics, while other elements have an ad hoc character.[14] For reasons discussed above, X and $\hat{X}$ are perceived as stochastic processes.

Beenstock et al. (2016) have used data for X and $\hat{X}$ produced by 22 selected GCMs for the period 1880-2010 to test whether the regression model $X(t) = \alpha + \beta \hat{X}(t) + v(t)$ fits the data, where α and β are unknown coefficients and $v = \{v(t)\}$ is the error process assumed to be stationary with zero expectation and to be independent of $\hat{X}(t)$. As data for X they use global temperature estimates given by NASA- GISS.

From statistical theory it follows that the regression model above can only be estimated consistently if the error process v is stationary. The most important characteristic of a zero mean stationary process is that it mean-reverts to zero over time. This implies that if a global climate model happens to over- or under-predict global temperatures during a specific period, its hindcasts are expected to come back on track over time. Given that the error process is stationary, α and β can be estimated by well-known methods. Otherwise, statistical methods may not lead to consistent estimates for α and β. In such situations it may happen that even though the true value of β is zero the estimate of β may not converge to zero as the sample increases. Beenstock et al. (2016) found that statistical tests rejected the hypothesis that the error process v is stationary, which means that the regression model postulated above does not hold. In other words, this means that the $\hat{X}$ process produced by the GCMs is unable to track the X process (Global temperature).

McKitrick and Christy (2020) have done a somewhat similar analysis for the period 1979-2014 and they found that the GCMs overpredict the global temperatures after 2000. For further details we refer to their paper. Fildes and Kourentzes (2011) compared the tracking behavior of one GCM to simple time series and neural network models, and found that the latter outperformed the former, despite their simplicity.

---

[14] In principle, the model may also depend on $Z(s)$ for $s < t$ but for simplicity this is disregarded in this summary description.

Although the predictions from the GCMs referred to above might be questionable, this does not mean that GCMs are unable to capture some of the temperature fluctuations in the past. According to Moberg et al. (2005) for example, graphs from simulation experiments using GCMs to hindcast temperatures for the period 1000–1990 show patterns that are qualitatively similar to the reconstructed temperature data shown in Figure B6 in Appendix B. Graphically, there may therefore seem to be some agreement between the reconstructed temperatures and the corresponding GCMs-based predictions.[15] The finding that the GCMs are only capable of reproducing some of the temperature variations in the past casts serious doubts about their ability to produce credible climate scenarios.

A weakness of the tests reviewed above is that the time series of measurement errors in the global temperature constructs most likely are non-stationary with unknown properties. Thus, it may be theoretically possible that the GCMs are able to track the "true" latent global temperature series reasonably well, despite the fact that they do not track the corresponding observed (constructed) one. In any case, the analyses of Beenstock et al. (2016), and McKitrick and Christy (2020) are startling and raise serious doubts about the quality of the GCMs, and in particular, if the CO_2 sensitivity has been correctly identified.

There are also other examples of informal tests, including some by IPCC. In an IPCC review it was claimed that *"There continues to be very high confidence that the models reproduce observed large-scale mean surface temperature patterns (pattern correlation ~0.99)"* (IPCC, 2014, p. 743)[16]. But as discussed above, the mere fact that these correlations are high does not necessarily mean that the GCMs that produced them have been validated successfully. When the temperatures predictions produced by GCMs have time trends, these correlations may be spurious, i.e., the models may happen to mimic global temperatures without there being any true relationship between them. Therefore, the usual empirical estimator of the correlation coefficient may not be consistent, that is, it may not converge to the true correlation coefficient as the sample increases. The statement by IPCC cited above is therefore misleading.[17]

---

[15] In the literature there are several other attempts to assess the performance of GCMs, see Beenstock et al. (2016) and references therein.

[16] IPCC (2014) Intergovernmental panel on climate change. 5th review.

[17] Gavin Schmidt, director of NASA's GISS says: «Many of the world's leading models are now projecting warming rates that most scientists, including the model makers themselves, believe are implausibly fast» (see Voosen, 2021).

6. Statistical time series analysis

In Section 3 we summarized theories of sources of climate variations. The effect on climate and temperature from some of these sources is not well understood and therefore partly unknown. Consequently, to the observing analyst observed or reconstructed temperature series appear to fluctuate in an unsystematic (stochastic) manner with local trends that may be hard to explain. Due to the seemingly stochastic pattern of temperature fluctuations, it thus seems worthwhile to study the temperature phenomenon as realizations from a statistical (stochastic) model, and to investigate what the properties of such a model might be. It is particularly interesting to test whether the observed and reconstructed temperature data indicate a rejection of the hypothesis of stationarity (absence of systematic trends). Although it seems clear from the reconstructed temperatures that the temperature process is not stationary in time frames that are longer than the interglacial periods, the stationary hypothesis may still appear as a possible benchmark in time frames of a few hundred years, or even up to two millennia.

The current paper extends the analysis of Dagsvik et al. (2020) by using observed temperature series up to 2021 for a set of weather stations, in contrast to the analysis of Dagsvik et al. (2020) who only analyzed a few temperature series up to 2012 whereas most of the temperature series used in their analysis ended between 1980 and 2012, see Section 2.2 and Appendices C and D for details.

As mentioned above, the temperature process is affected by a set of variables (drivers), such as aerosols, greenhouse gases and variations in radiation from the sun, etc. Some of the drivers that affect the climate might appear to be stationary (including cyclical drivers such as sunspots and grand solar cycles) and others might appear to be non-stationary (CO_2 emissions in the period after the industrial revolution). Although some of the drivers may be non-stationary, the temperature process may still be approximately stationary.

Both annual and monthly temperature series are used in the empirical analysis we have conducted. The monthly temperature series have been seasonally adjusted and are normalized to have zero mean (for convenience).[18] Both observed and reconstructed temperature series have the property that they are, or can be interpreted as, temporal aggregates of data generated at a finer (original) time scale where the aggregation takes place over a 'large' number of original time units. For example, weekly temperatures are defined as the average of daily (average) temperatures per week, monthly temperatures are the average of daily temperatures per month, etc. A formal

---

[18] See Dagsvik et al. (2020) for details about the seasonal adjustment procedure.

statement of this property is given as Property *A* below. As above, recall that $X = \{X(t), t \geq 0\}$ denotes the (observed) temperature process, which we view as a pure stochastic process. In the following, let *N* denote the set of integers, including zero, and let [*t*] denote the integer part of *t*.

Property *A*

The process $\{X(t), t \geq 0\}$ is generated as averages of observations at a finer (basic) timescale, i.e.

$$X(t) = \frac{1}{m} \sum_{q=[mt-m]+1}^{[mt]} \tilde{X}(q)$$

where $\{\tilde{X}(q), q \in N\}$ denotes the process defined at the basic timescale.

Suppose, for example, that the unit of the basic timescale is "day" and that *t* indexes "month". Then $\tilde{X}(q)$ is the temperature recorded at day *q* (properly adjusted for diurnal variation), $m \cong 30$, and *X*(*t*) is defined as the temperature of month *t*. Here, it is understood that the enumeration of the days goes from 1 to *mT* where *T* is the length of the time series when using the timescale that corresponds to the observed data, which in this case is "month". Alternatively, if *t* instead indexes "year", then *X*(*t*) is defined as the temperature of year *t* and *m* = 365. In our case Property *A* is simply a formalized statement of how the observed time series (suitably adjusted for seasonal variations) have been constructed.

If the temperature process $\tilde{X} = \{\tilde{X}(q), q \in N\}$ is strictly stationary and certain mild mathematical regularity conditions are met,[19] the temporal aggregation property (Property *A*) of data implies surprisingly strong restrictions on the model of the observed temperature process, namely that it is, asymptotically (that is, when *m* is large), a so-called fractional Gaussian noise process (FGN) (Giraitis et al., 2012, Proposition 4.4.1, p. 77).[20] In other words, the implied model (under strict stationarity) for the average annual or monthly temperatures is, asymptotically, FGN. The FGN process is a strictly stationary zero mean long memory Gaussian process with autocovariance function given by

---

[19] For details about regularity conditions, see Theorem 3, Appendix A in Dagsvik et al. (2020).

[20] Proposition 4.4.1 in Giraitis et al. (2012) requires that $\tilde{X}$ is a (causal) linear process. Fortunately, Bickel and Bühlmann (1996) have proved that any strictly stationary process can be approximated arbitrarily closely (under a suitable metric) by linear processes.

$$Cov(X(t), X(t-k)) = 0.5\sigma^2((k+1)^{2H} - 2k^{2H} + |k-1|^{2H})$$

where $\sigma^2 = VarX(t), 0 < H < 1$. When k is large the autocovariance function reduces to (approximately)

$$Cov(X(t), X(t-k)) \cong \sigma^2 H(2H-1)k^{2H-2}.$$

Thus, the model is completely determined by two unknown parameters, namely the variance σ^2 of the temperature fluctuations and H (in our context H assumes values between 0.5 and 1) which determines how strongly the temperatures covary over time. In addition to being stationary and Gaussian, FGN has fractal properties. The term 'fractal properties' means that the structure of the model is invariant under scale transformations of the time unit. Furthermore, in continuous time the realized oscillation patterns are extremely irregular in the sense that although the sample paths are (almost surely) continuous they are (almost surely) not differentiable (Mandelbrot and van Ness, 1968, Mandelbrot and Wallis, 1968, 1969). Long-range dependence means that temperatures at time epochs that are far apart are noticeably correlated. The parameter H is called the Hurst index, named after the British engineer Harold Edwin Hurst (1880–1978), who seems to have been the first to use this type of modelling approach in empirical research. To get an impression of the irregularity and long-range dependence properties of FGN, different realizations of the model with $\sigma = 1$ and 3 levels of H have been simulated, see Figure B8 in Appendix B, which is taken from Dagsvik et al. (2020). The larger the value of H, the stronger the long-range dependence property of FGN. Remember that these simulations are stochastic, meaning that different simulations based on the same model parameters will produce different realized sample paths. These simulations display interesting variation patterns. Recall that the properties of the model are independent of which time unit is used. When $H = 0.7$, from about time unit 625 to about time unit 720 there seems to be a declining trend, while from about time unit 260 to about time unit 330 there is an increasing trend. When $H = 0.8$ and 0.9, this type of pattern is more pronounced. Thus, in this case, local trends can last several hundred units of time. Thus, unless the time series are long it may be difficult to distinguish systematic variations from pure stochastic variation in the presence of long-range dependence because stationary models can exhibit long local trends. When H is greater than or equal to 0.9 (see lower panel of Figure B8), it may, unless the time series are very long, be almost impossible to separate systematic from stochastic trends without further a priori theoretical restrictions.

As mentioned, the FGN model follows from temporal aggregation, given that the basic process defined at a finer time scale is stationary. In other words, the properties of this model do not necessarily reflect properties of the original series realized on the basic time scale, but is solely

a consequence of temporal aggregation. A crucial point is therefore whether the observed temperature process is in fact stationary, and if so, whether it is consistent with FGN. Recall that FGN is implied by the aggregation properties of data, under stationarity, given that certain mathematical regularity conditions are met, and that aggregation takes place over a large enough (unknown) number of days. Consequently, it is of interest to test both the hypothesis of stationarity and whether the data are consistent with FGN. Thus, the hypotheses to be tested are:

Hypothesis *B*: the process *X* is stationary.

Hypothesis *C*: the process *X* can be represented by FGN.

Since FGN is stationary, hypothesis *C* implies hypothesis *B*. One method used to test hypothesis *B* is non-parametric and has been proposed by Cho (2016). This test is not based on specific model assumptions beyond general regularity conditions for the statistical distributions involved, and it uses random selected sub-samples from the temperature series and checks if there are possible local deviations from stationarity. It is therefore, to a certain extent, dependent on the researcher's choice of the number of sub-samples (*M*) and the smallest size of the sub-samples (*m*). The method used to test hypothesis *C*, on the other hand, does not depend on *M* and *m*. Hypothesis *C* is tested by using a Chi-square type statistic (called the *Q* statistic) which measures how well the FGN model fits the data. Under hypothesis *C*, this measure will be approximately standard normally distributed. Hypothesis *C* has also been tested by using a more informal graphical method which will not be discussed here (see Dagsvik et al., 2020).

7. Empirical results from statistical time series analysis

For the monthly observed time series, hypothesis *B* was rejected for 10 series when using the non-parametric test with significance level 5%. On the other hand, hypothesis *B* was rejected for only 3 series when annual data were used (with a 5% significance level). Note that the monthly and annual time series cover the same time interval. Rejection of hypothesis *B* for some of the monthly series may be due to weaknesses in the method used for seasonal adjustment.[21] A striking feature of these estimates is that the Hurst index *H* does not vary very much between weather stations (when accounting for standard errors). It was found that hypothesis *C* was rejected for four series when using the monthly data and three series when using the annual data (details are given in Appendices C and D). We have also analyzed the HadCET time series as well as the mean time series where the mean was taken across 74 weather stations used in the analysis. By using the same

---

[21] See Dagsvik et al. (2020) where our approach to seasonal adjustment is described.

tests as above, we found that the HadCET and the aggregate series were stationary and consistent with FGN. Further results are displayed in Table 1. Here, H_c and H_w denote the estimate of H based on the characteristics function approach and the Whittle approach, respectively. See Dagsvik et al. (2020) for details. The statistics Q_{H_c} and Q_{H_w} are goodness of fit measures based on the estimates H_c and H_w, respectively. These statistics are standard normally distributed. Thus, if $|Q|>1.96$ it signifies that the model is rejected at the 5 per cent significance level. Table 1 shows that the model fit is sensitive to the estimates. Specifically, when the estimate H_c is used the model based on the annual aggregate data is rejected whereas when the estimate H_w is used the model

Table 1. Estimates of *H* and *Q*

	H_c	H_w	SE H_w	Q_{H_c}	Q_{H_w}
Annual aggregate	0.854	0.904	0.057	-2.052	-0.384
Monthly aggregate	0.798	0.766	0.016	-0.502	-3.077
Annual HadCET	0.773	0.749	0.035	0.041	-0.780

is not rejected. For the monthly aggregate data the estimate H_w implies rejection whereas the estimate H_c implies that the model is not rejected.

Since global temperature constructions use different data sources at different time periods they become problematic to analyze with statistical time series methods, as mentioned above, because their statistical properties may vary over time in a way that is not known. Specifically, by looking at the HadCRUT3 time series (Figure B1 in Appendix B) it appears that the variance of the temperatures is greater the first 30 years than in the subsequent years. Indeed, by applying the non-parametric test described above we found that the HadCRUT3 time series (Figure 1B in Appendix B) is far from stationary. However, when comparing the HadCRUT3 series with the aggregate series obtained from 74 weather stations we see from Figure B7 in Appendix B that the overall trends of these series seem to be more or less similar. Still, as mentioned above, the aggregate series were found to be stationary in contrast to the HadCRUT3 series. This means that the trend in the aggregate series is unsystematic (stochastic). The reason why the HadCRUT3 series is non-stationary may not be because of the increasing trend but because of the systematic change in the pattern of variations over time (variance and auto-correlation, not visible in the figure). We also found that the HadCET time series is stationary and consistent with the FGN model.

Finally, we have checked if the reconstructed temperature series from Greenland is consistent with FGN. We found that this time series is also non-stationary. From Figure B4 in

Appendix B it is apparent that the temperature at several instances in the past were higher than recent observed temperatures. Kobashi et al. (2011) concluded that the current decadal mean snow temperature in central Greenland has not exceeded the envelope of natural variability of the past 4000 years.

Dagsvik et al. (2020) found that the reconstructed temperature data from the last two millennia (Moberg et al., 2005), see Figure B6 in Appendix B, were consistent with FGN. Recall that according to the theory of Zharkova et al. (2015) there are systematic grand solar cycles with durations 350-400 years. However, the statistical tests we have used do not reject stationarity. One reason for this may be that since the long-range dependence is very strong ($H = 0.95$) it appears difficult to detect departure from stationarity unless the observed time series are very long, or if a priori theoretical restrictions are imposed on the statistical model (cf. Figure B8 in Appendix B).

8. Extreme temperature values

In this section we shall establish bounds on the variation of the temperature process, under the FGN assumption. Given such bounds it is possible to assess whether extreme temperature observations are consistent with FGN or not. Pickands (1969) and others have obtained almost sure asymptotic bounds on extreme values of stationary Gaussian processes. A drawback with these results is that they are asymptotic (with slow convergence properties) and can therefore not be applied to compute corresponding bounds on extreme temperatures over finite time intervals. We shall therefore use an alternative approach. Let M_T denote the maximum temperature within the interval $[0, T]$, where it is understood that the temperature process is normalized to have zero mean. We have the following result:

Theorem 1

Assume that $\{X(t), t = 1, 2, ...\}$ is a stationary Gaussian sequence with $EX(t) = 0$, $VarX(t) = \sigma^2$ and $E(X(t)X(s)) \geq 0$. Then for $x \geq 0$ we have

$$P(M_T \leq y) \geq \Phi\left(\frac{y}{\sigma}\right)^T$$

where $\Phi(x)$ is the standard normal c.d.f.

The proof of Theorem 1 is given in Appendix A.

When $H = 0.5$, FGN reduces to a white noise process and in this case the inequality in Theorem 1 becomes an equality. When H increases the inequality becomes less and less sharp. Theorem 1 can be used to calculate asymptotic upper bounds for the temperatures of the respective weather stations for a given connected time interval of length T. Specifically, this can be done by solving the equation $\Phi\left(x_{T\delta}\right)^T = \delta$ for x where δ is close to one. Let $x_{T\delta}$ denote the solution of the above equation. Then it follows from Theorem 1 that $M_T \le \sigma x_{T\delta}$ with probability greater than or equal to δ. Let σ_M and σ_D be the standard deviation of the monthly and daily mean temperature, respectively (seasonally adjusted). Consider the daily upper bound over 50 years with $\delta = 0.999$.[22] Then we get that $x_{T\delta} \cong 5.24$.

In our data we only have observations of monthly and annual temperatures. Under the hypothesis of FGN it is easy to compute variances for other averages, such as daily or weekly average temperatures. It is easy to show that under the FGN hypothesis then $\sigma_M 30^{1-H}$ is the approximate standard deviation of the daily temperature (maximum or average). Consider the upper bound for Oslo, for example. Estimates for Oslo are $\sigma_M \cong 2.08$ and $H \cong 0.72$ implying that $\sigma_D \cong 5.39$. From these estimates and the formula above it follows that the upper bound for the daily normalized maximum temperature for a period of 50 years is about 21.3 degrees.[23] Thus, the upper bound for the maximum daily temperature for a period of 50 years for Oslo in July becomes 28.3 degrees Celsius plus the average maximum daily temperature for Oslo in July. Since the average maximum temperature for July is 22.7 degrees it follows that the upper bound of the temperatures in July in Oslo becomes 51.0 degrees Celsius. The highest temperature ever recorded in Oslo is 35 degrees (21 July 1901), which we note is substantially lower than the upper bound. If we consider New York City, $H \cong 0.7$ and $\sigma_M = 1.83$. The average maximum temperature in July in New York is about 29 degrees Celsius. With $\delta = 0.999$ this implies that the upper bound for the maximum temperature for a period of 50 years in July in New York becomes about 55.6 degrees Celsius. Thus, even in a stationary model with normally distributed variations, such as FGN, quite extreme temperature realizations are possible.

---

[22] This value of δ means that the corresponding upper bound may be crossed once each thousand years, on average.

[23] The normalized temperature series have zero mean.

9. Concluding remarks

In this paper we have reviewed data on climate and temperatures in the past and ascertained that there have been large (non-stationary) temperature fluctuations resulting from natural causes.

Subsequently, we have summarized recent work on statistical analyses on the ability of the GCMs to track historical temperature data. These studies have demonstrated that the time series of the difference between the global temperature and the corresponding hindcast from the GCMs is non-stationary. Thus, these studies raise serious doubts about whether the GCMs are able to distinguish natural variations in temperatures from variations caused by man-made emissions of CO_2.

Next, we have updated the statistical time series analysis of Dagsvik et al. (2020) based on observed temperature series recorded during the last 200 years and further back in time. Despite long trends and cycles in these temperature series, we have found that the hypothesis of stationarity was not rejected, apart from a few cases. These results are therefore consistent with the results obtained by Dagsvik et al. (2020). In other words, the results imply that the effect of man-made CO_2 emissions does not appear to be sufficiently strong to cause systematic changes in the pattern of the temperature fluctuations. In other words, our analysis indicates that with the current level of knowledge, it seems impossible to determine how much of the temperature increase is due to emissions of CO_2.

References

Bader, D. C., Covey, C., Gutkowski, W. J. Jr., Held, I. M., Kunkel, K. E., Miller, R. L, Tokmakian, R. T., and Zhang, M. H. (2008) Climate Models: An Assessment of strengths and limitations. U.S. Climate Change Science Program synthesis and assessment product 3.1. Department of Energy, Office of Biological and Environmental Research.

Beenstock, M., Reingewertz, Y. and Paldor, H. (2016) Testing the historic tracking of climate models. *International Journal of Forecasting,* **32**, 1234–1246.

Bickel, P. J. and Bühlmann, P. (1996) What is a linear process? *Proceedings of the National Academy of Sciences of the United States of America,* **93**, 12128–12131.

Brohan, P., Kennedy, J. J., Harris, I., Tett, S. F. B., and Jones, P. D. (2006) Uncertainty estimates in regional and global observed temperature changes: a new dataset from 1850. *Journal of Geophysical Research*, **111**, 2–21.

Cho, H. (2016) A test of second-order stationarity of time series based on unsystematic sub-samples. *Stat*, **5**, 262–277.

Curry, J. A. (2011) Reasoning about climate uncertainty. *Climatic Change*, **108**, 723–732.

Curry, J. A. (2017) *Climate models for the layman.* The global policy warming foundation. GWPF Briefing 24.

Curry, J. A. (2023) *Climate uncertainty and risk*. Athem Press, London.

Dagsvik, J. K., Fortuna, M. and Hov Moen, S. (2020) How does the temperature vary over time? Evidence on the stationary and fractal feature of temperature fluctuations. *Journal of the Royal Statistical Society, Series A*, **183**, 883–908.

Essex, C. (2022) Can computer models predict climate? Essay. https://wp.me/pSEKJ-bKY

Essex, C., McKitrick, R. and Andersen, B. (2006) Does a global temperature exist? *Journal of Non-Equilibrium Thermodynamics,* **32**, 1–27.

Fildes, R. and Kourentzes, N. (2011) Validation and forecasting accuracy in models of climate change. *International Journal of Forecasting*, **27,** 968–995.

Giraitis, L., Koul, H. L. and Surgailis, D. (2012) *Large sample inferences for long memory processes*. Imperial College Press, London.

Global temperature record, Climatic Research Unit web site http://www.cru.uea.ac.uk/cru/info/warming/, accessed December 2005.

Global temperature (Meteorological Stations), Goddard Institute of Space Studies web site http://data.giss.nasa.gov/gistemp/graphs/, accessed December 2005.

Hov Moen, S. (2020) www.rimfrost.no

Kaufmann, R. K. and Stern, D. I. 2004 A statistical evaluation of atmosphere-ocean general circulation models: complexity vs. simplicity. Rensselaer Working Papers in Economics 0411.

Kobashi, T., Kawamura, K., Severinghaus, J. P., Barnola, J.-M., Nakegawa, T., Vinther, M., Johnsen, S. J., and Box, J. E. (2011) High variability of Greenland surface temperature over trapped air in and ice core. *Geophysical Research Letters*, **38**, L21501.

Komatu, Y. (1955) Elementary inequalities for Mill's Ratio. *Reports of Statistical Application Research of the Union of Japanese Scientists and Engineers*, **4**, 69–70.

Koonin, S. E. (2021) *Unsettled*. BenBella Books, Inc. Dallas, Texas.

Lundqvist, F. C. (2010) A new reconstruction of temperature variability in the extra-tropical northern hemisphere during the last two millennia. *Geografiska Annaler*, Series A, **92**, 339–351.

Mandelbrot, B. B. and van Ness, J. W. (1968) Fractional brownian motions, Fractional noises and applications. *SIAM Review,* **10**, 422–437.

Mandelbrot, B. B. and Wallis, J. R. (1968) Noah, Joseph and operational hydrology. *Water Resource Research,* **4**, 909–918.

Mandelbrot, B. B. and Wallis, J. R. (1969) Some long-run properties of geophysical records. *Water Resource Research,* **5**, 321–340.

May, R. M. (1976): Simple mathematical models with very complicated dynamics. *Nature*, **261**, 459–467.

McKitrick, R. and Christy, J. (2020) Pervasive warming bias in CMIP6 tropospheric layers. *Earth and Space Science*, **7**, 1–8.

Milankovitch, M. (1941/1998) Canon of insolation and the ice age problem. Belgrade: Zavod za udžbenike i nastavna sredstva. ISBN 8617066199. See also Astronomical Theory of Climate Change (http://www.ncdc.noaa.gov/paleo/milankovitch).

Moberg, A., Sonechkin, D. M., Holmgren, K., Datsenko, N. M. and Karlén, W. (2005) Highly variable northern hemisphere temperatures reconstructed from low- and high-resolution proxy data. *Nature*, **433**, 613–617.

O'Neill, P., Connolly, R., Connolly, M., Soon, W., Chimani, B., Crok, M., de Vos, R., Harde, H., Kajaba, P., Nojarov, P., Przybylak, R., Rasol, D., Skrynyk, O., Skrynyk, O., Štepánek, P., Wypych, A., and Zahradnícek, P. (2022) Evaluation of the homogenization adjustments applied to european temperature records in the global historical climatology network dataset. *Atmosphere*, **13**, 285, 1–22.

Petit J. R., Jouzel, J., Raynaud, D., Barkov, N. I., Barnola, J. M., Basile, I., Bender, M., Chappellaz, J., Davis, J., Delaygue, G., Delmotte, M., Kotlyakov, V. M., Legrand, M., Lipenkov, V., Lorius, C., Pépin, L., Ritz, C., Saltzman, E. and Stievenard, M. (1999) Climate and atmospheric history of the past 420,000 years from the Vostok ice core, Antarctica, *Nature*, **399**, 429–436.

Petit, J. R. et al. (2001) Vostok ice core data for 420,000 years, IGBP PAGES/World Data Center for Paleoclimatology Data Contribution Series #2001-076. NOAA/NGDC Paleoclimatology Program, Boulder CO, USA.

Pickands, J. (1969) Asymptotic properties of the maximum in a stationary Gaussian process. *Transactions of the American Mathematical Society*, **145**, 75–86.

Rial, J. A., Pielke, R. A., Sr., Beniston, M., Clausen, M., Canadell, J., Cox, P., Held, H., de Noublet-Ducoudré, N., Prinn, R., Reynolds, J. F. and Salas, J. D. (2004) Nonlinearities, Feedbacks and Critical Thresholds within the Earth's Climate System. *Climate Change*, **65**, 11-38.

Schönwiese, C. D. (1995) *Klimaänderungen. Daten, analysen, prognosen*. Springer, Berlin.

Slepian, D. (1962) The one-sided barrier problem for Gaussian noise, *Bell System Technical Journal*, **41**, 463–501.

Scafetta, N. and Bianchini, A. (2022) The Planetary Theory of Solar Activity Variability: A Review. *Frontiers in Astronomy and Space Sciences. Sec. Stellar and Solar Physics*, **9**, 2022.

Stephenson, D. B. Collins, M., Rougier, J. C. and Chandler, R. E. (2012) Statistical problems in the probabilistic prediction of climate change. *Environmetrics*, **23**, 364–372.

Svensmark, J., M. B. Enghoff, Shaviv, N. J., and Svensmark, H. (2016) The Response of clouds and aerosols to cosmic ray decreases. *Journal of Geophysical Research: Space Physics,* **121**, 8152–8188.

Varenholt, F. and Lüning, S. (2015) *The neglected sun.* The Heartland Institute, Arlington Heights, Illinois.

Voosen, P. (2016) Climate scientists open up their black boxes to scrutiny. *Science*, **354**, 401–402.

Voosen, P, (2021) U.N. panel confronts implausibly hot forecasts of future warming. *Science*, **373**, 474–475.

Yan, Y., Bender, M. L., Brook, E. J., Clifford, H. M., Kemeny, P. C., Kurbatov, A. V., Mackay, S., Mayewski, P. A., Ng, J., Severinghaus, J. P., and Higgins, J. A. (2019) Two-million-year-old snapshots of atmospheric gases from Antarctic ice. *Nature*, **574**, 663–666.

Yndestad, H. (2022) Jovian planets and lunar Nodal cycles in the earth's climate variability. *Frontiers in Astronomy and Space Sciences*, **9**, 1–19.

Zharkova, V. V. (2020) Modern grand solar minimum will lead to terrestrial cooling. *Temperature*, **7**, 217–222.

Zharkova, V. V., Shepherd, S. J., Popova, E. and Zharkov, S. I. (2015) Heartbeat of the sun from principal component analysis and prediction of solar activity on a millennium timescale. *Scientific Report*, **5**, article no 15689.

Appendix A

Extreme values for stationary normal sequences

The following result is useful for proving Theorem 1.

Lemma 1

Assume that $\{X(t), t = 1, 2, ...\}$ is a stationary Gaussian sequence with $EX(t) = 0$, $VarX(t) = 1$ and $E(X(t)X(s)) \geq 0$. Then

$$P\left(\bigcap_{j \leq n}(X(t_j) \leq x_j)\right) \geq \prod_{j \leq n} P\left(X(t_j) \leq x_j\right).$$

The result of Lemma 1 follows from Slepian (1962).

Appendix B

Figure B1. Global air temperatures (HadCRUT3)
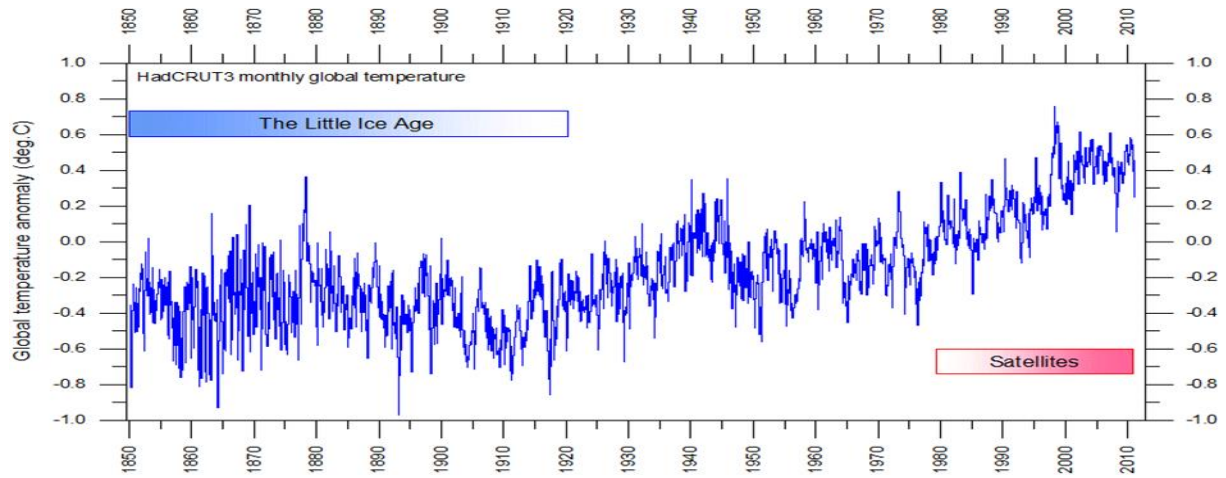
Figure B2. Reconstructed temperatures over the last 420,000 years
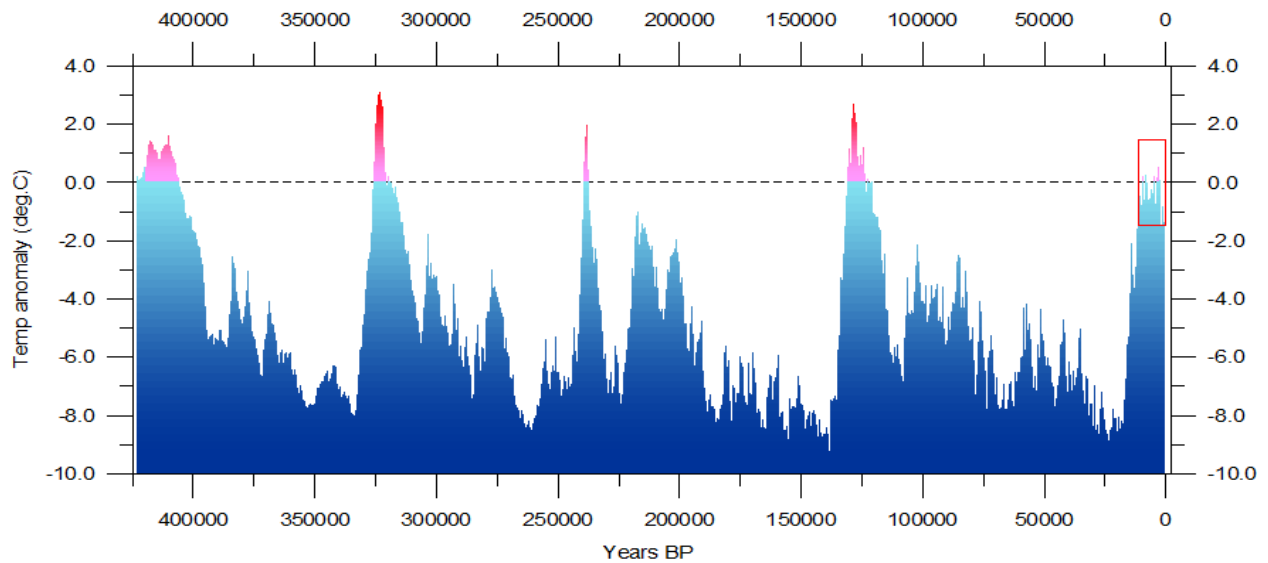
Reconstructed global temperature based on the Vostok ice core from the Antarctica. The horizontal line indicates the modern temperature level. The red square to the right indicates the time interval shown in greater detail in https://www.climate4you.com/

Figure B3. Reconstructed temperatures and CO₂ for the last 420,000 years

The Vostok (Antarctica) Ice Core Record.
Carbon Dioxide versus Temperature for the last 420,000 years.
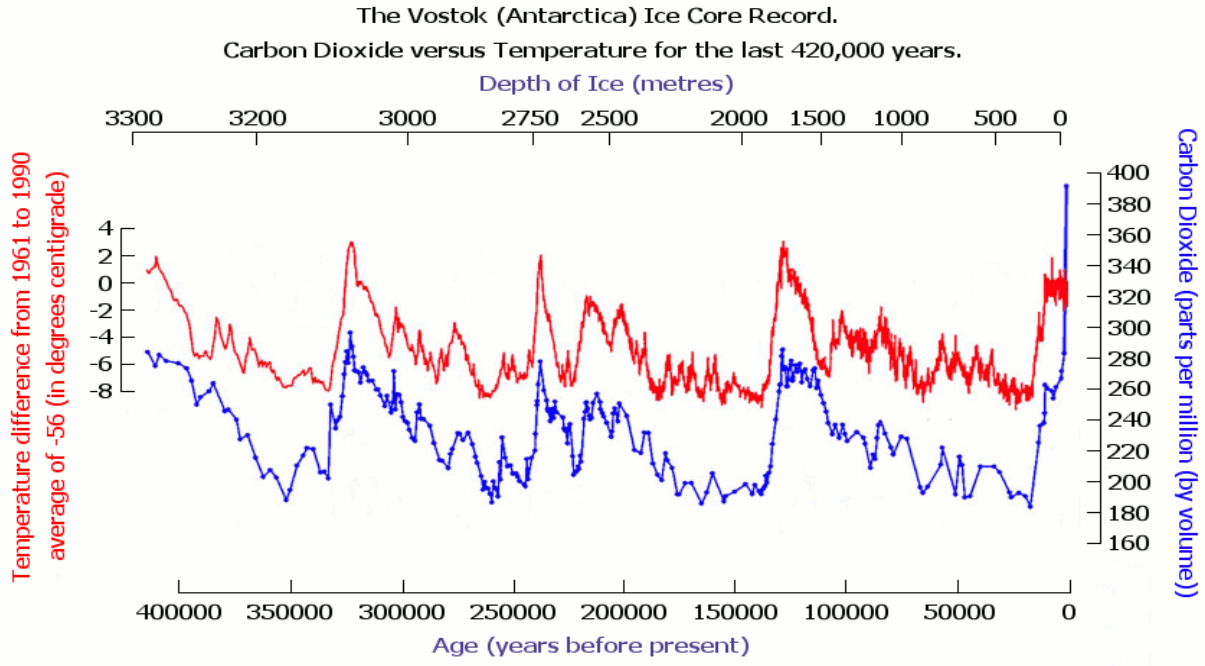
Figure B4. Reconstructed temperatures from Greenland, 2000 BC to 2000 AD

Greenland temperature
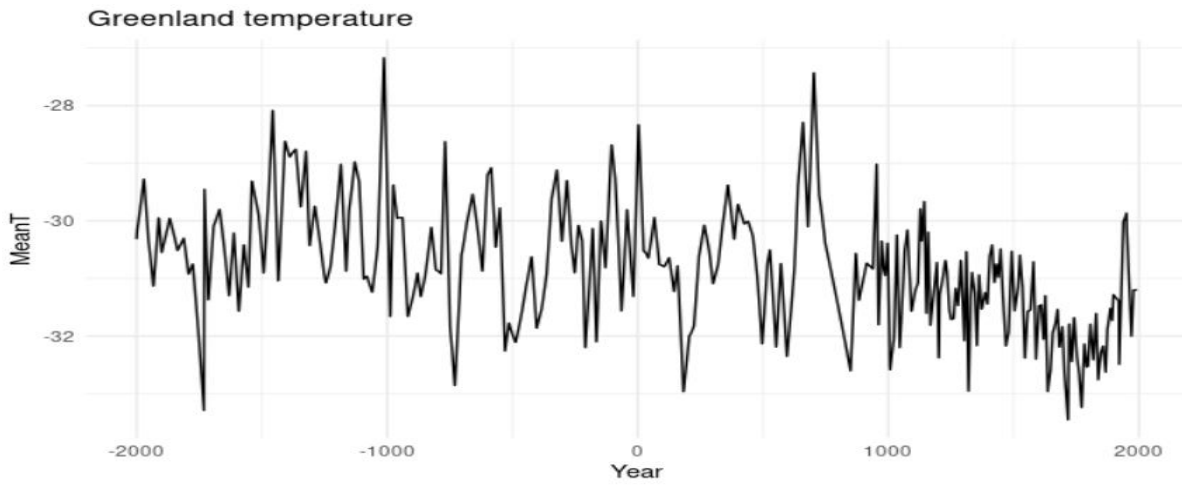
Figure B5. Reconstructed temperatures from Greenland for the last 11,000 (Schönwiese, 1995)
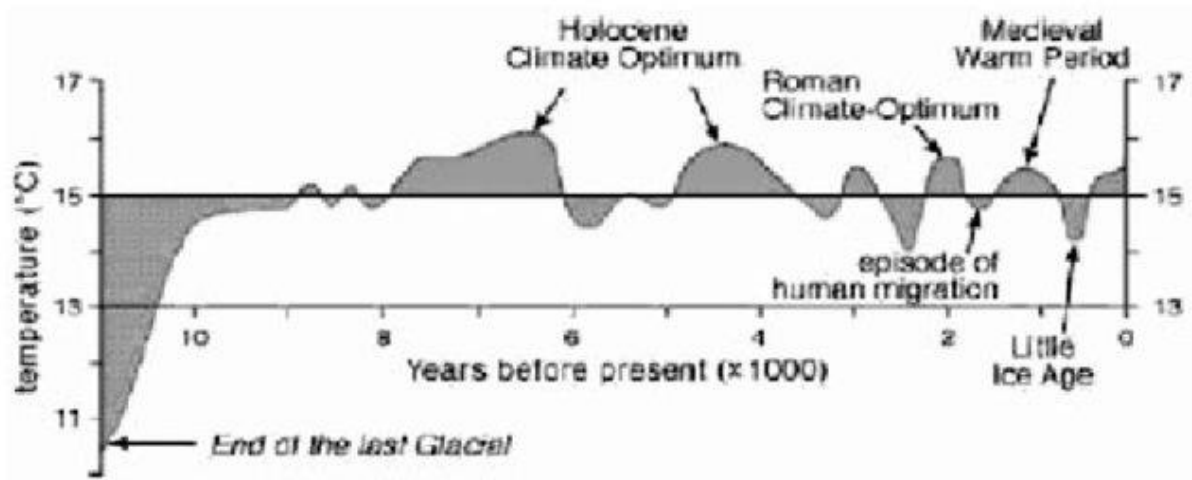
NB: The original graph also includes greenhouse-induced predictions for the next 130 years, not shown here.

Figure B6. Reconstructed temperatures (Moberg et al., 2005), AD 1–1979
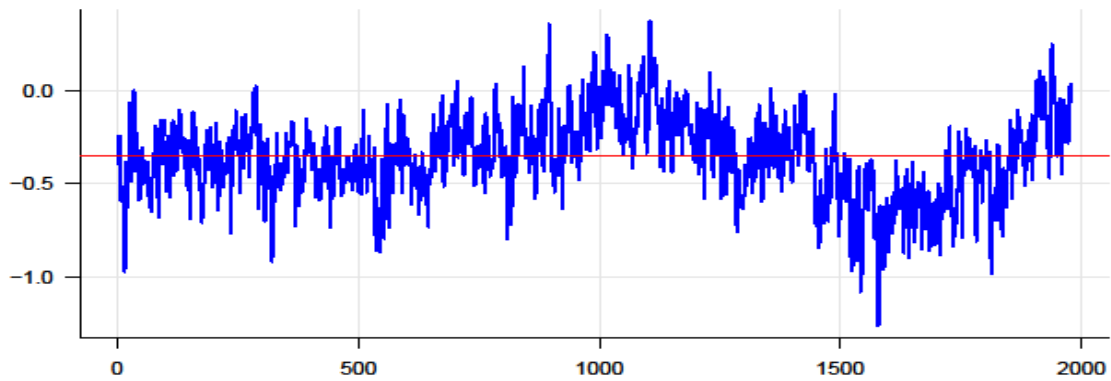
Figure B7. HadCRUT3 and aggregate annual air temperatures
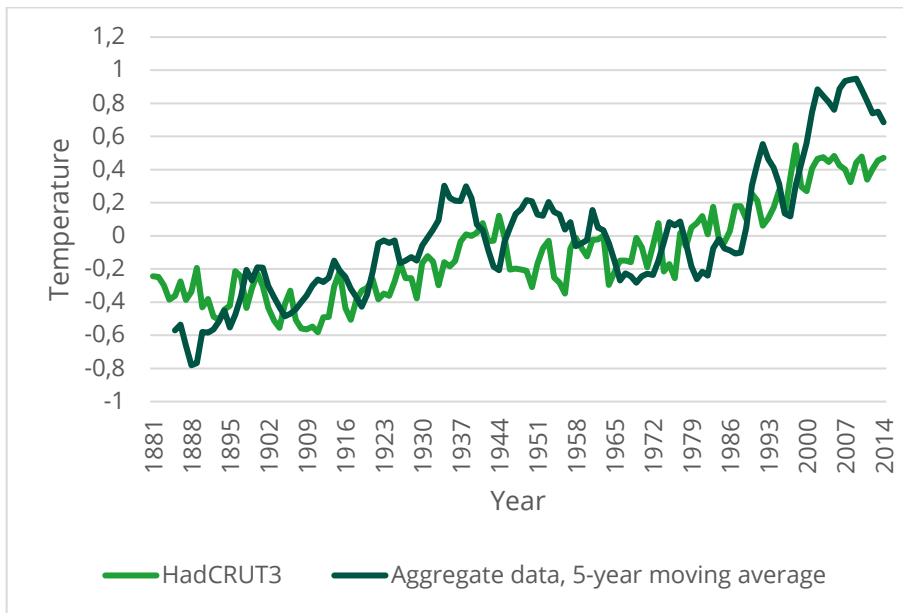
Figure B8. Simulated realizations of the FGN process with unit variance and different values of the Hurst parameter

FGN simulation, H = 0.7

FGN simulation, H = 0.8

FGN simulation, H = 0.9
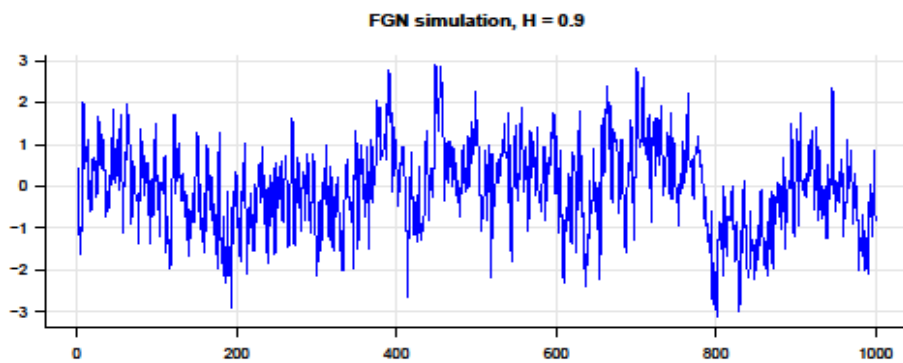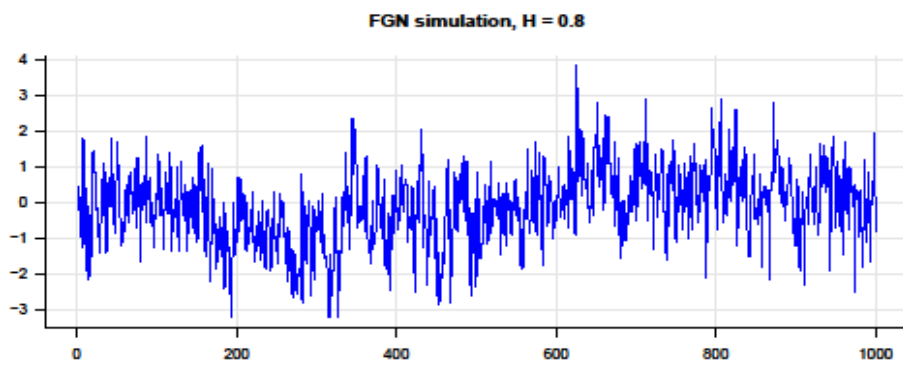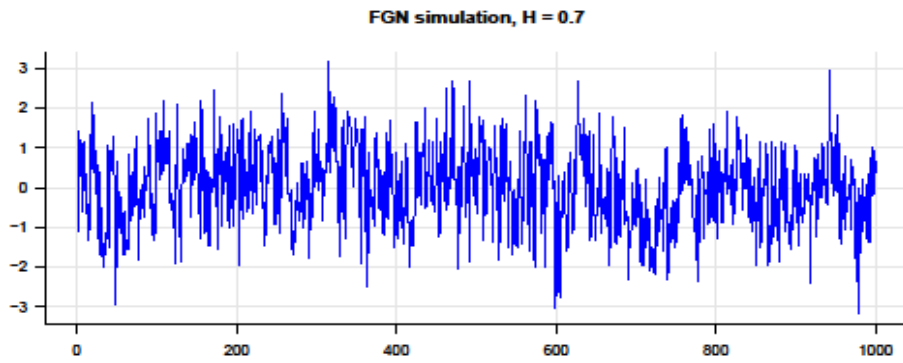
Online Resource 01, 2021 merged data - Supplementary appendix C

To what extent are temperature levels changing due to greenhouse gas emissions?

John Dagsvik and Sigmund H. Moen

Corresponding author:

John K. Dagsvik, E-mail: john.dagsvik@ssb.no

Mariachiara Fortuna, E-mail: mariachiara.fortuna1@gmail.com (reference for code and analysis)

Table C1. Summary information about data

Weather station	First year	Last year	Years	Nonmissing months	Full length in months	Missing months
Aberdeen	1880	2018	139	1657	1669	12
Adelaide	1881	2021	141	1681	1692	11
Alexandria	1870	2021	152	1796	1825	29
Alice Springs	1881	2021	141	1679	1692	13
Allahabad	1881	2014	134	1559	1610	51
Andoya	1868	2021	154	1842	1854	12
Archangelsk	1881	2019	139	1657	1668	11
Athens	1858	2015	158	1887	1899	12
Atlanta	1881	2021	141	1683	1695	12
Basel	1755	2019	265	3141	3188	47
Bergen	1858	2021	164	1963	1974	11
Berlin	1756	2021	266	3186	3198	12
Bismarck	1880	2013	134	1606	1617	11
Bodo	1868	2021	154	1843	1854	11
Boise	1880	2021	142	1697	1708	11
Bombay	1881	2021	141	1671	1694	23
Boston	1881	2021	141	1684	1695	11
Budapest	1780	2021	242	2898	2910	12
Cap Otway	1865	2021	157	1840	1884	44
Chattanooga	1880	2021	142	1695	1707	12
Cincinatti	1880	2021	142	1696	1707	11
Columbus	1880	2017	138	1646	1657	11
Concord	1881	2021	141	1684	1695	11
Copenhagen	1798	2021	224	2677	2689	12
Des Moines	1880	2021	142	1696	1707	11
Detroit	1880	2021	142	1696	1707	11
Dodge City	1880	2021	142	1696	1707	11
Dombas	1865	2021	157	1876	1890	14
Fargo	1881	2021	141	1684	1695	11
Galveston	1881	2021	141	1684	1695	11
Geneva	1753	2019	267	3201	3212	11
Gibraltar	1852	2021	170	1985	2045	60
Hohenpeissenberg	1781	2021	241	2885	2898	13
Illulisat	1873	2021	149	1778	1794	16
Indianapolis	1881	2021	141	1684	1695	11
Indore	1880	2021	142	1677	1696	19
Jacksonville	1880	2021	142	1695	1708	13
Karasjok	1876	2021	146	1747	1758	11
Kazalinsk	1881	2021	141	1687	1698	11
Knoxville	1881	2021	141	1684	1696	12
Kremsmunster	1876	2021	146	1741	1752	11
Lahore	1876	2021	146	1746	1758	12
Lisbon	1880	2021	142	1697	1710	13
Madison	1880	2021	142	1697	1708	11
Madras	1880	2021	142	1693	1706	13
Marquette	1881	2021	141	1681	1696	15
Milwaukee	1881	2021	141	1685	1696	11
Mobile	1880	2021	142	1697	1708	11
Nagasaki	1880	2021	142	1699	1710	11
Nagpur	1880	2020	141	1684	1702	18

Weather station	First year	Last year	Years	Nonmissing months	Full length in months	Missing months
Nantes	1851	2021	171	2038	2053	15
Nashville	1880	2021	142	1697	1708	11
New Orleans	1874	2021	148	1738	1779	41
New York	1822	2020	199	2379	2390	11
Oksoy Lighthouse	1870	2021	152	1818	1830	12
Ona	1868	2021	154	1831	1854	23
Oslo	1816	2021	206	2467	2478	11
Paris	1757	2021	265	3174	3186	12
Prague	1775	2021	247	2959	2970	11
Reykjavik	1870	2021	152	1819	1830	11
Roros	1871	2021	151	1806	1818	12
Sort	1881	2013	133	1566	1607	41
Sulina	1880	2021	142	1699	1710	11
Tokyo	1876	2021	146	1747	1758	11
Tromso	1868	2021	154	1842	1854	12
Uccle	1833	2021	189	2257	2268	11
Uppsala	1774	2021	248	2966	2979	13
Utsira	1868	2021	154	1843	1854	11
Vardo	1858	2021	164	1962	1974	12
Vestervig	1874	2021	148	1758	1770	12
Vienna	1855	2021	167	1929	2003	74
Wellington	1864	2021	158	1875	1902	27
Winnipeg	1880	2021	142	1694	1705	11
Zagreb	1861	2021	161	1915	1927	12

Table C2. Estimates and test statistics based on monthly data

Name	Hc	Hw	SE_Hw	Q_Hc	Q_Hw
Aberdeen	0.702	0.709	0.016	-0.411	-0.069
Adelaide	0.702	0.663	0.016	0.708	-0.953
Alexandria	0.825	0.827	0.016	-2.381	-2.170
Alice Springs	0.716	0.686	0.016	0.877	-0.556
Allahabad	0.678	0.679	0.017	-0.056	0.003
Andoya	0.724	0.717	0.015	-0.005	-0.405
Archangelsk	0.680	0.669	0.016	0.056	-0.358
Athens	0.697	0.704	0.015	-0.631	-0.322
Atlanta	0.637	0.635	0.016	-0.039	-0.070
Basel	0.654	0.639	0.012	-0.122	-0.736
Bergen	0.696	0.700	0.015	-0.485	-0.318
Berlin	0.685	0.682	0.012	-0.418	-0.529
Bismarck	0.663	0.656	0.016	0.062	-0.172
Bodo	0.692	0.696	0.015	-0.283	-0.138
Boise	0.672	0.661	0.016	0.037	-0.364
Bombay	0.802	0.818	0.016	-1.697	-0.091
Boston	0.694	0.668	0.016	0.473	-0.561
Budapest	0.666	0.671	0.012	-0.831	-0.609
Cap Otway	0.809	0.753	0.015	2.594	-2.582
Chattanooga	0.640	0.643	0.016	-0.175	-0.071
Cincinatti	0.649	0.640	0.016	0.038	-0.220
Columbus	0.618	0.637	0.016	-0.356	0.074
Concord	0.701	0.675	0.016	0.273	-0.874
Copenhagen	0.774	0.782	0.013	-0.976	-0.188
Des Moines	0.626	0.633	0.016	-0.108	0.060
Detroit	0.663	0.664	0.016	-0.131	-0.106
Dodge City	0.622	0.599	0.016	0.337	-0.163
Dombas	0.650	0.675	0.015	-0.754	0.065
Fargo	0.665	0.667	0.016	-0.247	-0.187
Galveston	0.690	0.697	0.016	-0.300	-0.041
Geneva	0.698	0.666	0.012	0.184	-1.654
Gibraltar	0.806	0.771	0.015	0.719	-2.642
Hohenpeissenberg	0.636	0.615	0.012	0.135	-0.535
Illulisat	0.743	0.773	0.016	-0.913	1.227
Indianapolis	0.610	0.618	0.016	-0.178	-0.029
Indore	0.740	0.713	0.016	0.597	-0.968
Jacksonville	0.634	0.660	0.016	-0.685	0.012
Karasjok	0.641	0.673	0.016	-0.594	0.380
Kazalinsk	0.680	0.730	0.016	-1.108	1.093
Knoxville	0.619	0.620	0.016	-0.138	-0.112
Kremsmunster	0.704	0.678	0.016	-0.012	-1.139
Lahore	0.657	0.700	0.016	-0.779	0.772
Lisbon	0.790	0.724	0.016	1.793	-3.143
Madison	0.645	0.656	0.016	-0.277	0.049
Madras	0.759	0.760	0.016	-0.816	-0.761
Marquette	0.720	0.711	0.016	-0.515	-0.989
Milwaukee	0.685	0.669	0.016	0.223	-0.395
Mobile	0.635	0.654	0.016	-0.406	0.097
Nagasaki	0.747	0.719	0.016	0.333	-1.386
Nagpur	0.690	0.704	0.016	-0.322	0.267
Nantes	0.667	0.655	0.014	-0.182	-0.651

Name	Hc	Hw	SE_Hw	Q_Hc	Q_Hw
Nashville	0.601	0.615	0.016	-0.230	0.014
New Orleans	0.711	0.694	0.016	0.165	-0.639
New York	0.749	0.703	0.013	0.768	-2.451
Oksoy Lighthouse	0.735	0.800	0.016	-1.434	3.667
Ona	0.730	0.750	0.015	-0.693	0.538
Oslo	0.711	0.746	0.013	-1.154	1.121
Paris	0.748	0.677	0.012	2.018	-3.327
Prague	0.684	0.675	0.012	0.012	-0.461
Reykjavik	0.737	0.705	0.015	0.484	-1.340
Roros	0.673	0.702	0.015	-0.690	0.486
Sort	0.658	0.703	0.017	-0.657	0.932
Sulina	0.684	0.720	0.016	-1.110	0.465
Tokyo	0.801	0.750	0.016	1.356	-2.954
Tromso	0.675	0.689	0.015	-0.346	0.186
Uccle	0.676	0.655	0.014	0.103	-0.763
Uppsala	0.723	0.741	0.012	-1.021	0.319
Utsira	0.755	0.781	0.016	-0.898	1.192
Vardo	0.787	0.759	0.015	0.907	-1.540
Vestervig	0.753	0.802	0.016	-1.397	2.739
Vienna	0.709	0.676	0.015	0.254	-1.294
Wellington	0.843	0.783	0.015	3.334	-3.715
Winnipeg	0.675	0.683	0.016	-0.493	-0.165
Zagreb	0.710	0.686	0.015	-0.033	-1.232

Table C3. Estimates and test statistics based on annual data

Name	Hc	Hw	SE_Hw	Q_Hc	Q_Hw
Aberdeen	0.794	0.781	0.057	0.289	-0.058
Adelaide	0.910	0.793	0.056	7.018	-0.552
Alexandria	0.879	0.936	0.055	-1.818	3.067
Alice Springs	0.675	0.755	0.056	-0.560	0.495
Allahabad	0.710	0.783	0.058	-0.415	0.882
Andoya	0.797	0.773	0.054	1.018	0.303
Archangelsk	0.749	0.781	0.057	-0.652	-0.040
Athens	0.760	0.833	0.053	-1.127	0.787
Atlanta	0.731	0.749	0.056	-0.009	0.318
Basel	0.719	0.764	0.041	-1.753	-0.886
Bergen	0.793	0.747	0.052	0.588	-0.607
Berlin	0.739	0.750	0.041	-0.686	-0.424
Bismarck	0.753	0.753	0.057	0.186	0.176
Bodo	0.744	0.723	0.053	0.005	-0.357
Boise	0.779	0.739	0.056	0.608	-0.280
Bombay	0.807	0.915	0.057	-2.039	3.539
Boston	0.744	0.741	0.056	-0.374	-0.423
Budapest	0.721	0.753	0.043	-1.500	-0.892
Cap Otway	0.887	0.843	0.055	2.821	0.161
Chattanooga	0.732	0.729	0.056	0.271	0.213
Cincinatti	0.746	0.749	0.056	0.253	0.309
Columbus	0.722	0.717	0.056	0.451	0.370
Concord	0.814	0.766	0.056	0.676	-0.631
Copenhagen	0.825	0.789	0.045	0.568	-0.823
Des Moines	0.651	0.645	0.055	0.095	0.041
Detroit	0.722	0.699	0.055	0.410	0.043
Dodge City	0.675	0.741	0.056	-0.505	0.341
Dombas	0.689	0.657	0.052	-0.026	-0.379
Fargo	0.744	0.727	0.056	0.319	0.017
Galveston	0.713	0.737	0.056	-0.590	-0.265
Geneva	0.862	0.817	0.041	1.295	-1.204
Gibraltar	0.821	0.917	0.054	-2.032	3.351
Hohenpeissenberg	0.723	0.733	0.043	-0.742	-0.553
Illulisat	0.832	0.791	0.055	1.836	0.324
Indianapolis	0.686	0.680	0.055	0.025	-0.048
Indore	0.828	0.894	0.057	-0.506	3.053
Jacksonville	0.660	0.739	0.056	-0.621	0.282
Karasjok	0.695	0.672	0.054	0.238	-0.052
Kazalinsk	0.786	0.708	0.055	1.265	-0.474
Knoxville	0.736	0.706	0.056	0.205	-0.258
Kremsmunster	0.789	0.888	0.056	-2.375	1.019
Lahore	0.665	0.753	0.055	-0.303	0.921
Lisbon	0.948	0.933	0.057	4.772	2.035
Madison	0.676	0.680	0.055	0.047	0.097
Madras	0.836	0.902	0.057	-1.202	2.320
Marquette	0.757	0.775	0.056	-0.795	-0.461
Milwaukee	0.681	0.736	0.056	-0.693	-0.042
Mobile	0.669	0.739	0.056	-0.492	0.374
Nagasaki	0.835	0.791	0.056	0.529	-0.837
Nagpur	0.685	0.734	0.056	-0.224	0.450
Nantes	0.759	0.756	0.051	-0.682	-0.739

Name	Hc	Hw	SE_Hw	Q_Hc	Q_Hw
Nashville	0.601	0.698	0.055	-0.370	0.361
New Orleans	0.854	0.877	0.056	0.272	1.525
New York	0.917	0.860	0.048	5.050	-0.366
Oksoy Lighthouse	0.699	0.696	0.053	-0.326	-0.358
Ona	0.715	0.751	0.055	-0.691	-0.122
Oslo	0.717	0.720	0.046	-0.700	-0.652
Paris	0.885	0.833	0.041	0.882	-2.348
Prague	0.771	0.724	0.042	0.797	-0.484
Reykjavik	0.914	0.887	0.055	3.868	1.217
Roros	0.738	0.703	0.054	0.122	-0.426
Sort	0.643	0.595	0.056	0.227	-0.102
Sulina	0.708	0.743	0.056	-0.917	-0.478
Tokyo	0.934	0.856	0.056	5.734	-1.325
Tromso	0.681	0.676	0.053	-0.007	-0.059
Uccle	0.791	0.759	0.048	0.161	-0.715
Uppsala	0.749	0.735	0.042	-0.507	-0.805
Utsira	0.761	0.793	0.054	-0.639	0.097
Vardo	0.802	0.823	0.052	-0.233	0.502
Vestervig	0.729	0.766	0.055	-1.041	-0.466
Vienna	0.826	0.852	0.054	-1.109	-0.117
Wellington	0.868	0.937	0.055	-1.233	5.063
Winnipeg	0.768	0.764	0.056	0.090	0.003
Zagreb	0.783	0.863	0.053	-2.304	0.102

Table C4. Stationarity test. Annual data

Name	Test_statistics	Test_result	Test_criterion
Aberdeen	2.086	No rejection	5.783
Adelaide	3.273	No rejection	5.890
Alexandria	4.063	No rejection	5.527
Alice Springs	3.797	No rejection	5.774
Allahabad	2.590	No rejection	5.762
Andoya	4.899	No rejection	5.936
Archangelsk	3.568	No rejection	5.717
Athens	4.090	No rejection	5.570
Atlanta	3.606	No rejection	5.889
Basel	4.573	No rejection	5.963
Bergen	2.515	No rejection	5.834
Berlin	4.486	No rejection	5.982
Bismarck	3.335	No rejection	5.641
Bodo	4.479	No rejection	5.917
Boise	3.463	No rejection	5.632
Bombay	4.763	No rejection	5.861
Boston	3.319	No rejection	5.805
Budapest	4.501	No rejection	5.941
Cap Otway	3.901	No rejection	5.858
Chattanooga	3.598	No rejection	5.843
Cincinatti	4.177	No rejection	5.851
Columbus	2.884	No rejection	5.828
Concord	2.945	No rejection	5.855
Copenhagen	3.784	No rejection	5.958
Des Moines	2.720	No rejection	5.776
Detroit	3.489	No rejection	5.810
Dodge City	2.811	No rejection	5.823
Dombas	4.591	No rejection	5.850
Fargo	2.107	No rejection	5.463
Galveston	2.885	No rejection	5.879
Geneva	4.158	No rejection	5.952
Gibraltar	5.364	No rejection	5.855
Hohenpeissenberg	6.153	Rejection	5.997
Illulisat	3.701	No rejection	5.835
Indianapolis	3.003	No rejection	5.801
Indore	2.554	No rejection	5.849
Jacksonville	3.832	No rejection	5.821
Karasjok	4.224	No rejection	5.863
Kazalinsk	3.484	No rejection	5.755
Knoxville	3.523	No rejection	5.887
Kremsmunster	5.685	No rejection	5.773
Lahore	3.092	No rejection	5.893
Lisbon	5.661	No rejection	5.854
Madison	2.146	No rejection	5.793
Madras	4.372	No rejection	5.742
Marquette	2.616	No rejection	5.750
Milwaukee	2.522	No rejection	5.752
Mobile	2.679	No rejection	5.903
Nagasaki	3.997	No rejection	5.743
Nagpur	4.199	No rejection	5.869
Nantes	3.307	No rejection	5.847

Name	Test_statistics	Test_result	Test_criterion
Nashville	3.314	No rejection	5.854
New Orleans	4.297	No rejection	5.881
New York	4.566	No rejection	5.576
Oksoy Lighthouse	3.471	No rejection	5.876
Ona	3.670	No rejection	5.907
Oslo	4.438	No rejection	5.931
Paris	4.227	No rejection	5.954
Prague	3.994	No rejection	5.991
Reykjavik	3.708	No rejection	5.706
Roros	3.160	No rejection	5.814
Sort	3.892	No rejection	5.597
Sulina	4.297	No rejection	5.545
Tokyo	3.581	No rejection	5.576
Tromso	5.150	No rejection	5.891
Uccle	4.063	No rejection	5.945
Uppsala	2.854	No rejection	5.924
Utsira	3.879	No rejection	5.860
Vardo	3.108	No rejection	5.895
Vestervig	3.832	No rejection	5.856
Vienna	3.285	No rejection	5.783
Wellington	3.456	No rejection	5.484
Winnipeg	3.220	No rejection	5.584
Zagreb	4.396	No rejection	5.856

Table C5. Stationarity test. Monthly data

Name	Test_statistics	Test_result	Test_criterion
Aberdeen	3.818	No rejection	5.856
Adelaide	5.527	No rejection	6.064
Alexandria	4.473	No rejection	5.876
Alice Springs	3.768	No rejection	6.033
Allahabad	6.386	Rejection	5.727
Andoya	4.380	No rejection	5.981
Archangelsk	3.711	No rejection	5.563
Athens	5.573	No rejection	6.030
Atlanta	3.325	No rejection	6.067
Basel	3.873	No rejection	6.120
Bergen	3.345	No rejection	6.037
Berlin	5.279	No rejection	6.111
Bismarck	5.307	No rejection	6.026
Bodo	3.074	No rejection	6.028
Boise	6.780	Rejection	6.053
Bombay	4.124	No rejection	5.724
Boston	3.151	No rejection	6.017
Budapest	4.419	No rejection	6.120
Cap Otway	5.931	No rejection	6.025
Chattanooga	3.941	No rejection	6.042
Cincinatti	3.448	No rejection	6.041
Columbus	5.500	No rejection	6.046
Concord	3.853	No rejection	5.902
Copenhagen	5.233	No rejection	6.110
Des Moines	5.692	No rejection	6.049
Detroit	5.039	No rejection	6.031
Dodge City	4.780	No rejection	6.039
Dombas	5.196	No rejection	5.977
Fargo	3.972	No rejection	6.043
Galveston	4.581	No rejection	6.064
Geneva	5.030	No rejection	6.128
Gibraltar	6.070	Rejection	6.008
Hohenpeissenberg	3.238	No rejection	6.096
Illulisat	4.394	No rejection	6.043
Indianapolis	6.068	Rejection	6.039
Indore	5.084	No rejection	6.040
Jacksonville	4.216	No rejection	5.896
Karasjok	4.383	No rejection	5.878
Kazalinsk	3.728	No rejection	6.020
Knoxville	3.552	No rejection	6.071
Kremsmunster	4.519	No rejection	5.837
Lahore	6.268	Rejection	6.008
Lisbon	3.721	No rejection	5.828
Madison	4.101	No rejection	6.050
Madras	2.798	No rejection	5.938
Marquette	4.132	No rejection	5.945
Milwaukee	5.249	No rejection	6.057
Mobile	5.786	No rejection	5.827
Nagasaki	4.490	No rejection	6.060
Nagpur	4.037	No rejection	6.038
Nantes	6.136	Rejection	6.058

Name	Test_statistics	Test_result	Test_criterion
Nashville	5.682	No rejection	6.047
New Orleans	4.802	No rejection	5.978
New York	2.916	No rejection	5.956
Oksoy Lighthouse	4.470	No rejection	5.909
Ona	4.193	No rejection	6.037
Oslo	3.908	No rejection	6.041
Paris	5.169	No rejection	6.139
Prague	6.494	Rejection	6.108
Reykjavik	8.775	Rejection	6.006
Roros	3.609	No rejection	5.975
Sort	5.211	No rejection	5.823
Sulina	5.215	No rejection	6.066
Tokyo	4.151	No rejection	5.990
Tromso	2.912	No rejection	5.959
Uccle	3.492	No rejection	6.057
Uppsala	4.764	No rejection	6.131
Utsira	5.016	No rejection	5.994
Vardo	6.728	Rejection	6.063
Vestervig	5.105	No rejection	5.907
Vienna	4.187	No rejection	5.976
Wellington	7.499	Rejection	5.721
Winnipeg	3.764	No rejection	5.998
Zagreb	4.134	No rejection	6.017

Table C6. Monthly and annual standard deviations of the temperature series

Name	SD_annual	SD_monthly_des
Aberdeen	0.585	1.225
Adelaide	0.570	1.229
Alexandria	0.701	1.047
Alice Springs	0.806	1.558
Allahabad	0.521	1.149
Andoya	0.789	1.530
Archangelsk	1.356	3.014
Athens	0.687	1.441
Atlanta	0.662	1.744
Basel	0.818	1.954
Bergen	0.766	1.616
Berlin	0.986	2.139
Bismarck	1.229	2.924
Bodo	0.867	1.824
Boise	0.932	2.061
Bombay	0.467	0.760
Boston	0.773	1.649
Budapest	0.929	2.047
Cap Otway	0.599	1.004
Chattanooga	0.723	1.818
Cincinatti	0.895	2.119
Columbus	0.804	2.088
Concord	0.878	1.810
Copenhagen	1.059	1.832
Des Moines	0.930	2.384
Detroit	0.892	2.006
Dodge City	0.814	2.124
Dombas	1.048	2.313
Fargo	1.183	2.683
Galveston	0.655	1.446
Geneva	0.841	1.775
Gibraltar	0.629	1.008
Hohenpeissenberg	0.897	2.183
Illulisat	1.665	3.225
Indianapolis	0.810	2.150
Indore	0.525	1.052
Jacksonville	0.648	1.561
Karasjok	1.301	3.130
Kazalinsk	1.256	2.834
Knoxville	0.708	1.846
Kremsmunster	0.933	1.941
Lahore	0.537	1.318
Lisbon	0.765	1.276
Madison	0.974	2.306
Madras	0.409	0.753
Marquette	1.208	2.243
Milwaukee	1.030	2.146
Mobile	0.607	1.597
Nagasaki	0.623	1.125
Nagpur	0.487	1.070
Nantes	0.754	1.654

Name	SD_annual	SD_monthly_des
Nashville	0.709	1.952
New Orleans	0.764	1.641
New York	0.976	1.833
Oksoy Lighthouse	0.869	1.738
Ona	0.695	1.338
Oslo	1.006	2.078
Paris	1.051	1.953
Prague	0.962	2.102
Reykjavik	0.792	1.556
Roros	1.134	2.615
Sort	0.660	1.605
Sulina	0.872	1.874
Tokyo	0.750	1.230
Tromso	0.784	1.720
Uccle	0.833	1.841
Uppsala	1.145	2.315
Utsira	0.741	1.383
Vardo	0.977	1.620
Vestervig	0.949	1.789
Vienna	0.994	2.045
Wellington	0.679	1.043
Winnipeg	1.323	2.873
Zagreb	1.025	2.099

Online Resource 01, 2021 merged data - Supplementary appendix D

To what extent are temperature levels changing due to greenhouse gas emissions?

John Dagsvik **and** Sigmund H. Moen

Corresponding author:

John K. Dagsvik, E-mail: john.dagsvik@ssb.no

Mariachiara Fortuna, E-mail: mariachiara.fortuna1@gmail.com (reference for code and analysis)
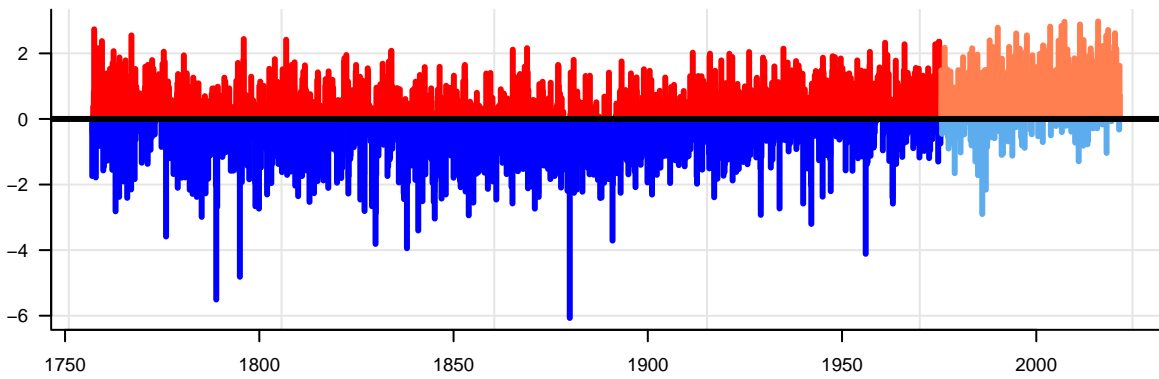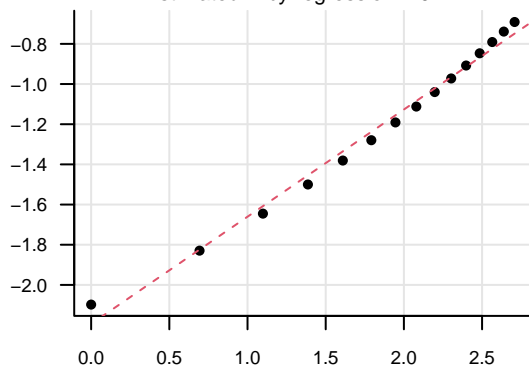
Aberdeen

Autocorrelation
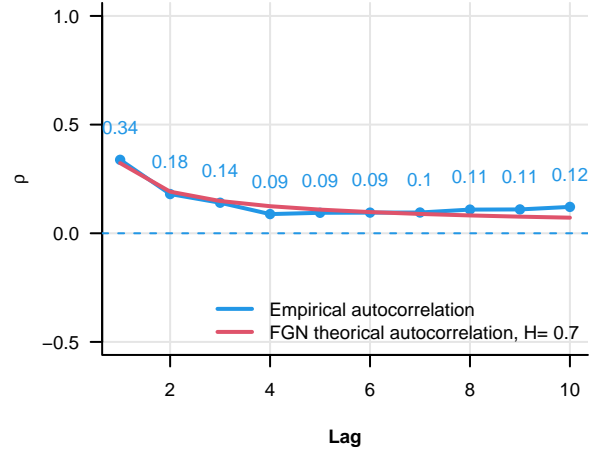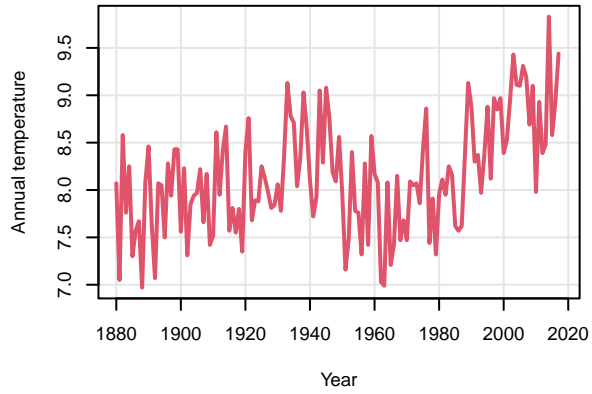
Deviation from the mean
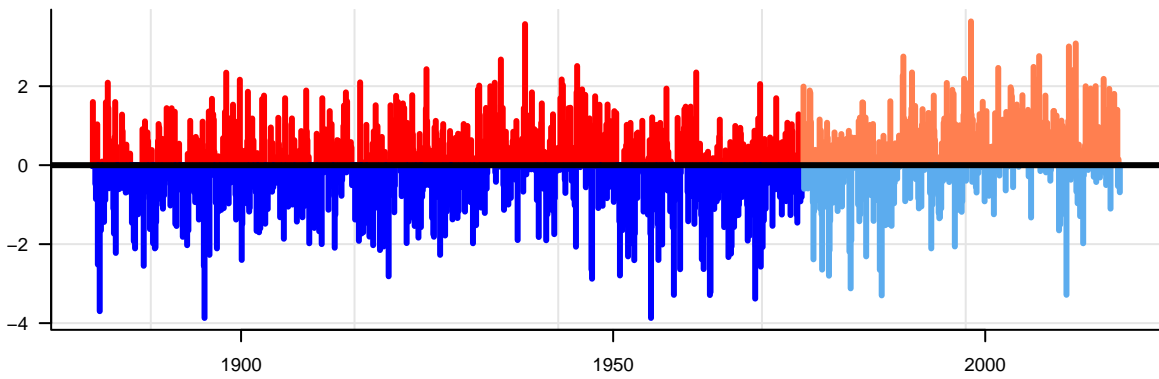
Self−similarity test

Estimated H by regression = 0.71
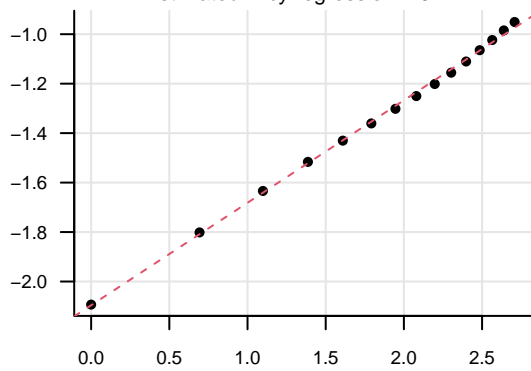
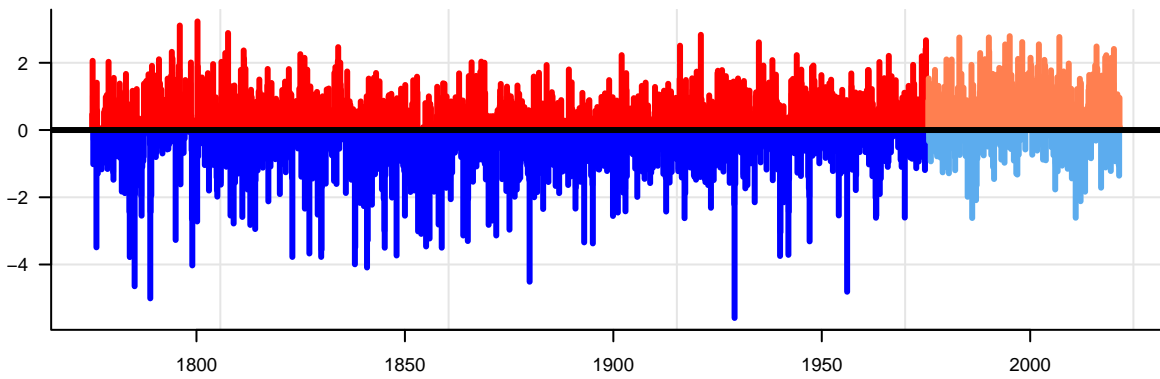## Normality test

Estimated alpha = 1.98

Adelaide
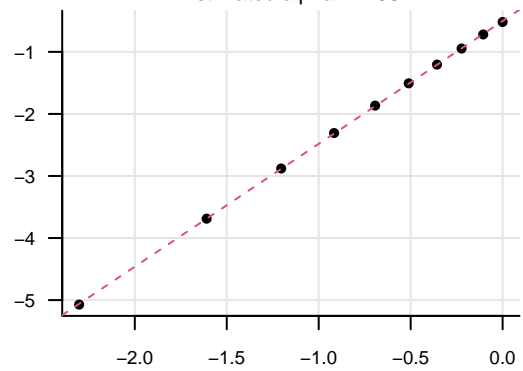
Alexandria
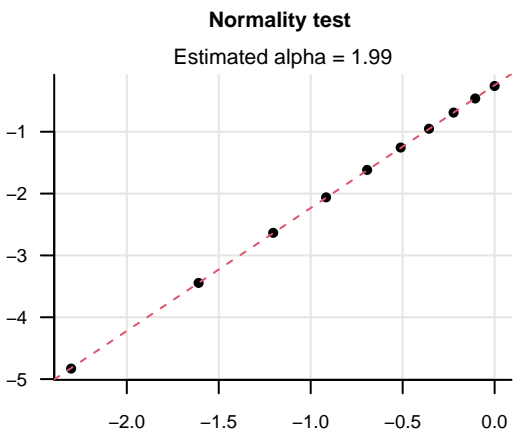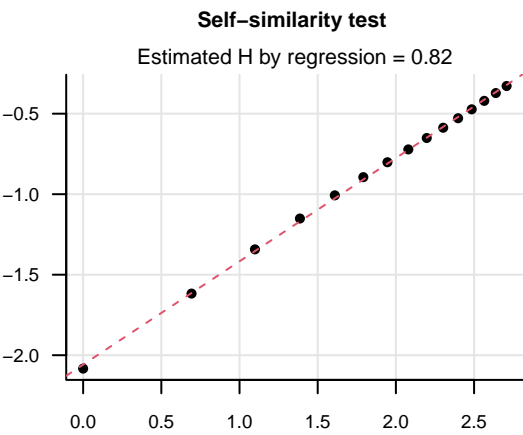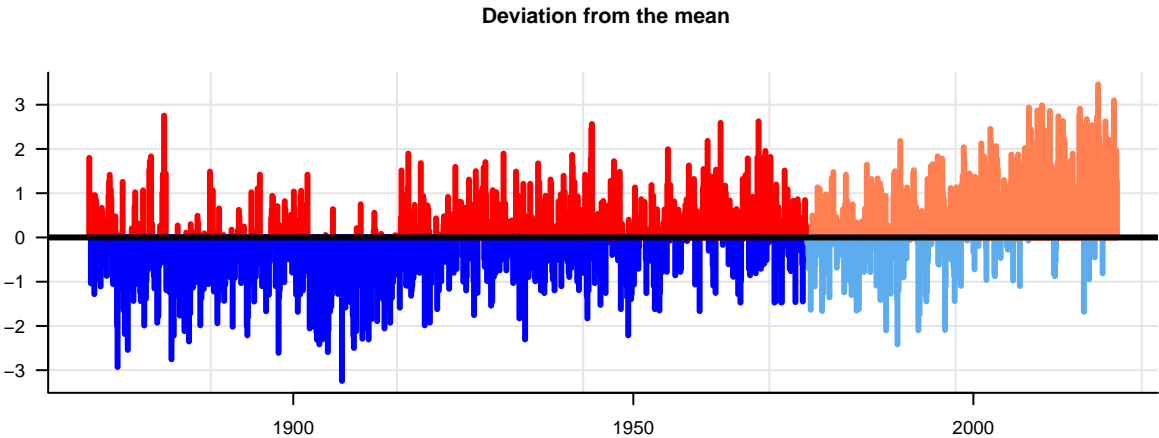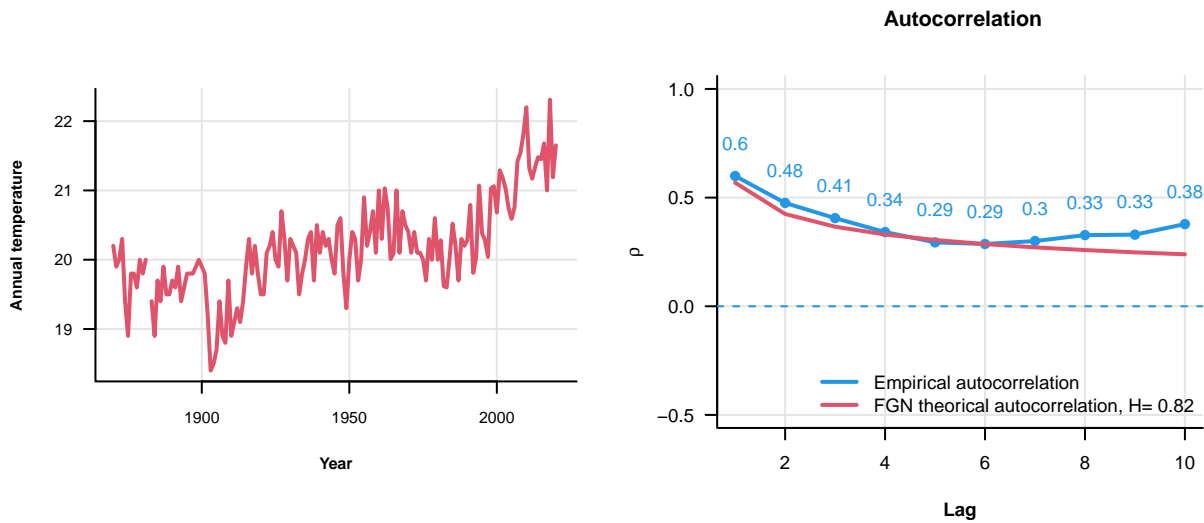
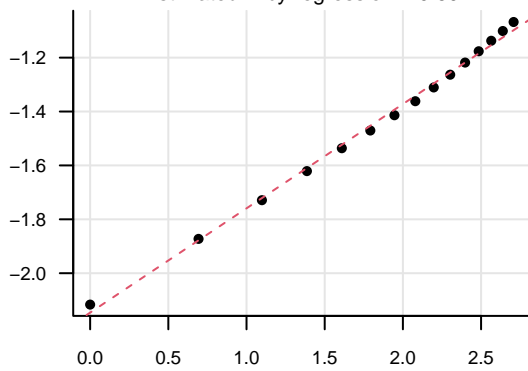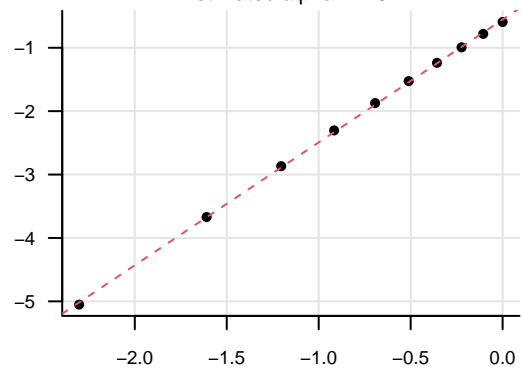# Alice Springs

Autocorrelation

Deviation from the mean

Self−similarity test

Estimated H by regression = 0.73

Normality test

Estimated alpha = 2

Allahabad

Andoya

Archangelsk

Athens

Atlanta

Autocorrelation

Deviation from the mean

Self−similarity test
Estimated H by regression = 0.64

Normality test
Estimated alpha = 1.96

Basel

Autocorrelation
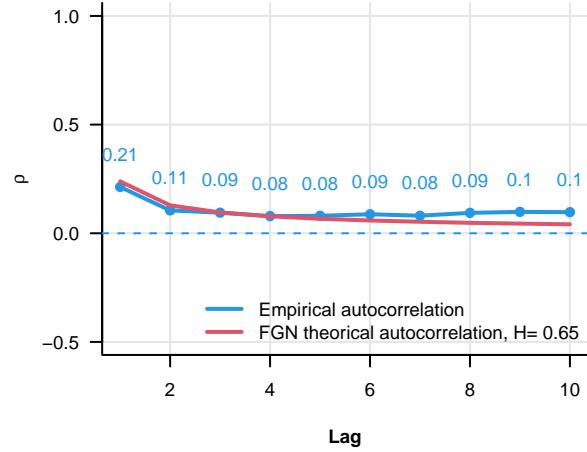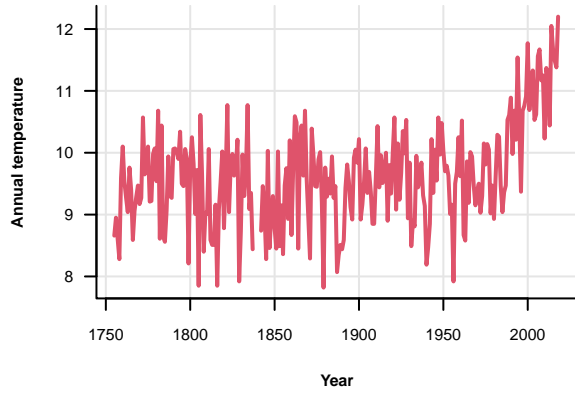
Deviation from the mean
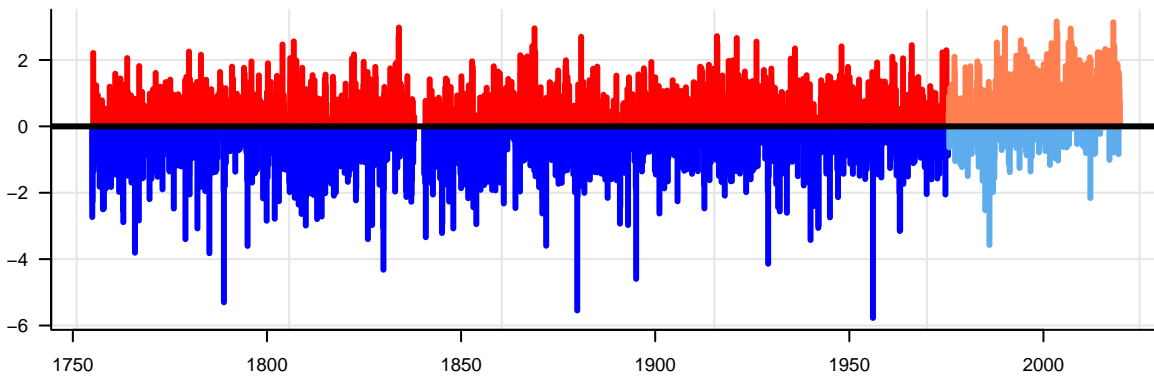
Self−similarity test
Estimated H by regression = 0.67
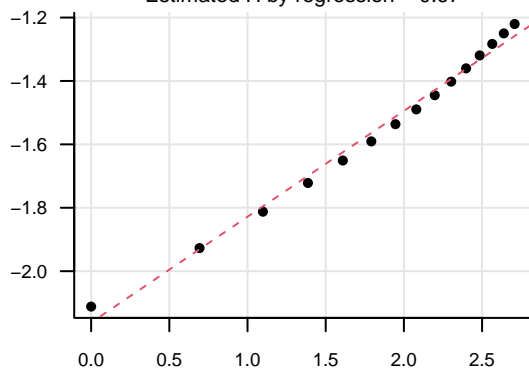
Normality test
Estimated alpha = 1.95
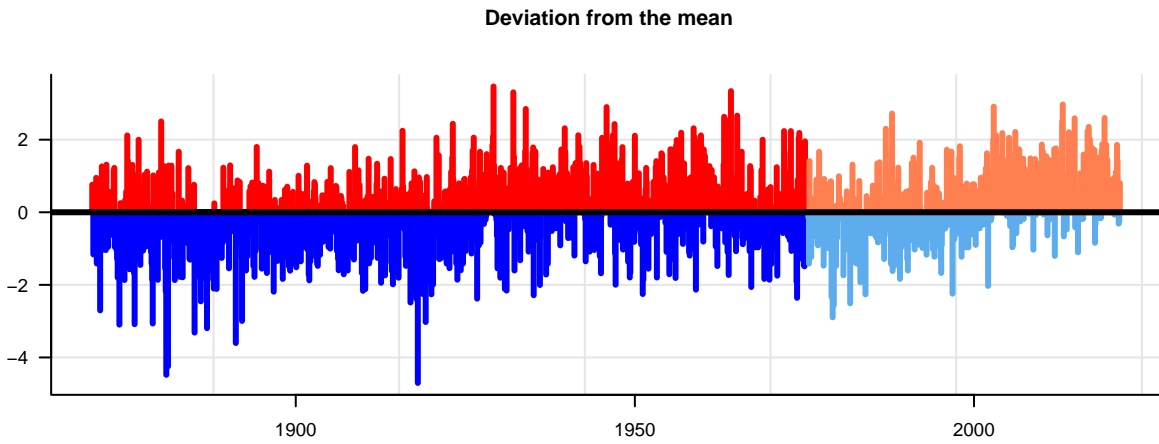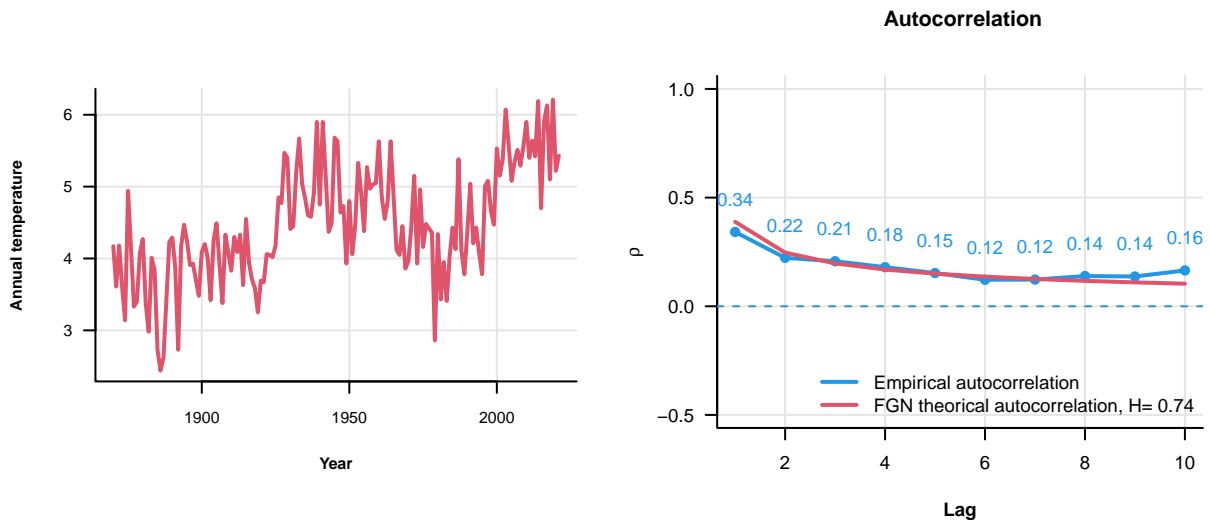
Bergen
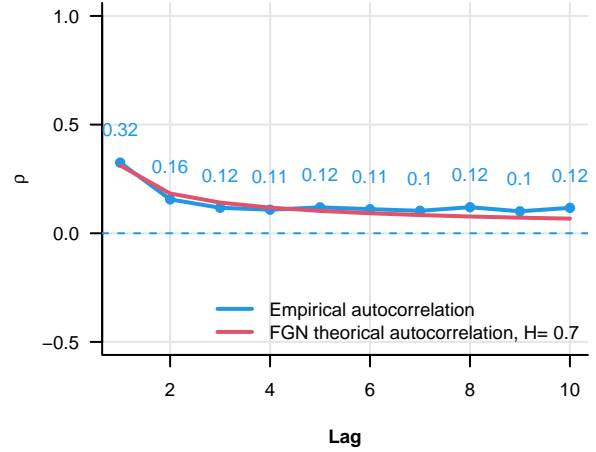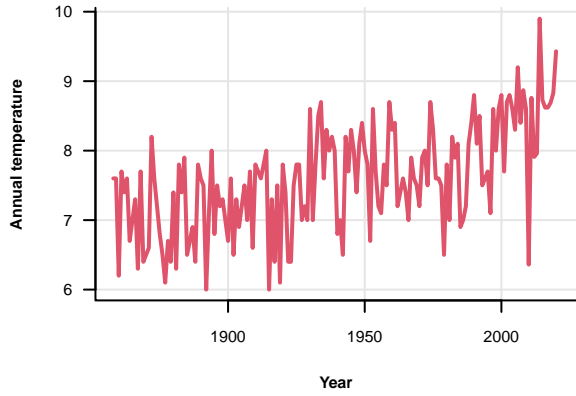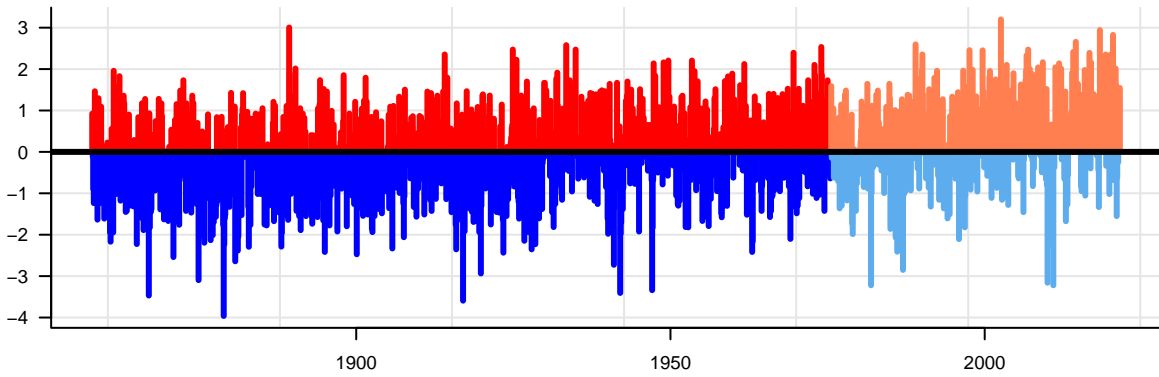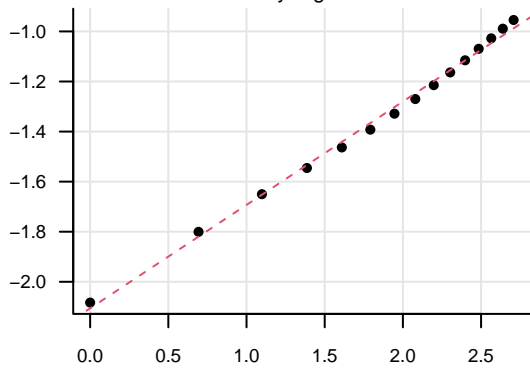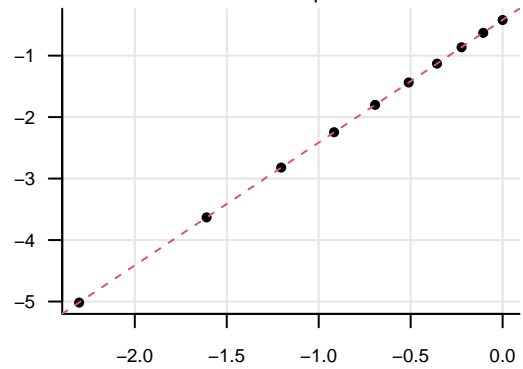
Berlin
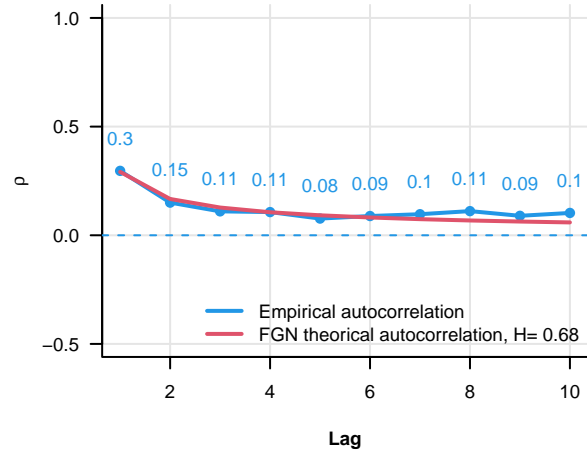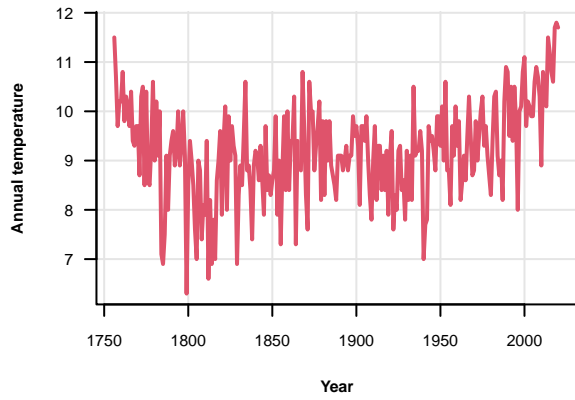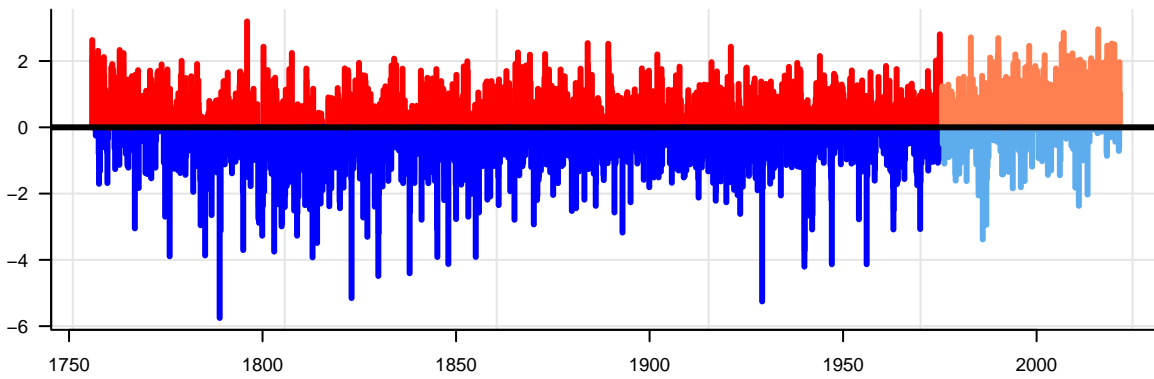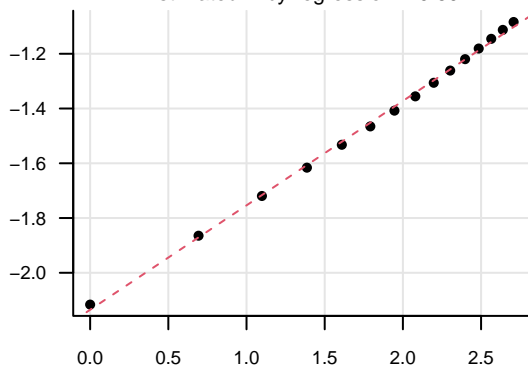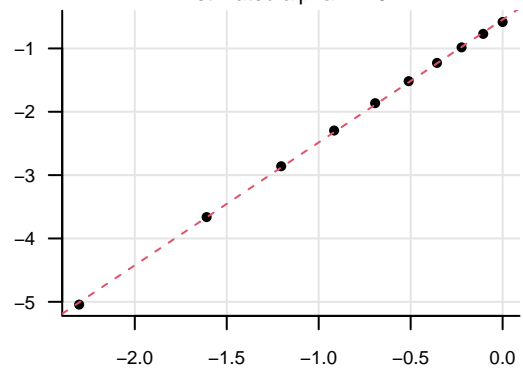
Bismarck

Autocorrelation
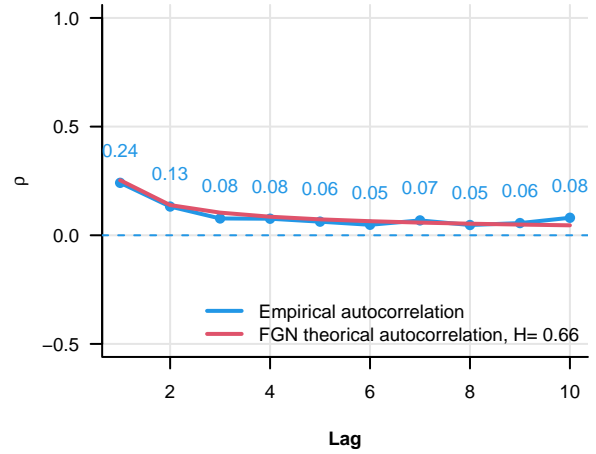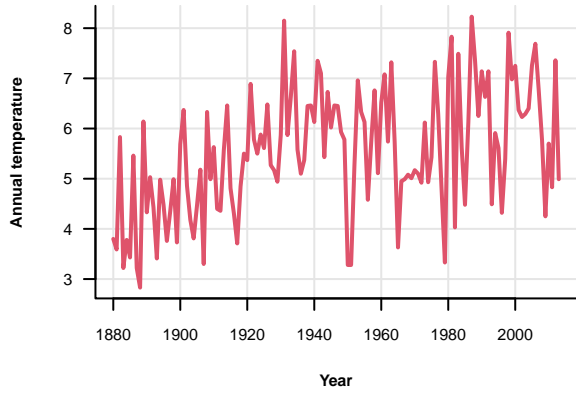
Deviation from the mean
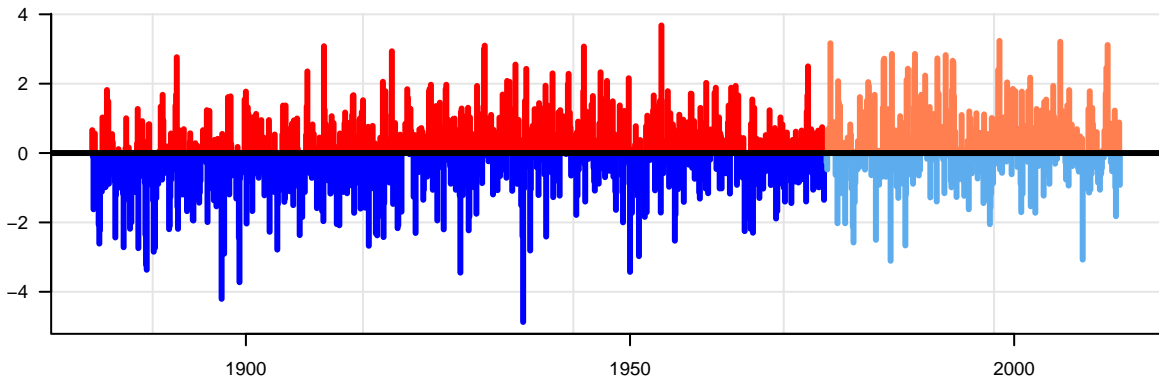
Self−similarity test
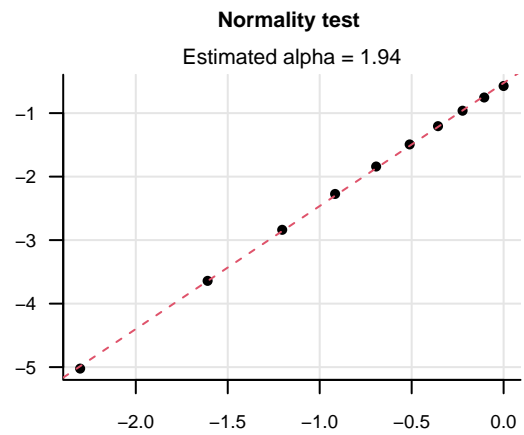Estimated H by regression = 0.67
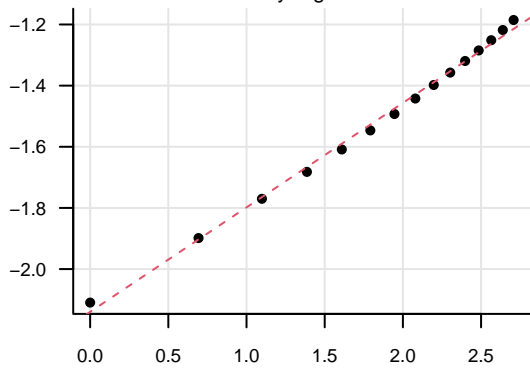
Normality test
Estimated alpha = 1.94

Bodo

Autocorrelation

- Empirical autocorrelation
- FGN theorical autocorrelation, H= 0.69
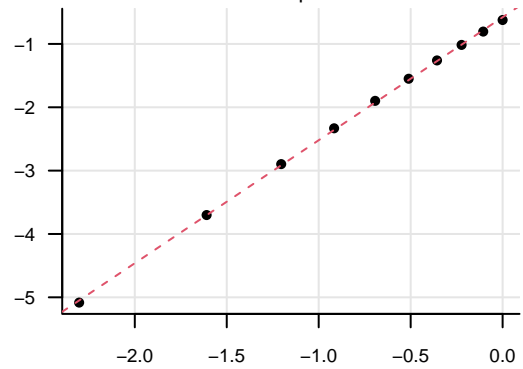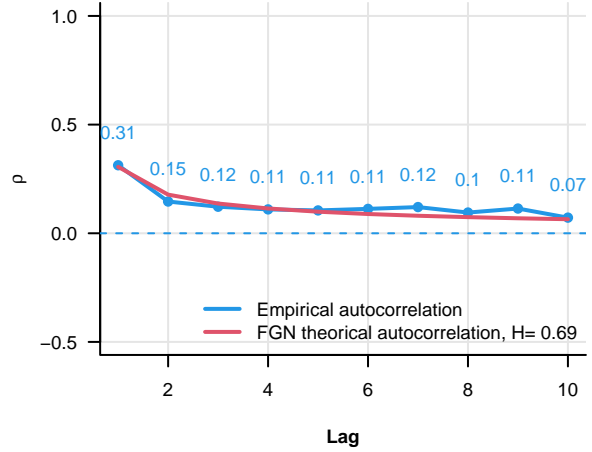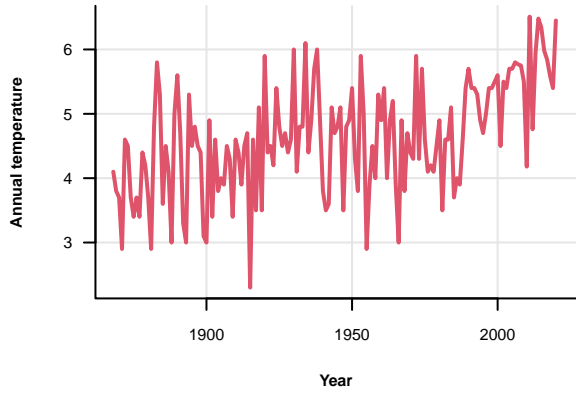
Deviation from the mean
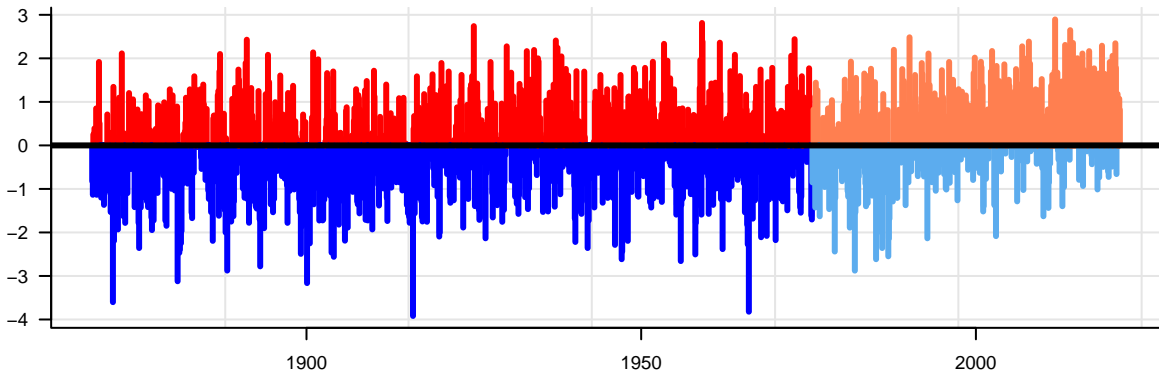
Self–similarity test

Estimated H by regression = 0.7
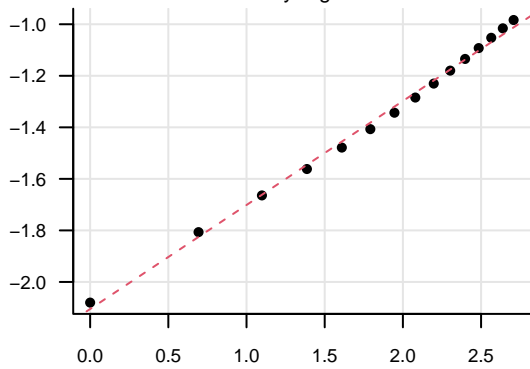
Normality test

Estimated alpha = 2
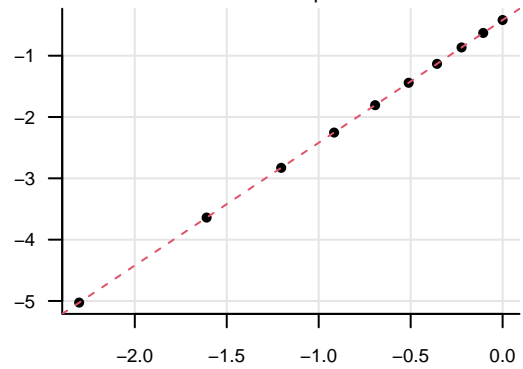
Boise

Autocorrelation
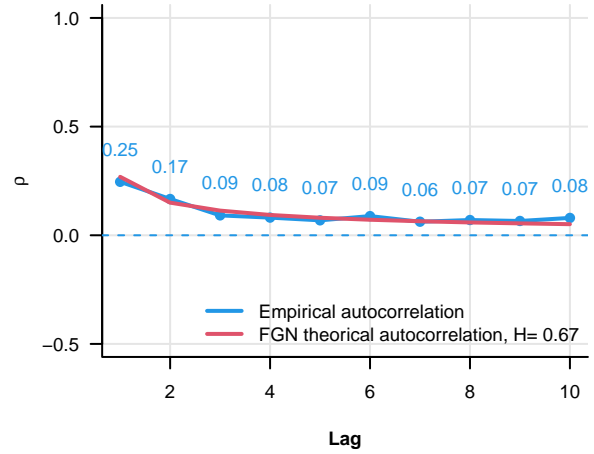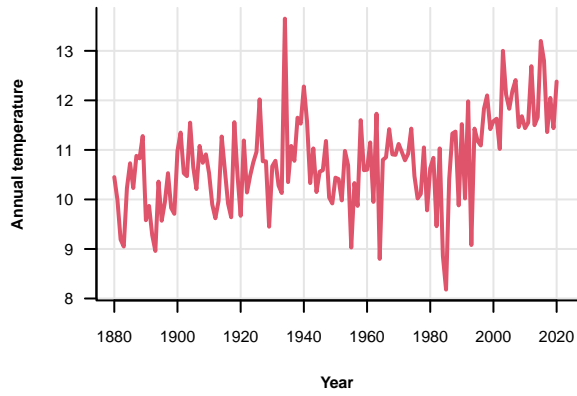
Deviation from the mean
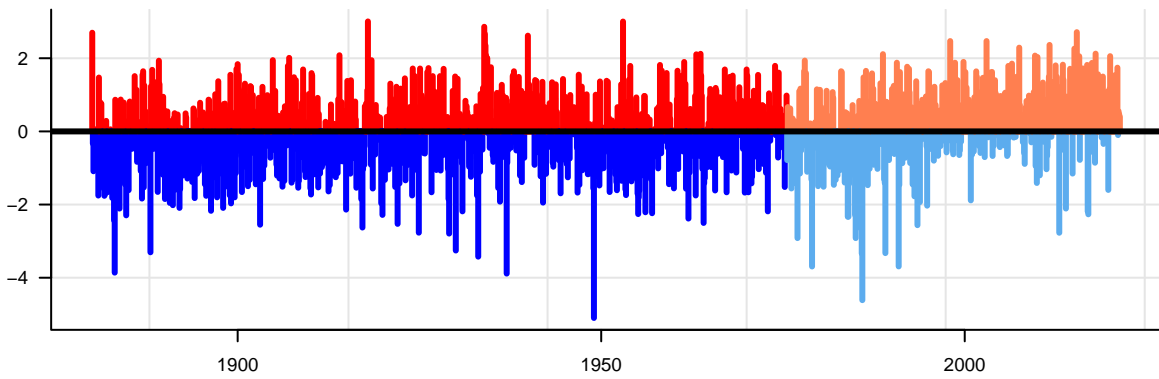
Self−similarity test
Estimated H by regression = 0.68
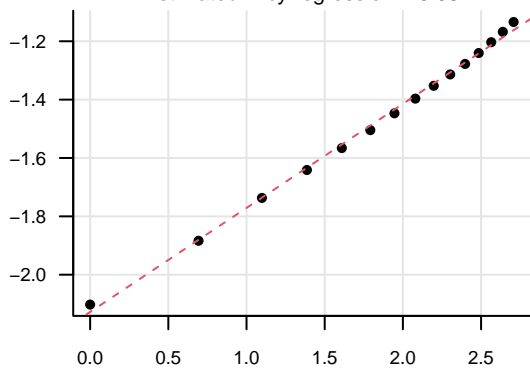
Normality test
Estimated alpha = 1.97
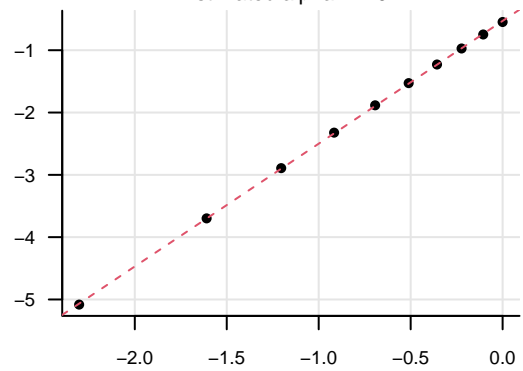
Bombay

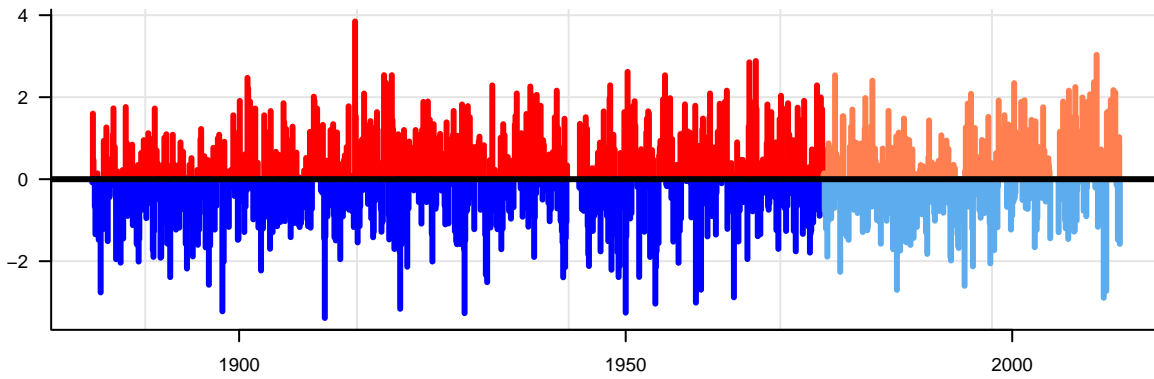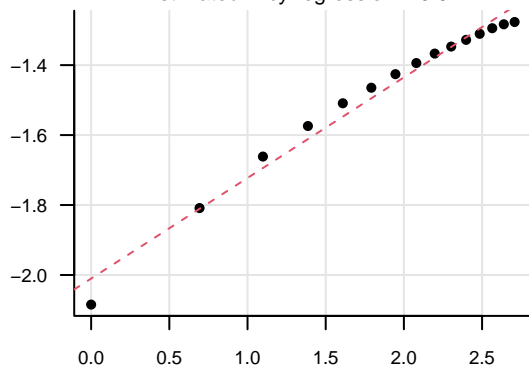## Autocorrelation

Deviation from the mean

Self−similarity test
Estimated H by regression = 0.81

Normality test
Estimated alpha = 1.96

Boston
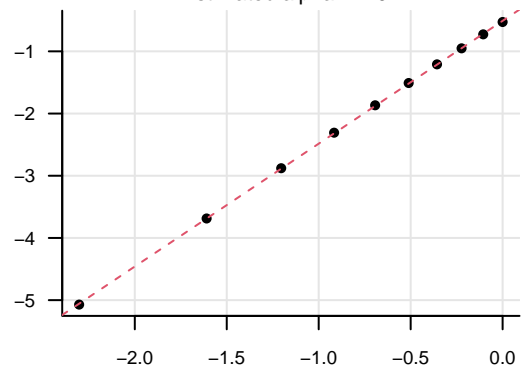
Budapest
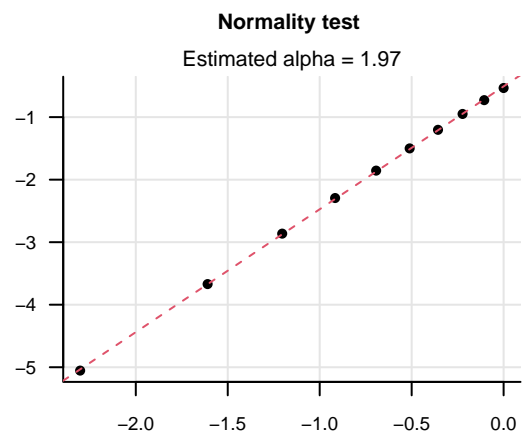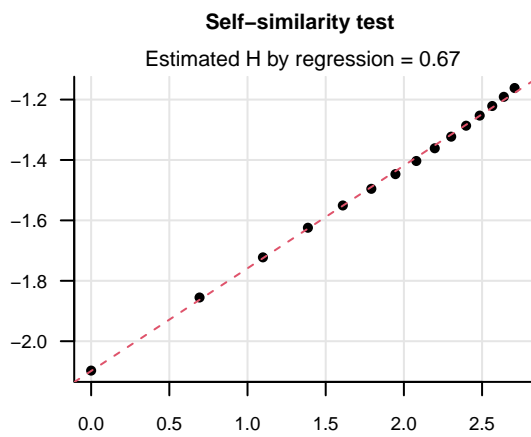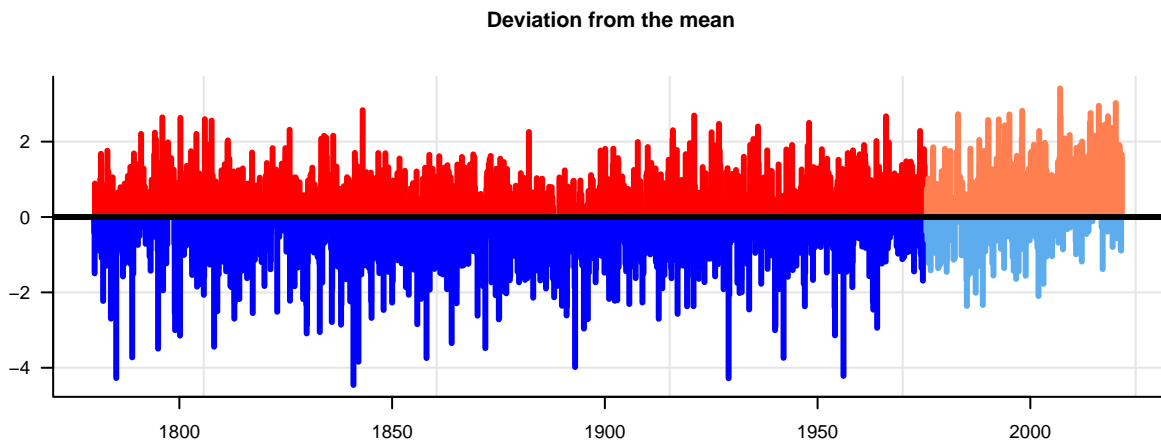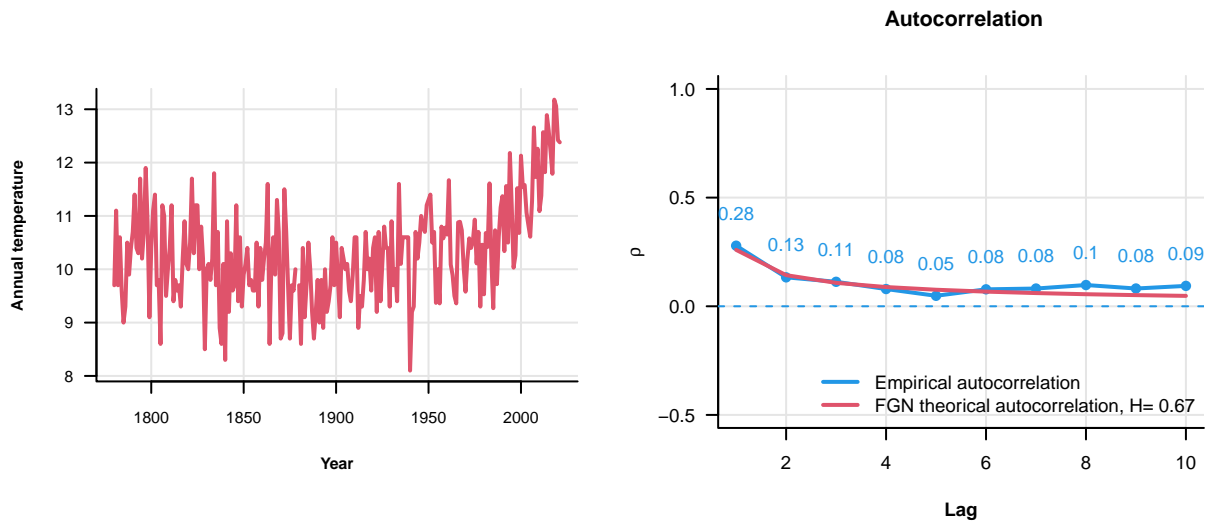
Cap Otway

Autocorrelation
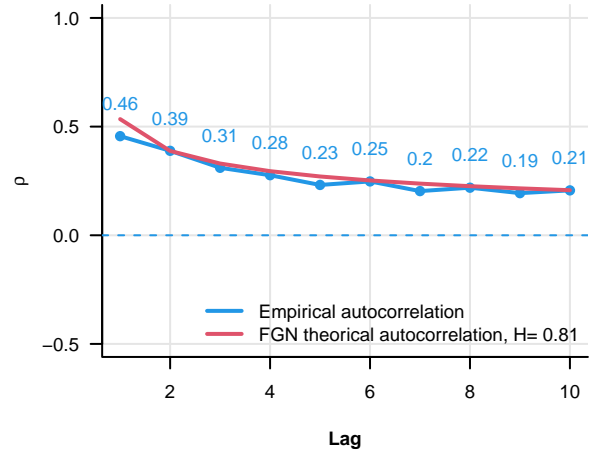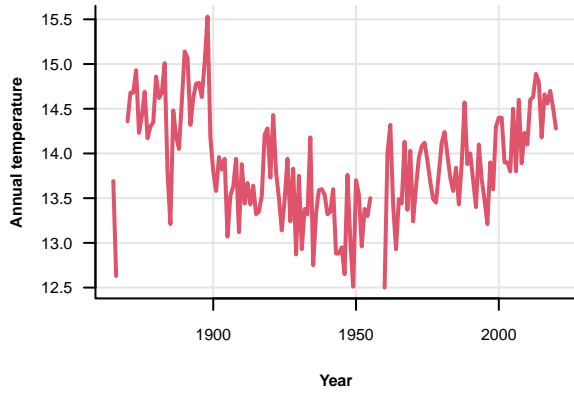
Deviation from the mean
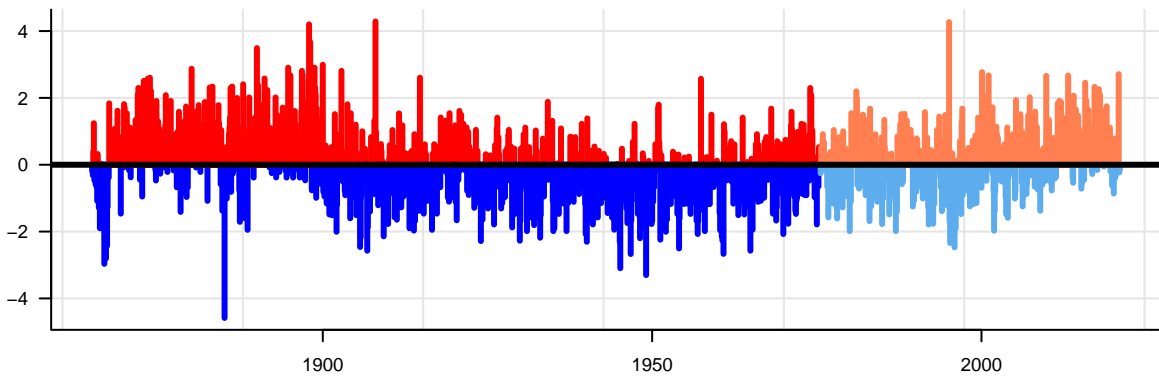
Self−similarity test
Estimated H by regression = 0.82
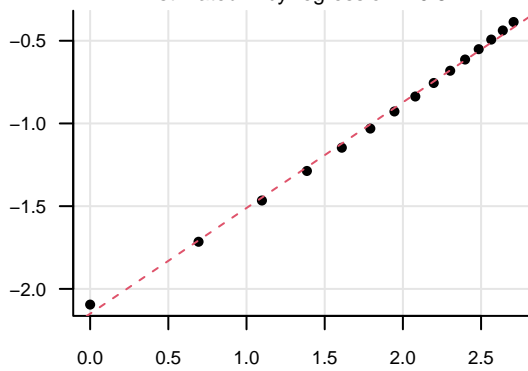
Normality test
Estimated alpha = 1.98

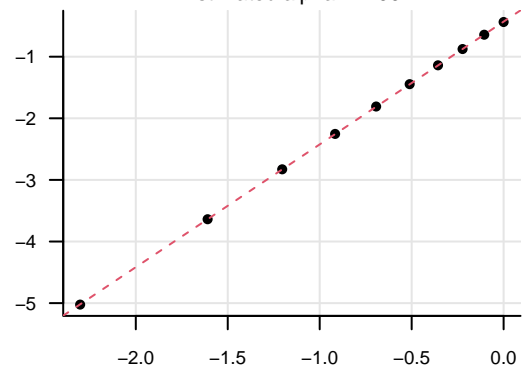# Chattanooga
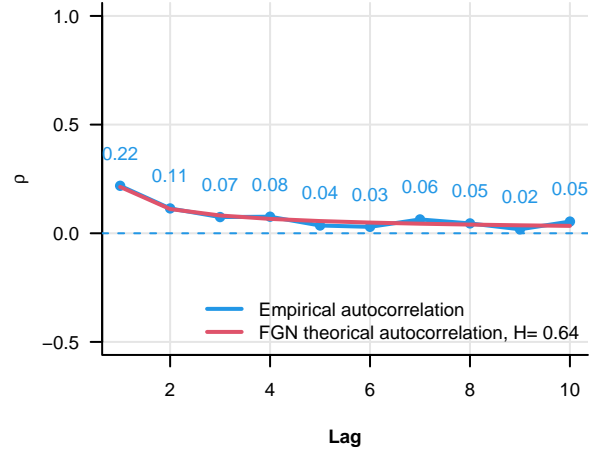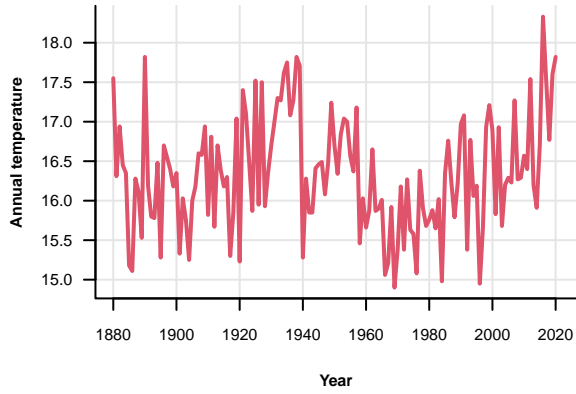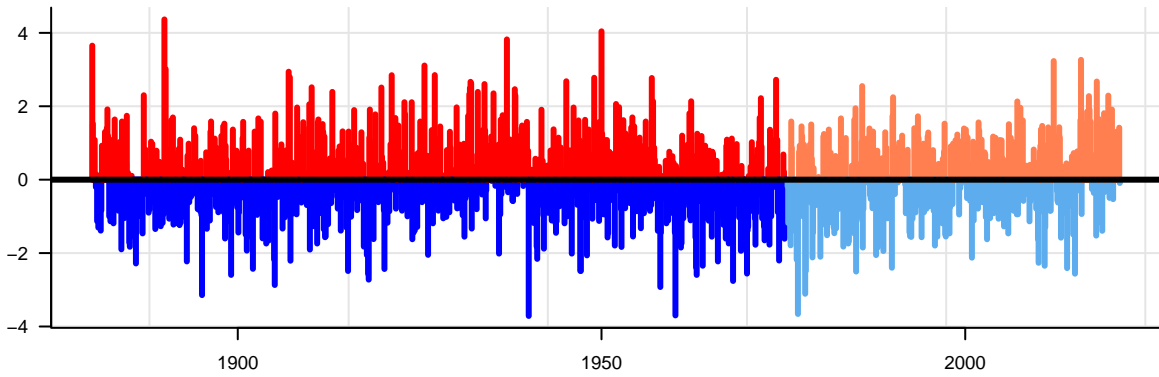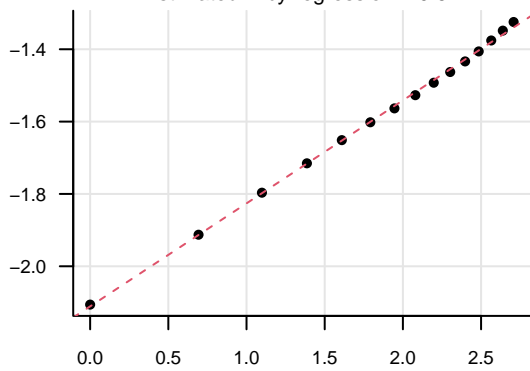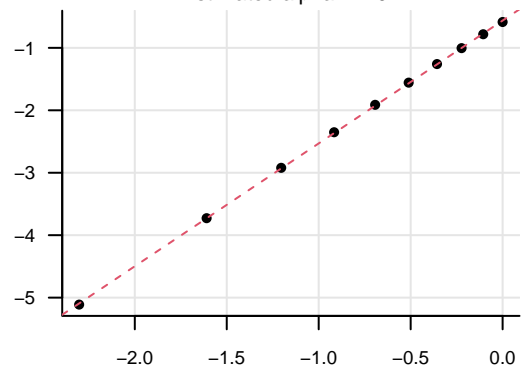
Cincinatti

Autocorrelation
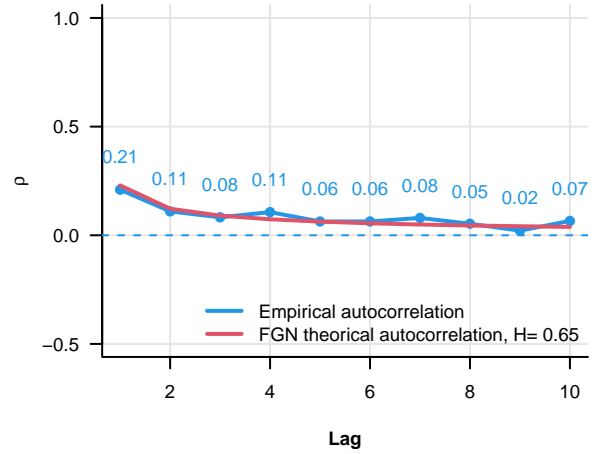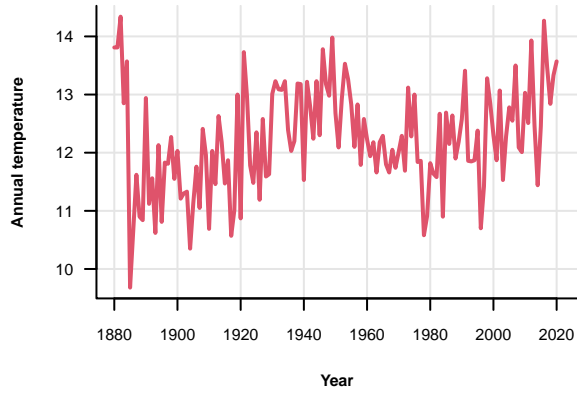
Deviation from the mean
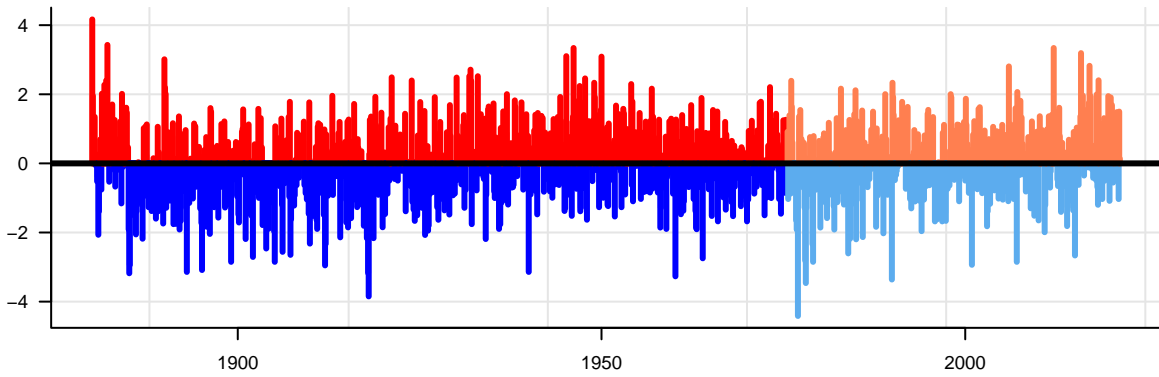
Self-similarity test
Estimated H by regression = 0.66
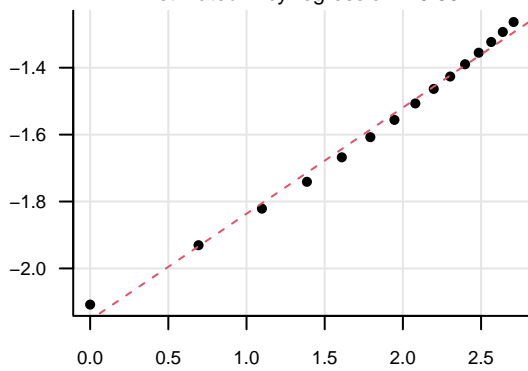
Normality test
Estimated alpha = 1.96

Columbus
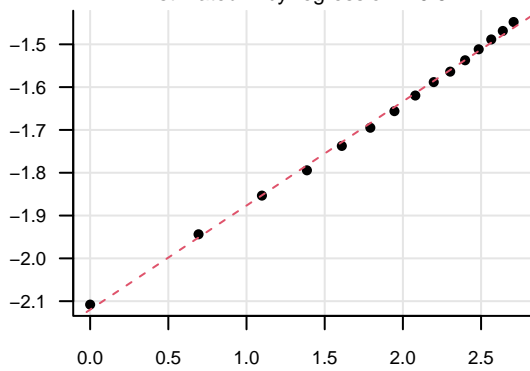
Concord

Autocorrelation
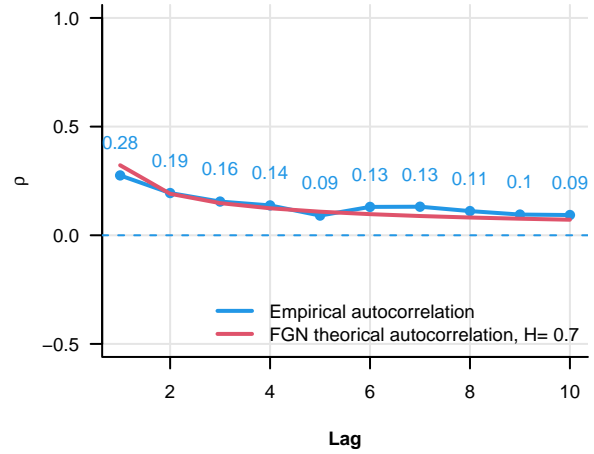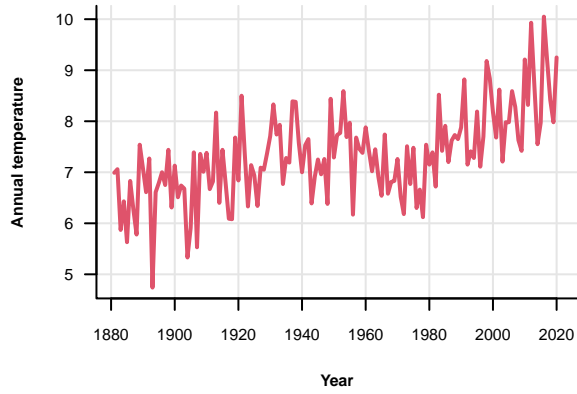
Deviation from the mean
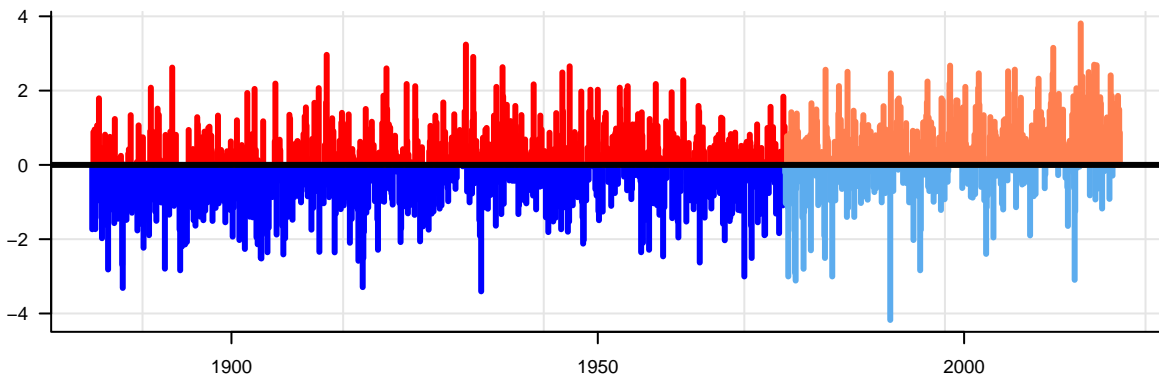
Self−similarity test
Estimated H by regression = 0.71
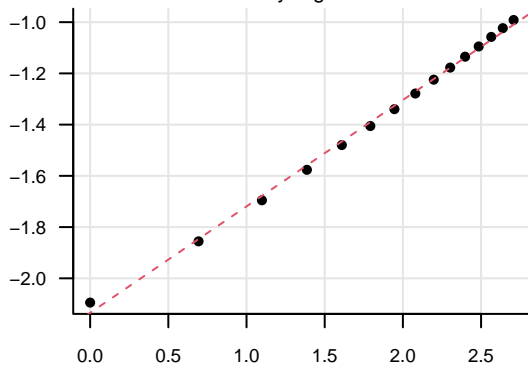
Normality test
Estimated alpha = 1.97

Copenhagen
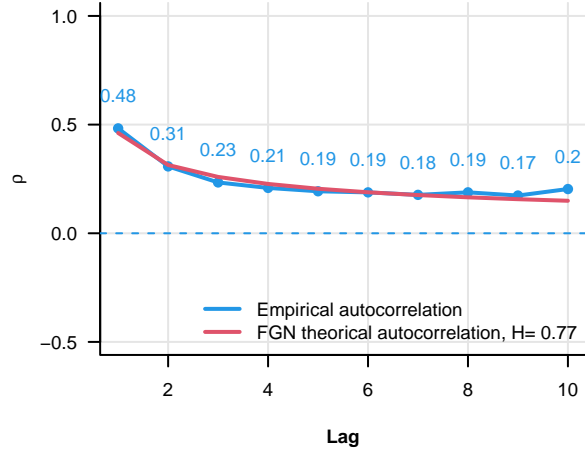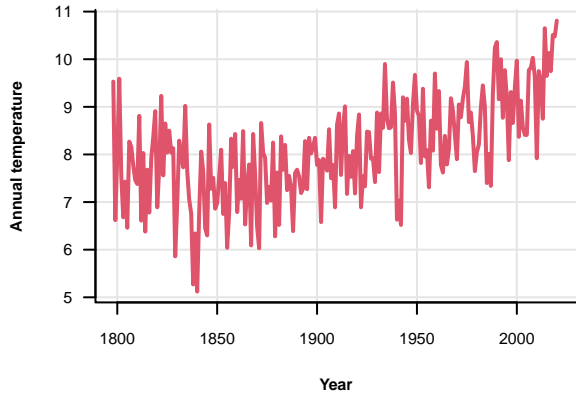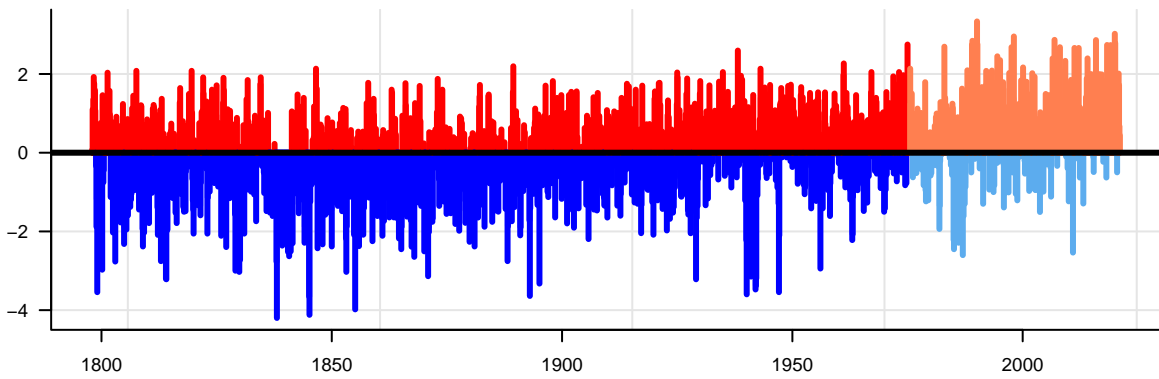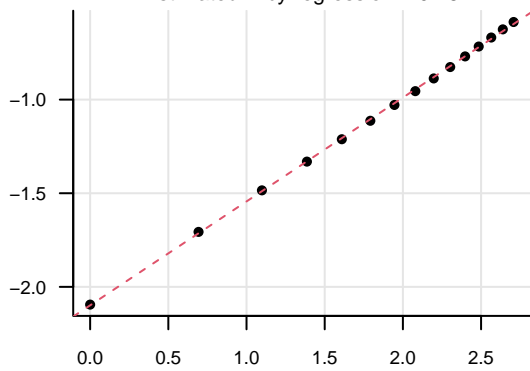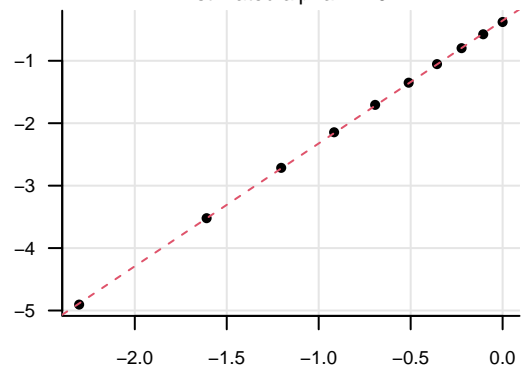
Des Moines
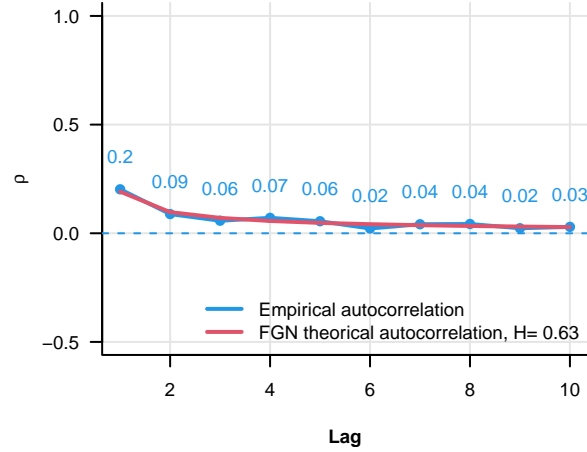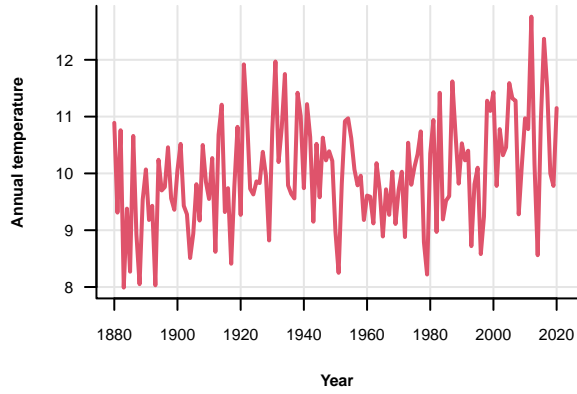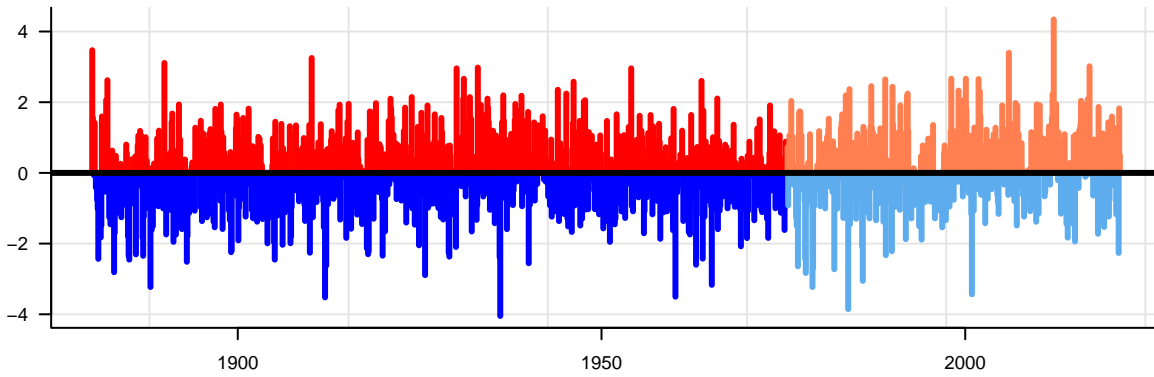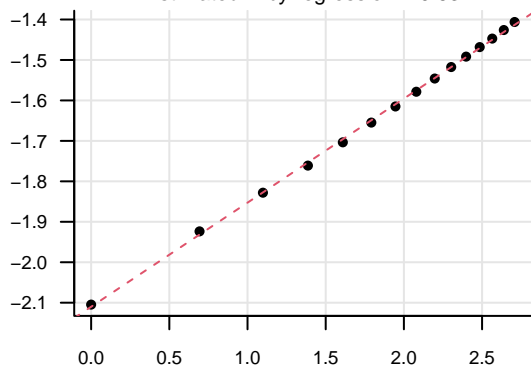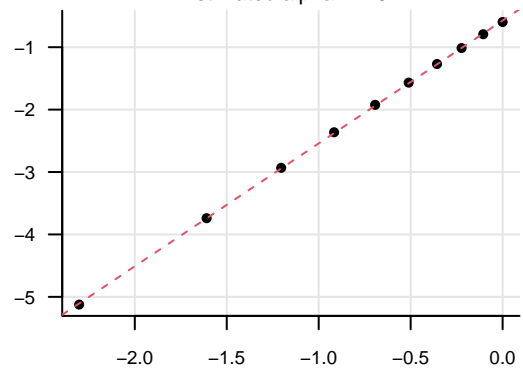
Detroit

Autocorrelation
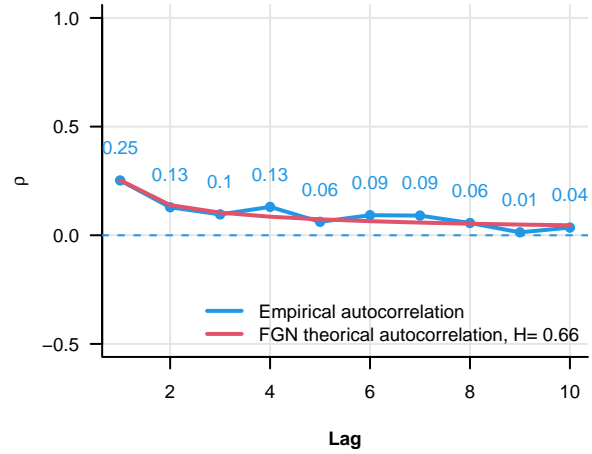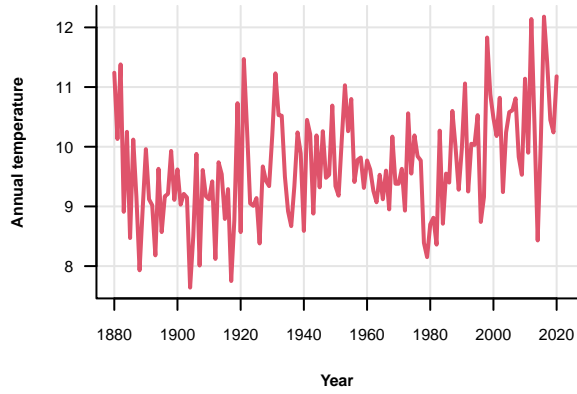
Deviation from the mean
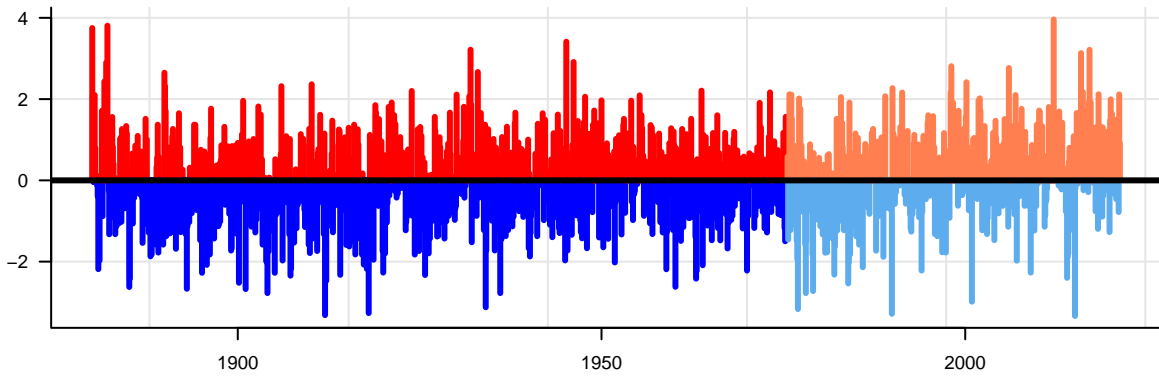
Self−similarity test
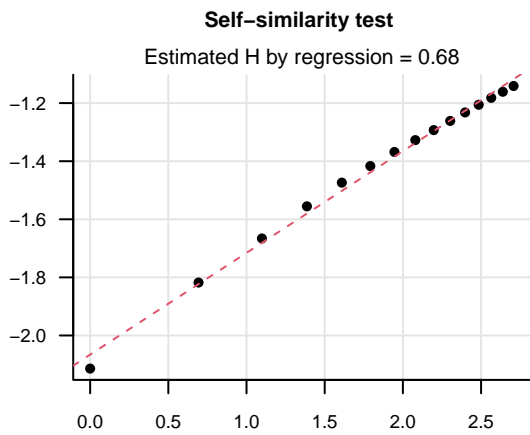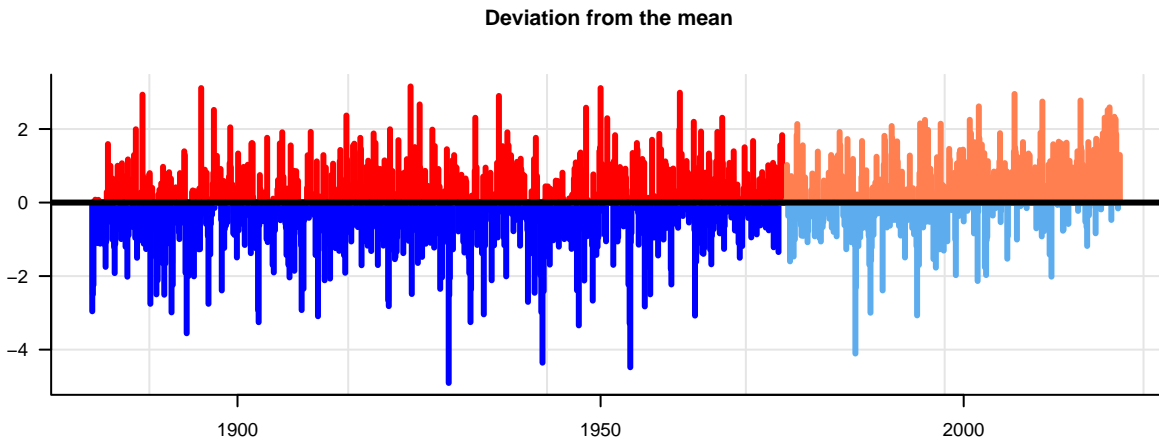Estimated H by regression = 0.67
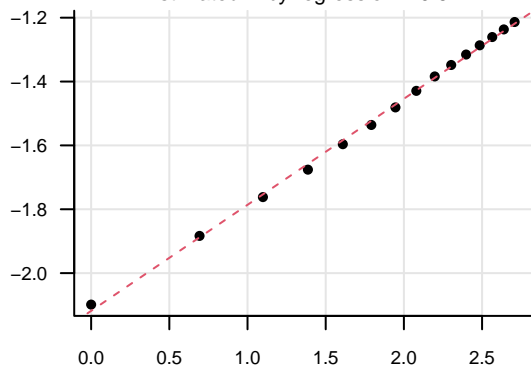
Normality test
Estimated alpha = 1.97
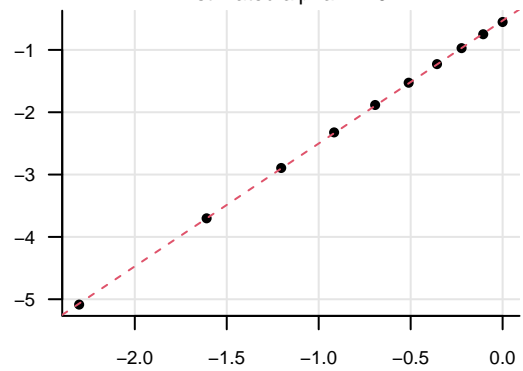
Dodge City

Autocorrelation
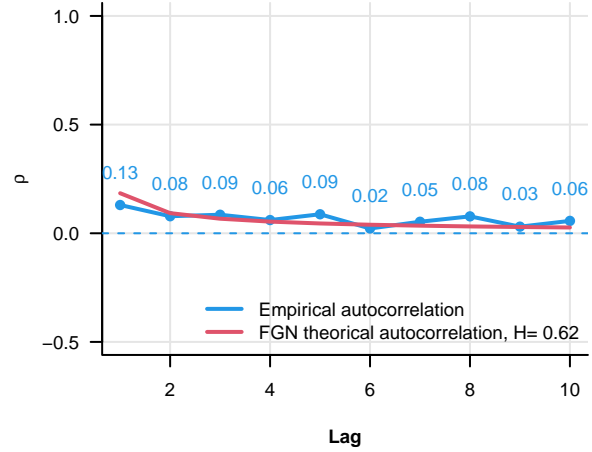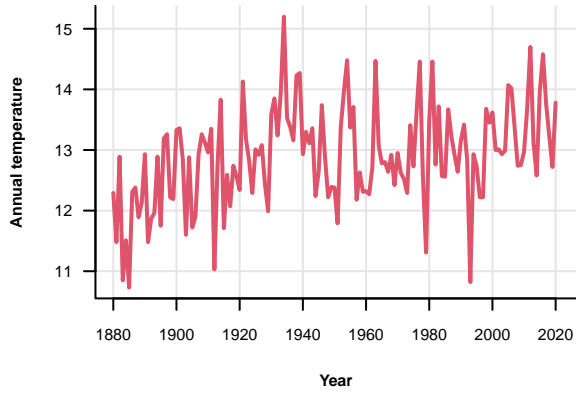
Deviation from the mean
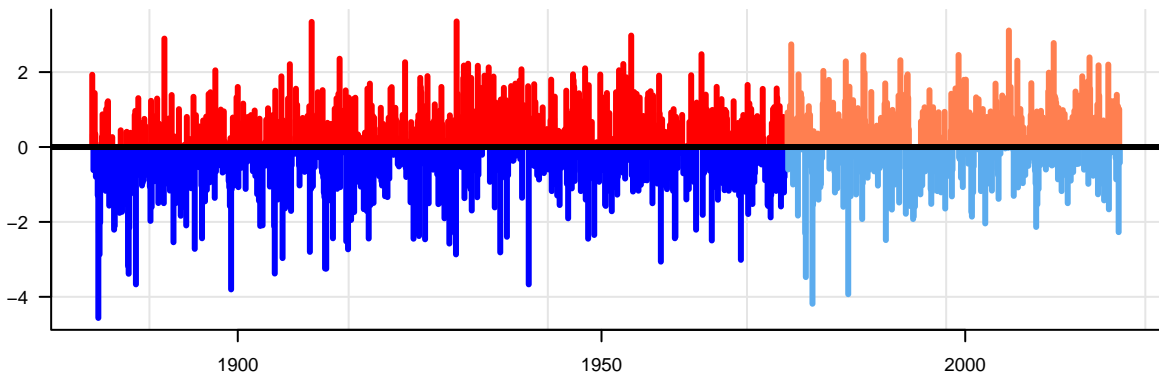
Self−similarity test
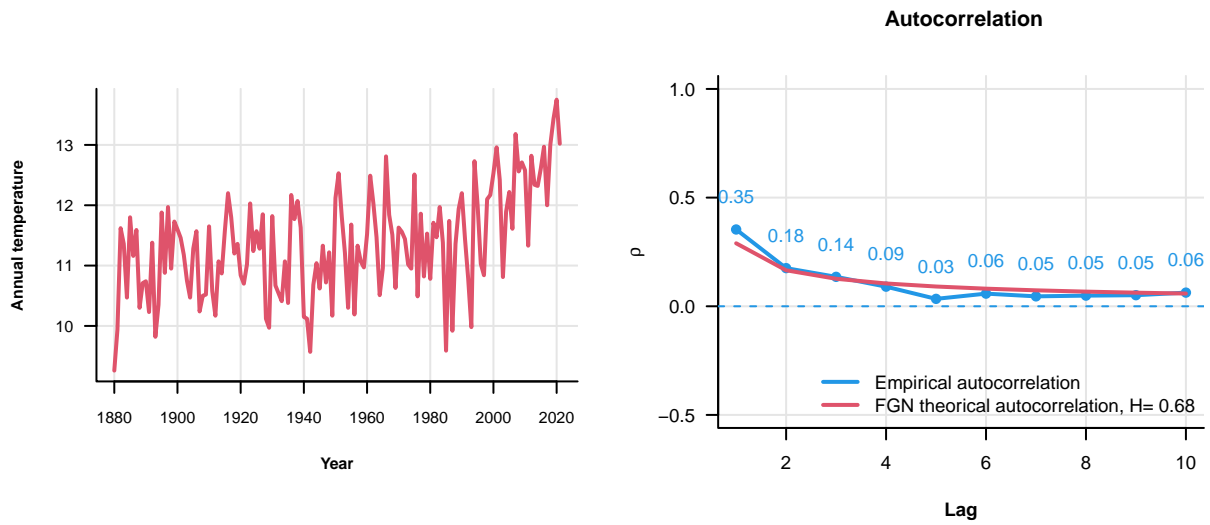Estimated H by regression = 0.63
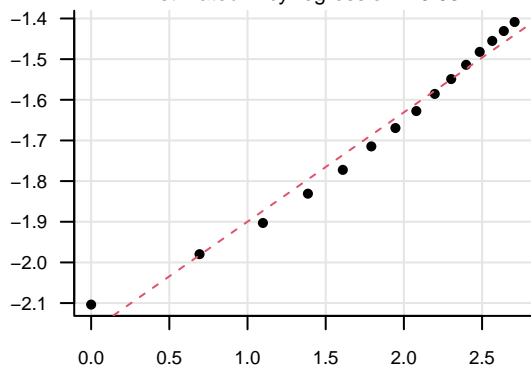
Normality test
Estimated alpha = 1.97
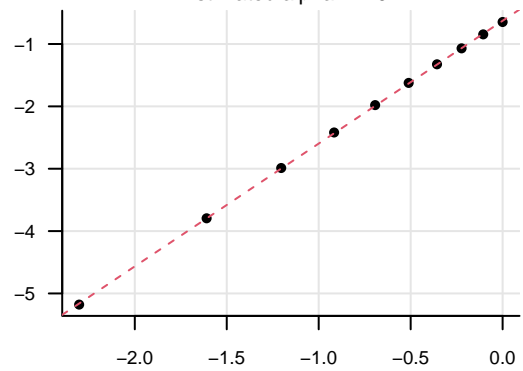
Dombas

Autocorrelation
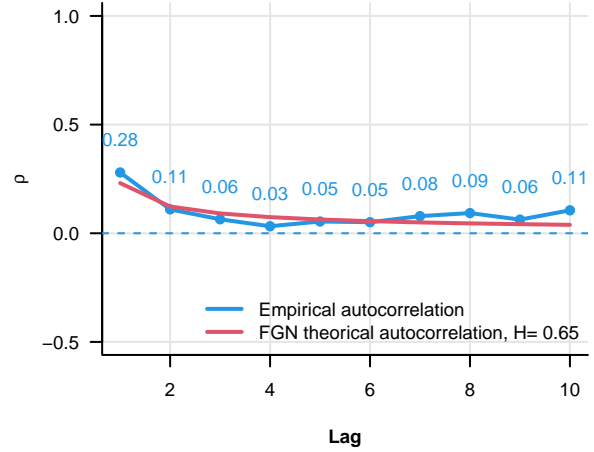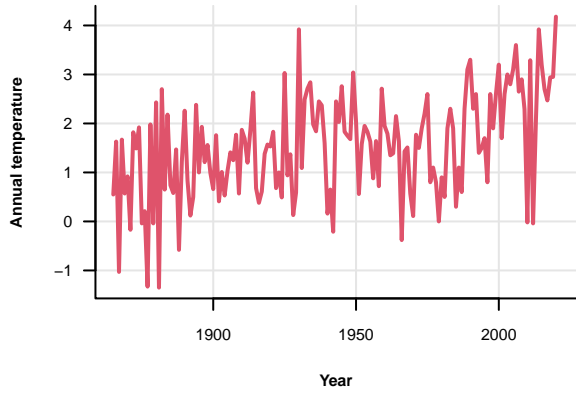
Deviation from the mean
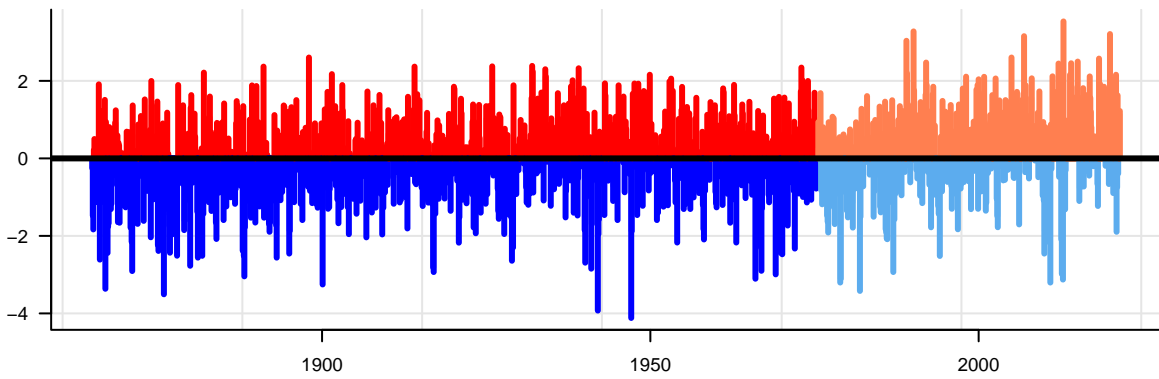
Self−similarity test
Estimated H by regression = 0.66
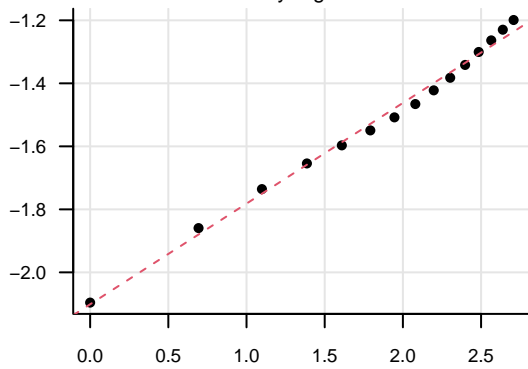
Normality test
Estimated alpha = 1.96
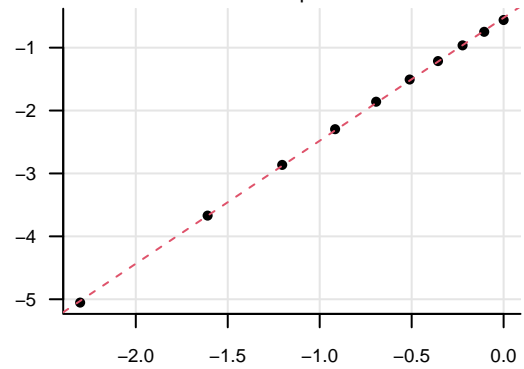
Fargo

Autocorrelation
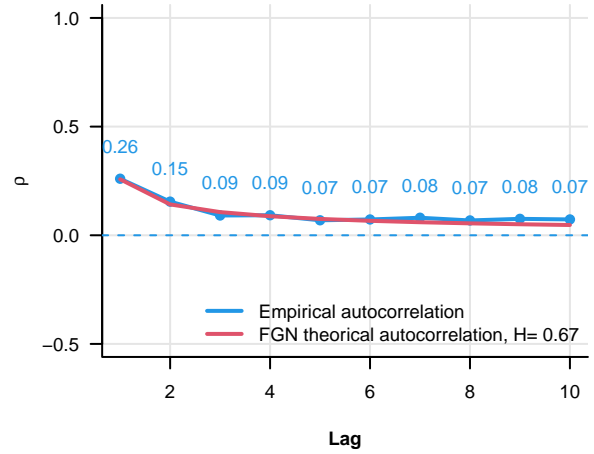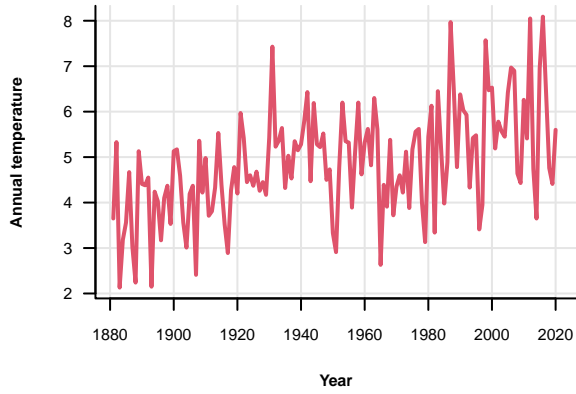
Deviation from the mean
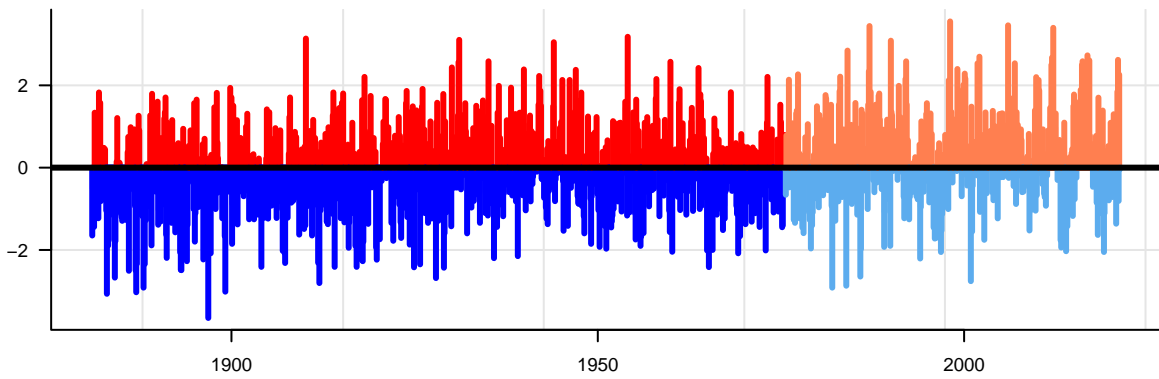
Self−similarity test
Estimated H by regression = 0.67
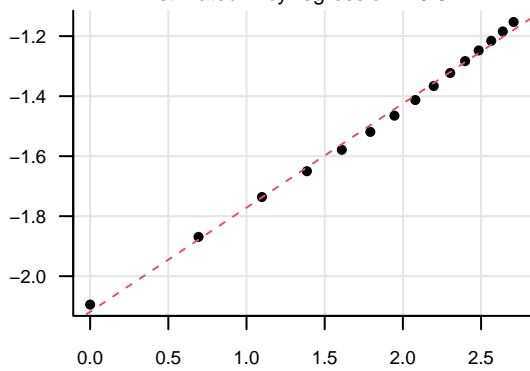
Normality test
Estimated alpha = 1.97
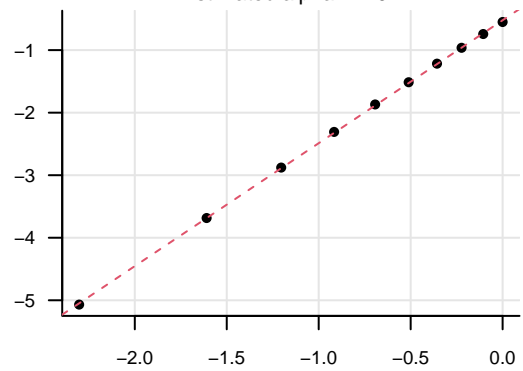
Galveston

Autocorrelation
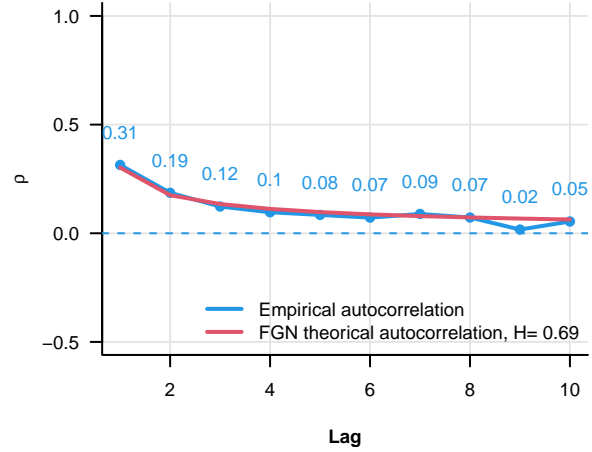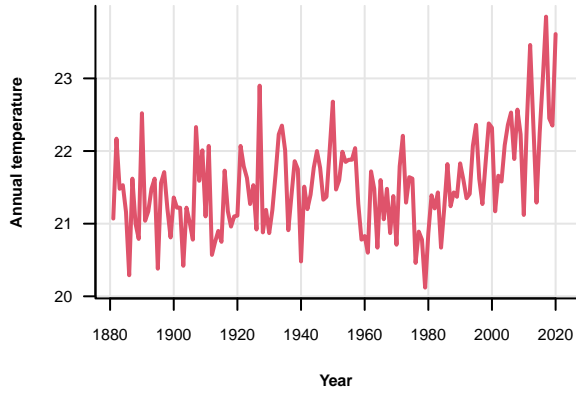
Deviation from the mean
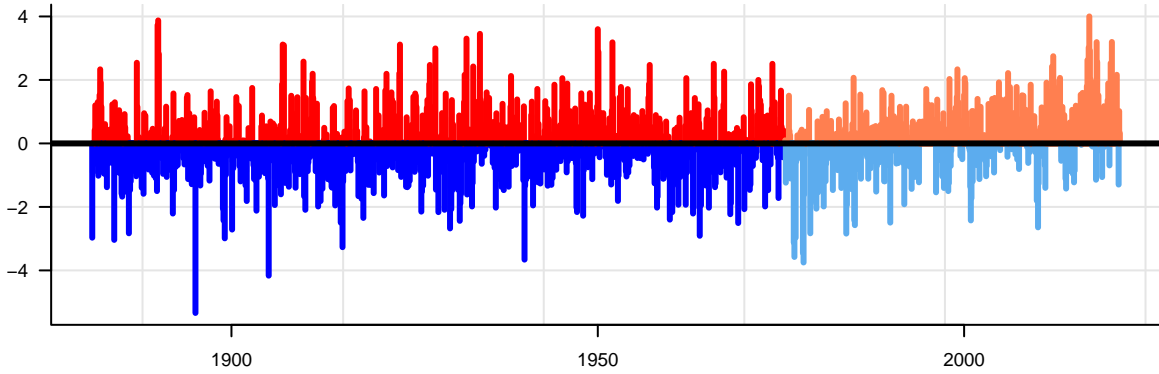
Self−similarity test
Estimated H by regression = 0.69
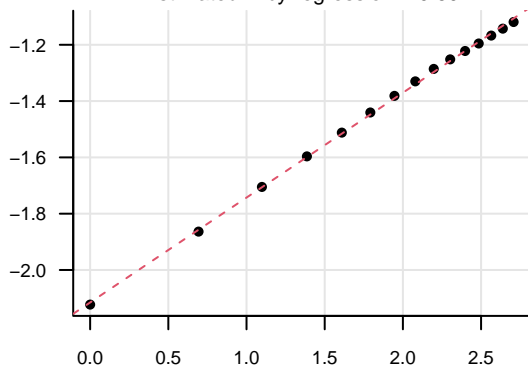
Normality test
Estimated alpha = 1.92
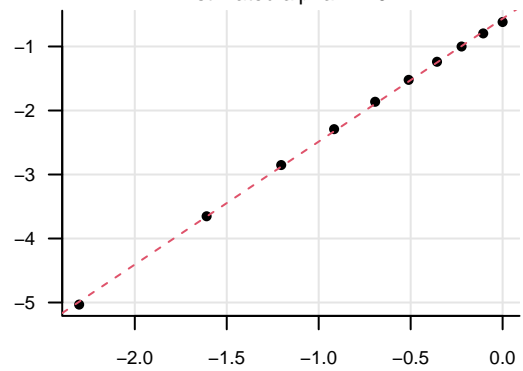
Geneva

Autocorrelation
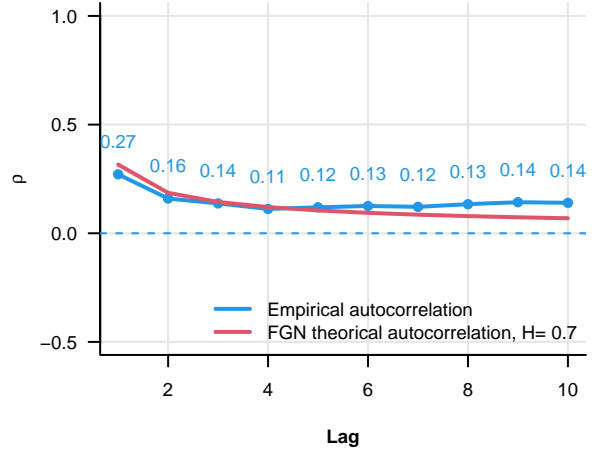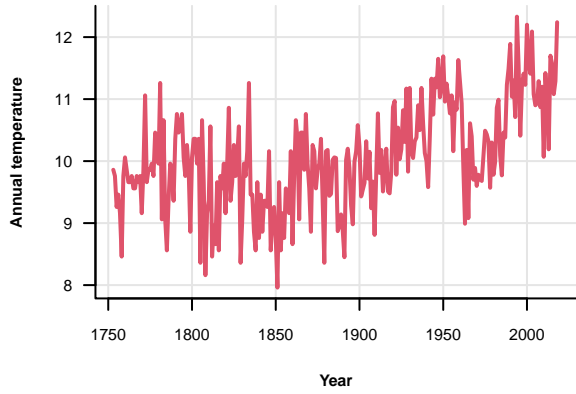
Deviation from the mean
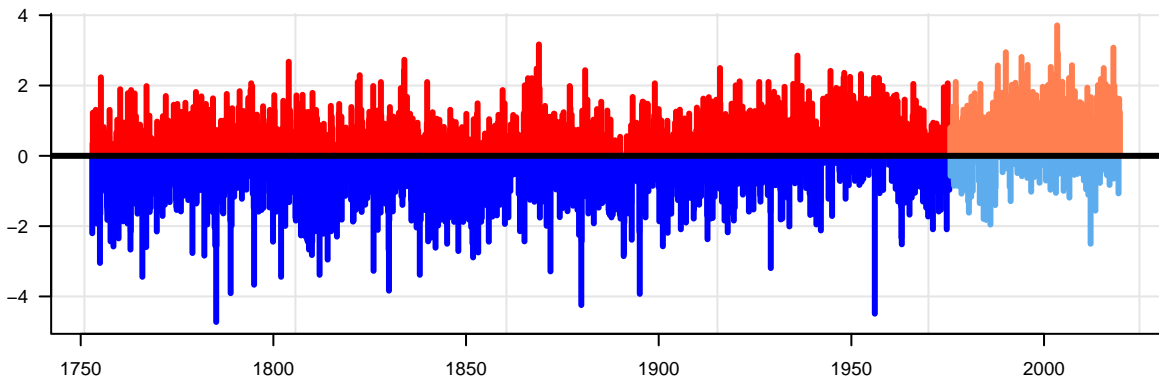
Self−similarity test
Estimated H by regression = 0.72
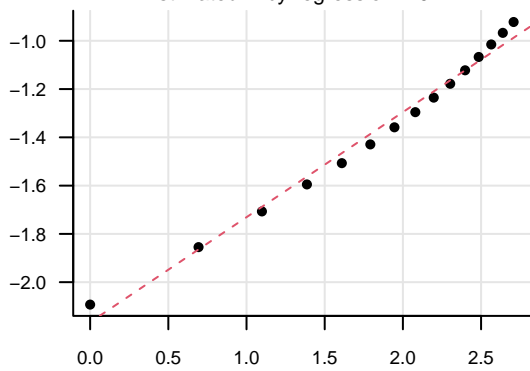
Normality test
Estimated alpha = 1.98
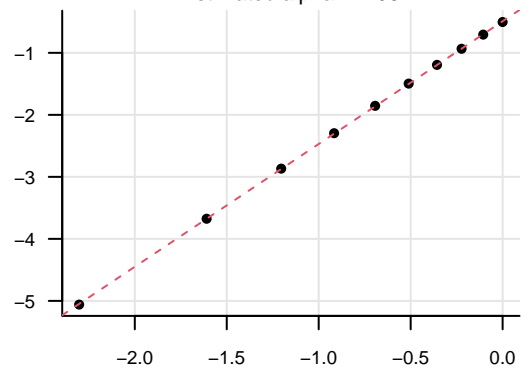
Gibraltar
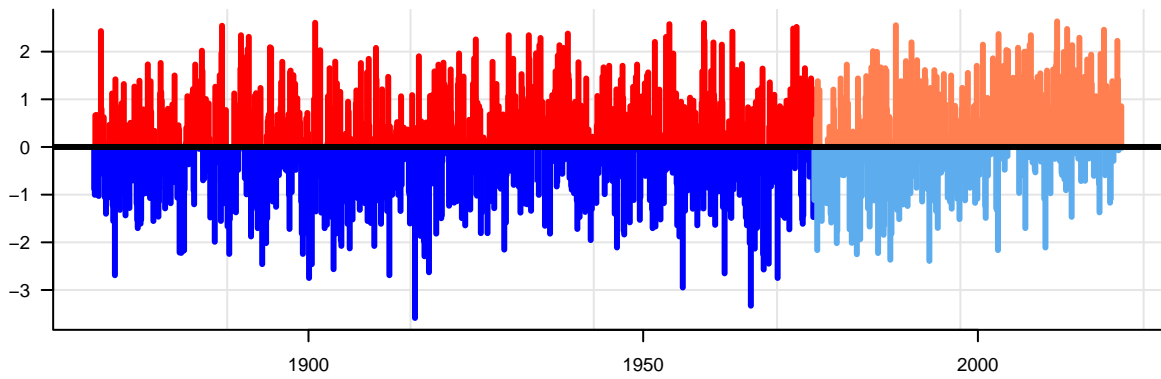
Autocorrelation
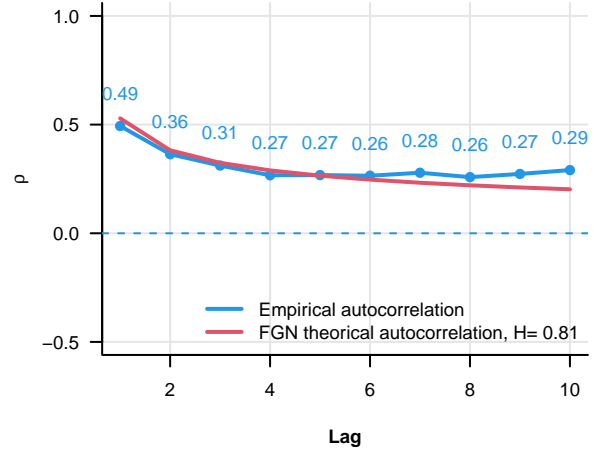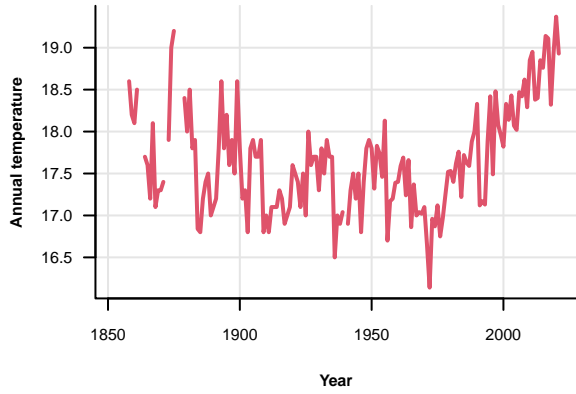
Deviation from the mean
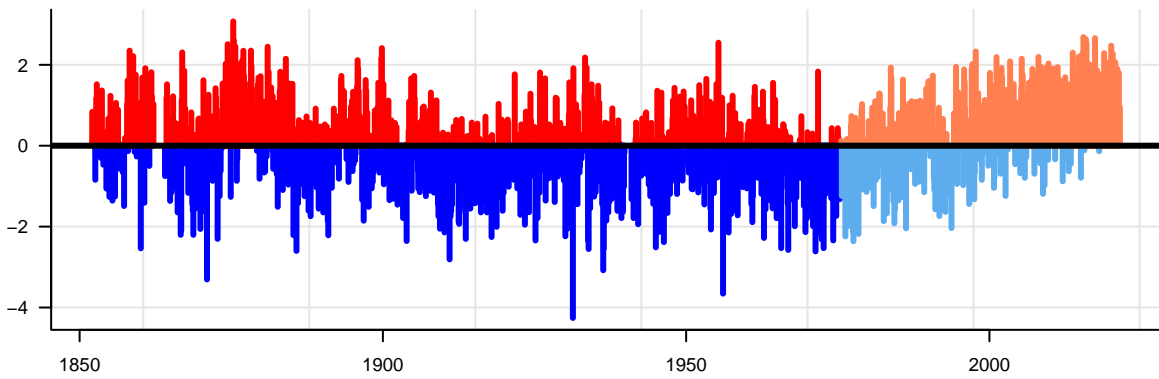
Self–similarity test
Estimated H by regression = 0.81
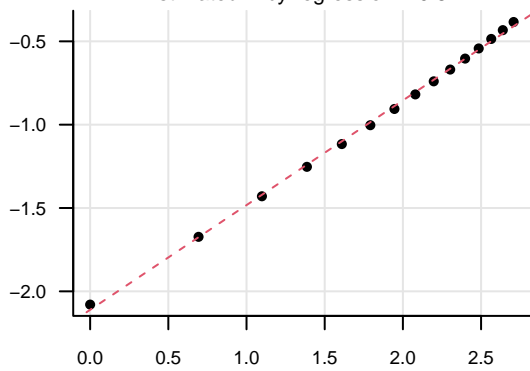
Normality test
Estimated alpha = 2.01

Hohenpeissenberg
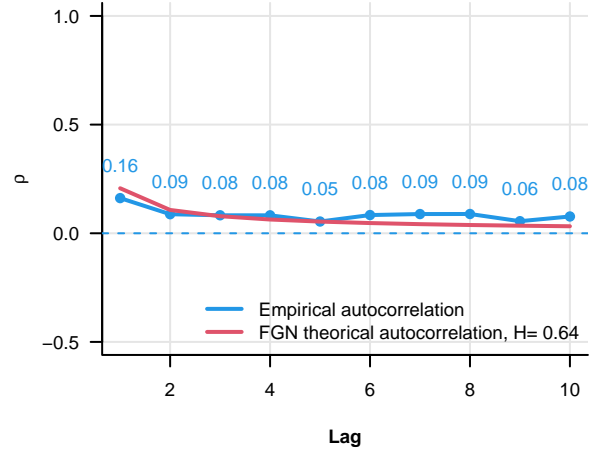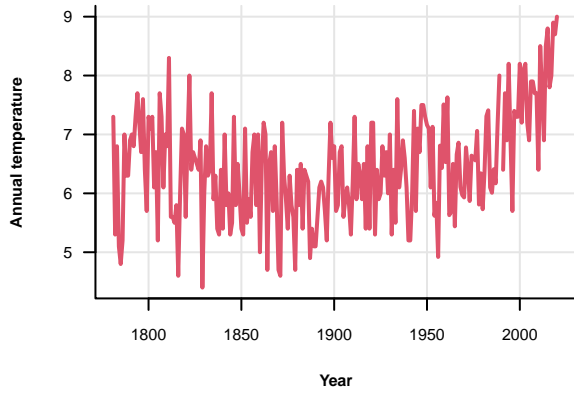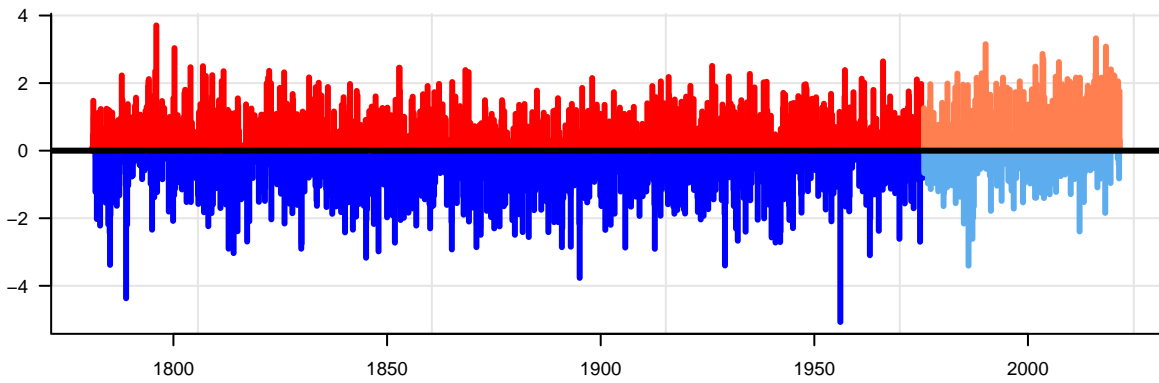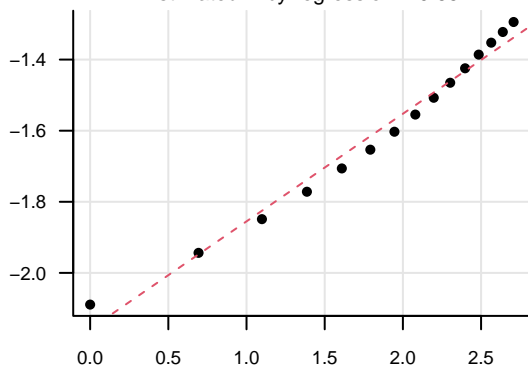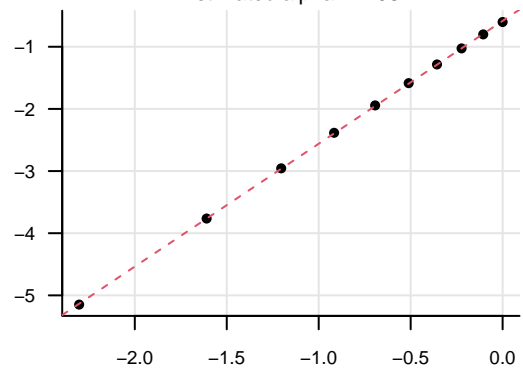
Illulisat
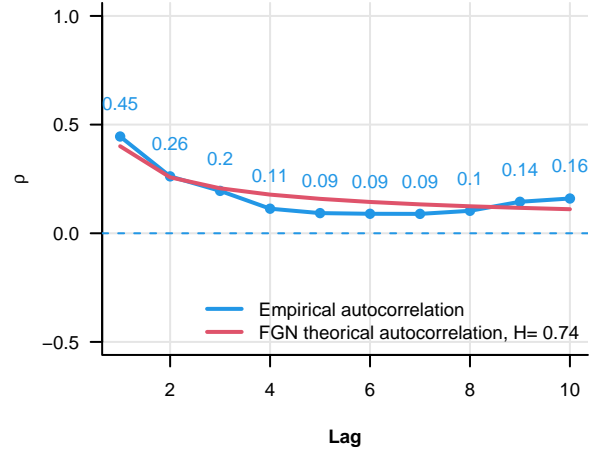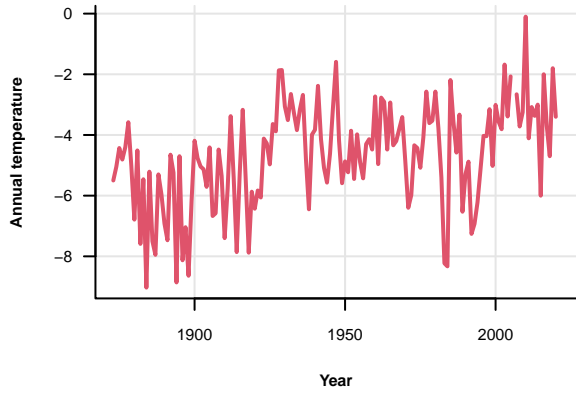
Autocorrelation

Deviation from the mean
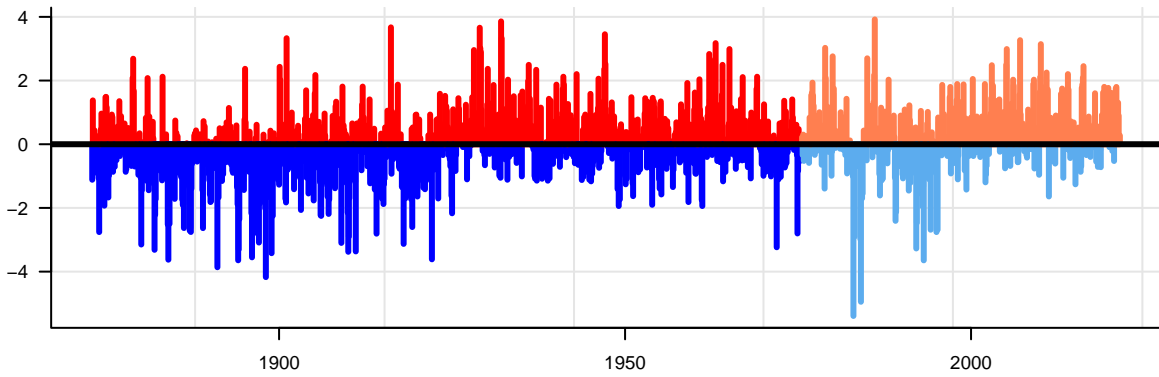
Self−similarity test
Estimated H by regression = 0.75
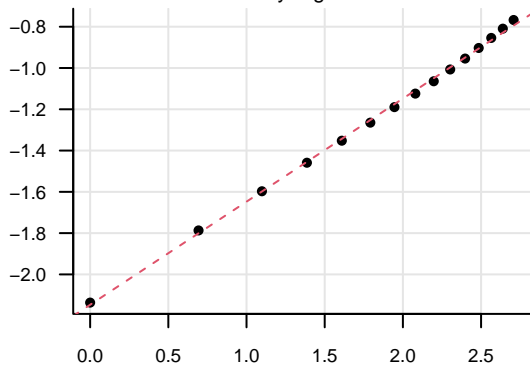
Normality test
Estimated alpha = 1.88
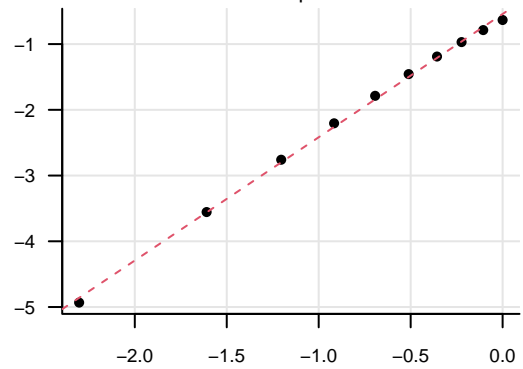
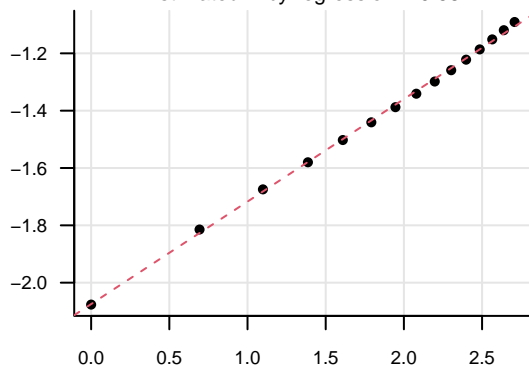# Indianapolis

Autocorrelation
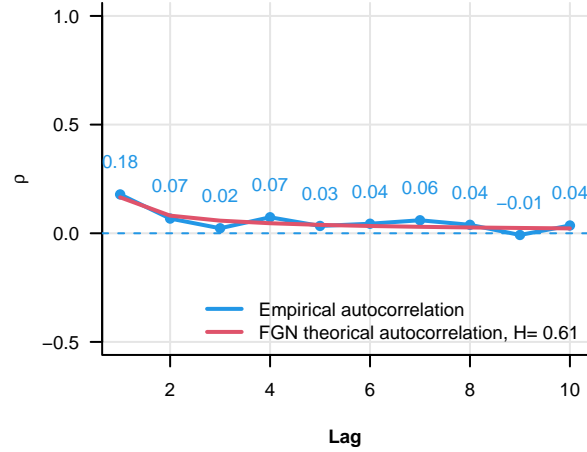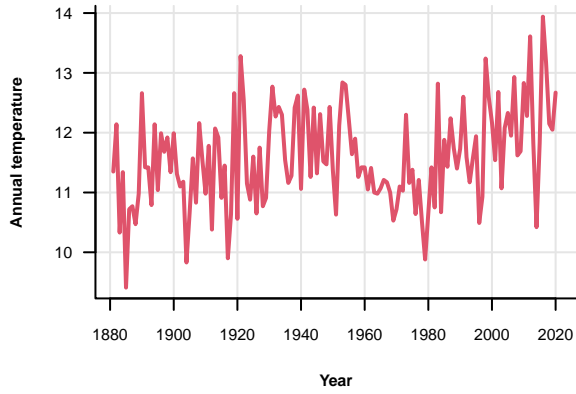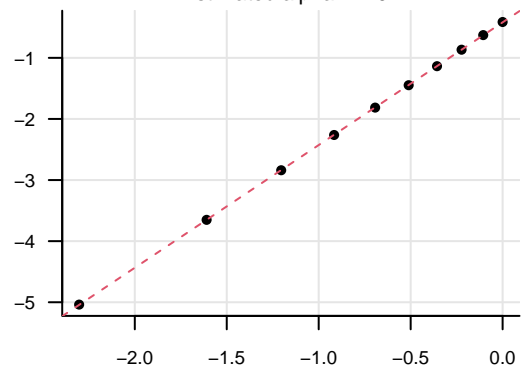
Deviation from the mean
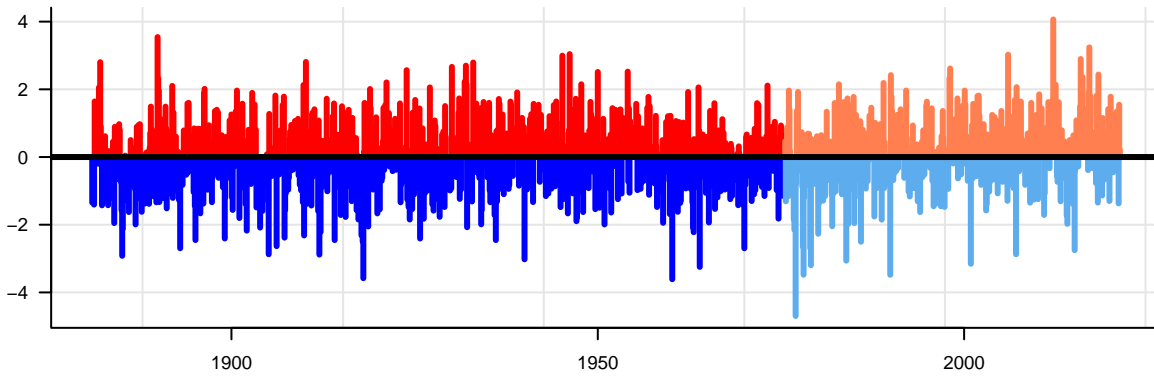
Self-similarity test
Estimated H by regression = 0.62
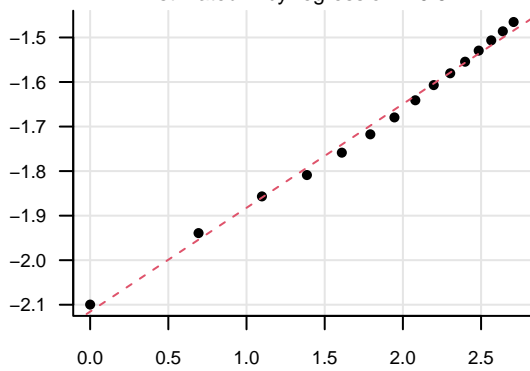
Normality test
Estimated alpha = 1.96
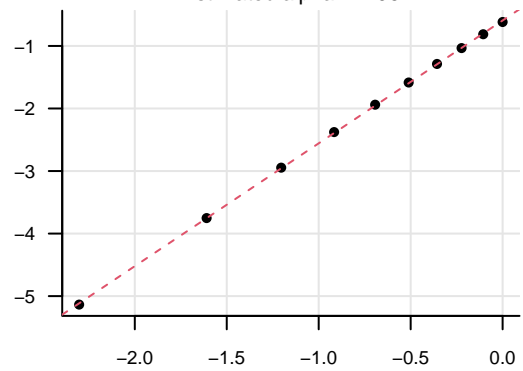
Indore
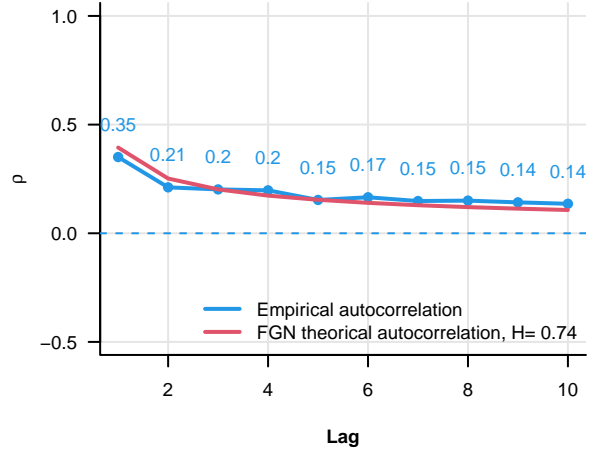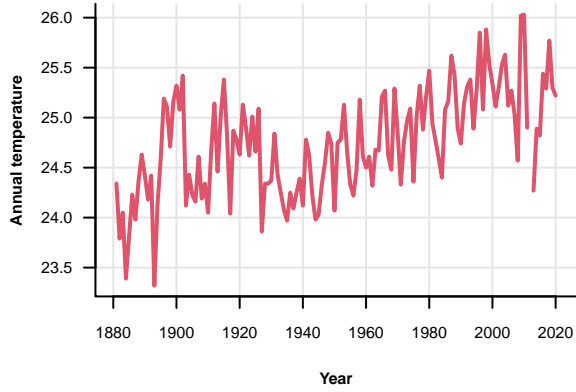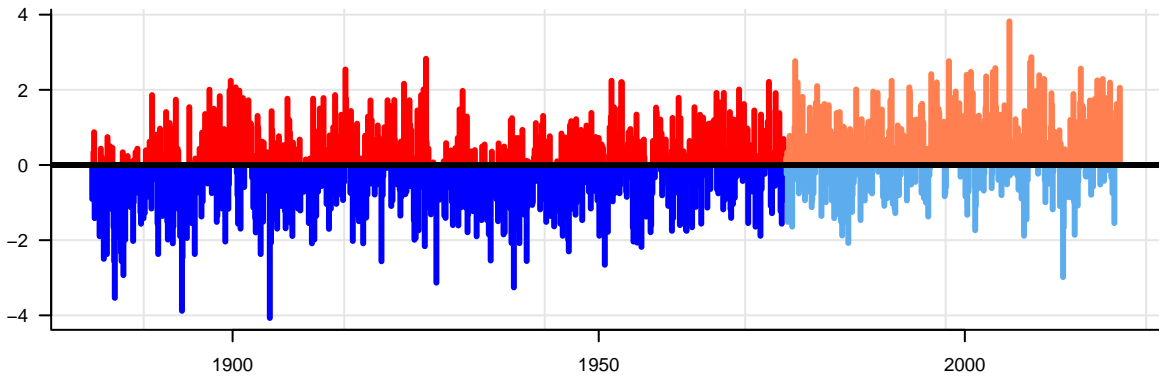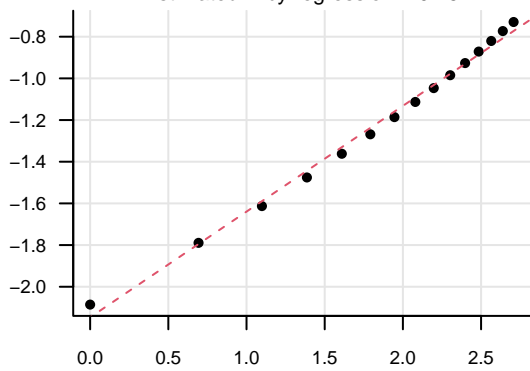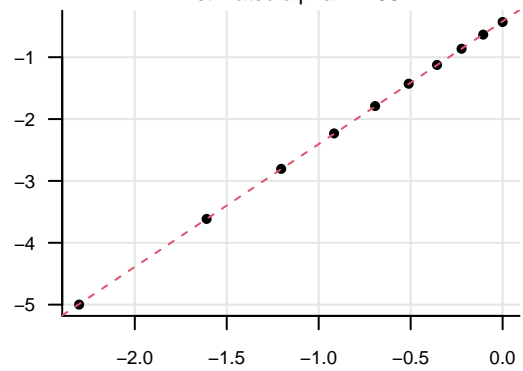
Jacksonville
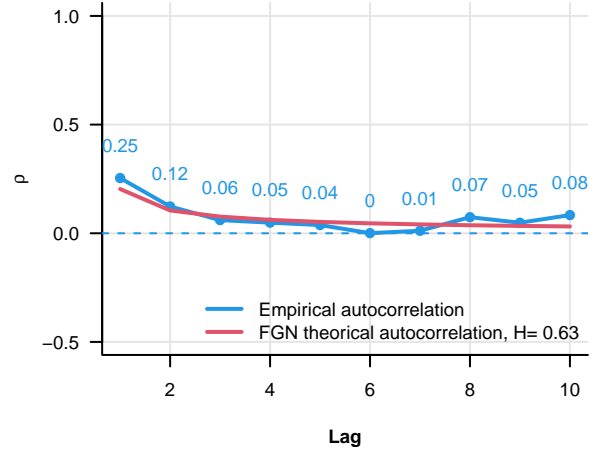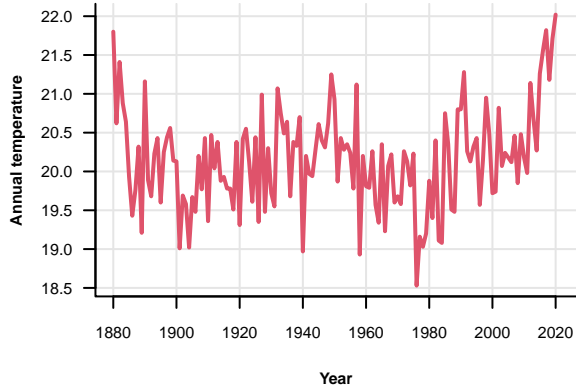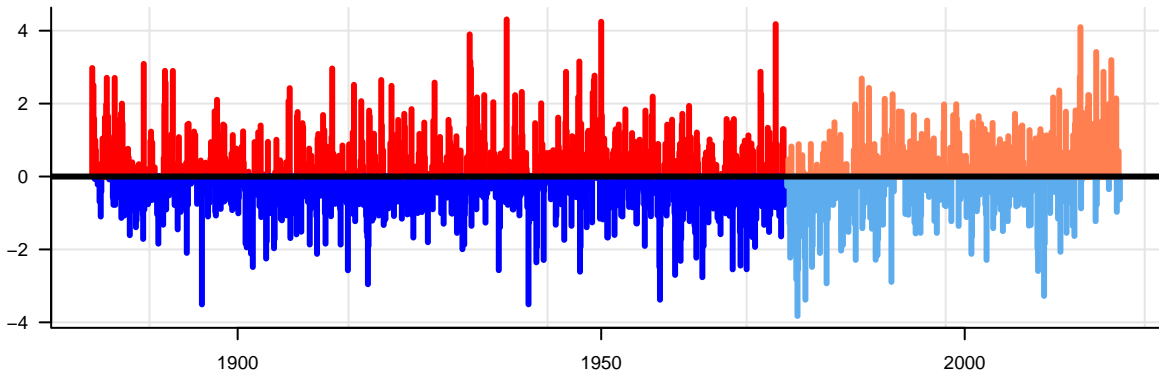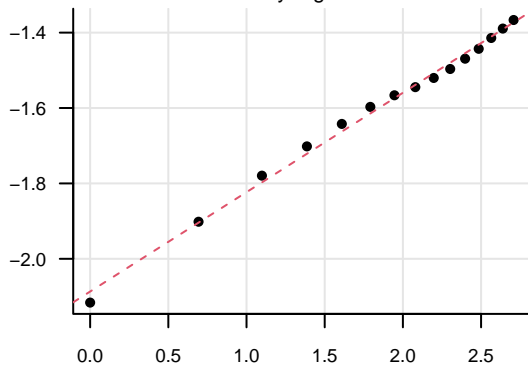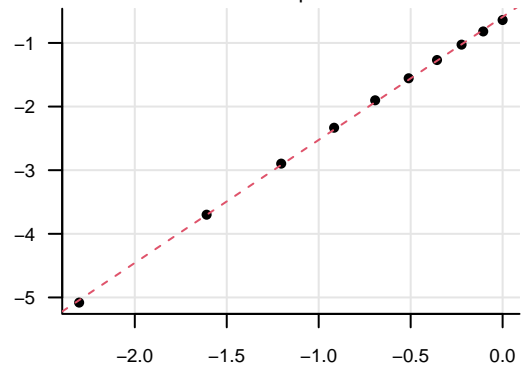
Karasjok

Autocorrelation
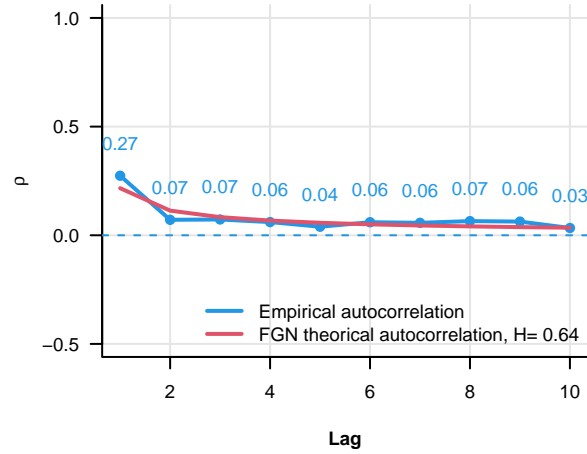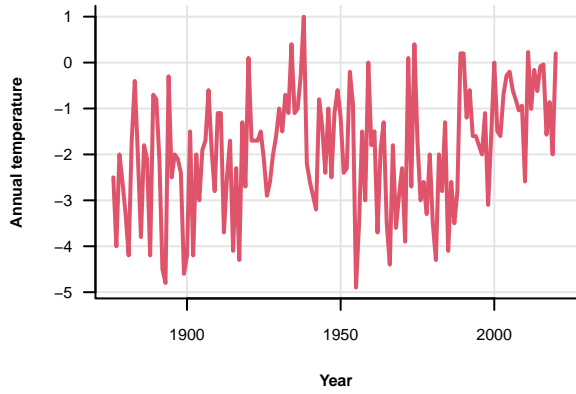
Deviation from the mean
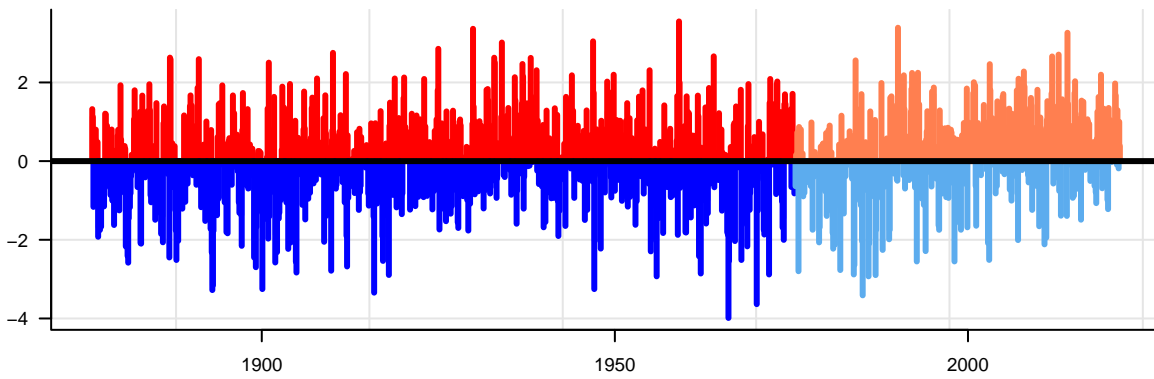
Self-similarity test
Estimated H by regression = 0.65
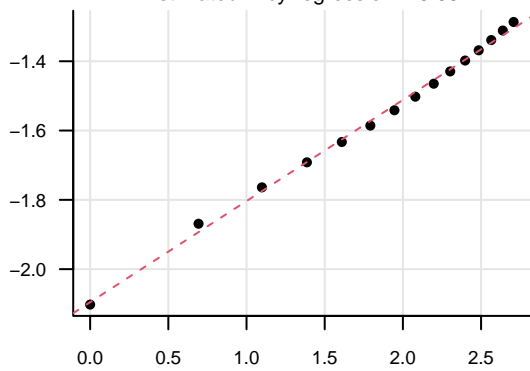
Normality test
Estimated alpha = 1.95
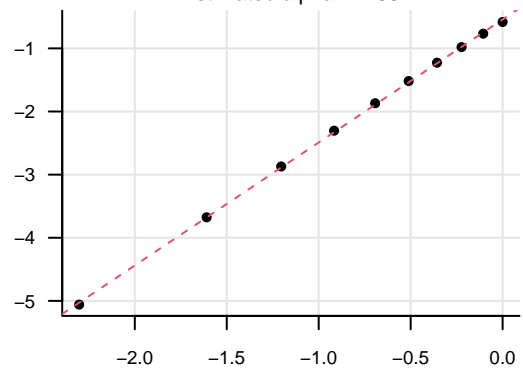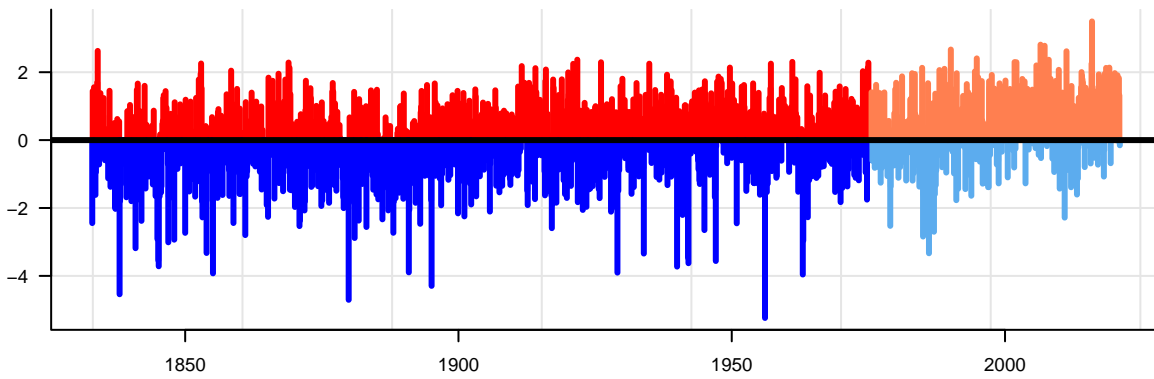
Kazalinsk

Autocorrelation
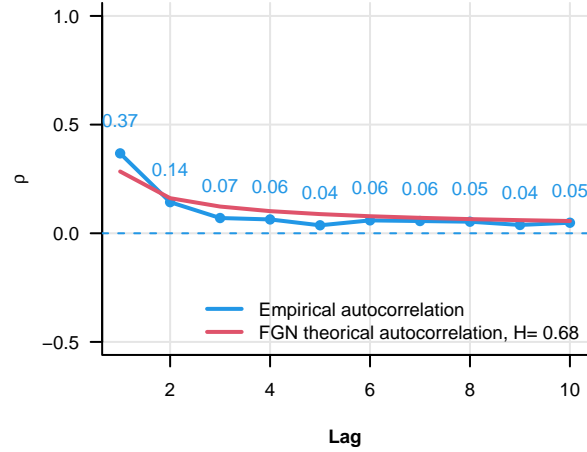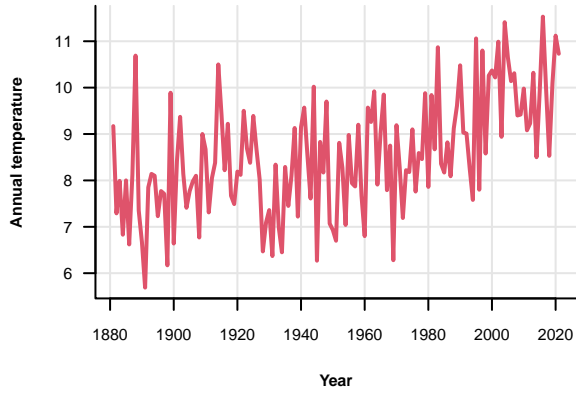
Deviation from the mean
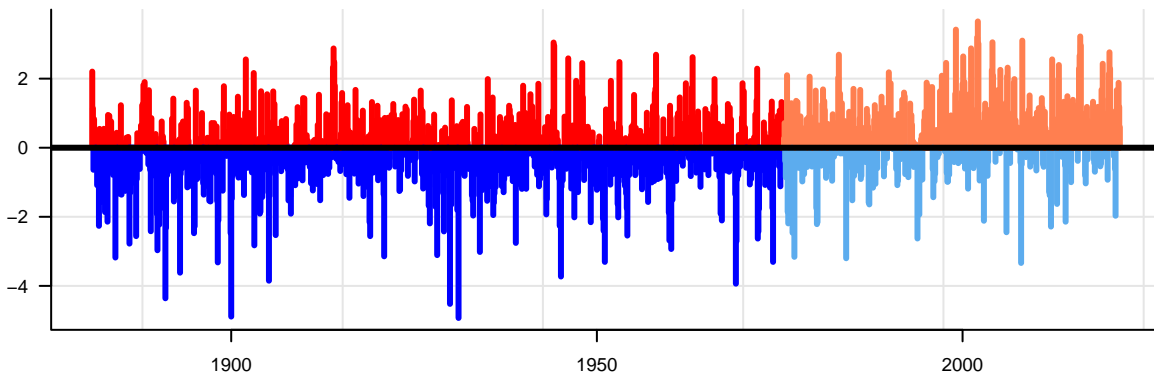
Self–similarity test
Estimated H by regression = 0.68
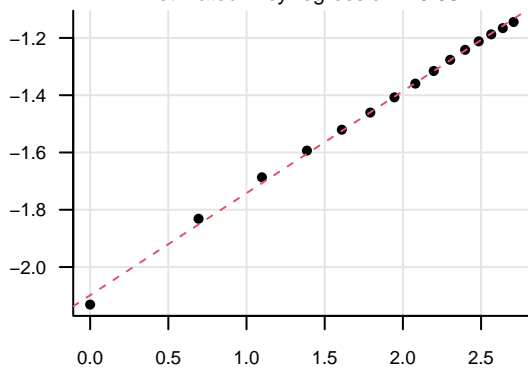
Normality test
Estimated alpha = 1.9

Knoxville
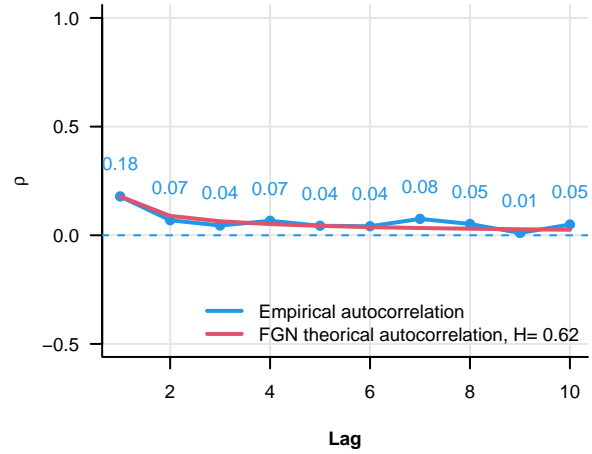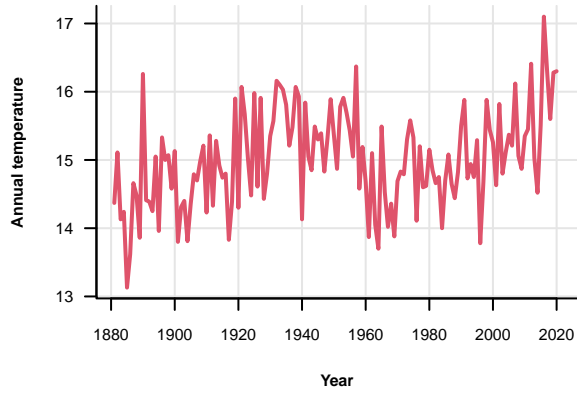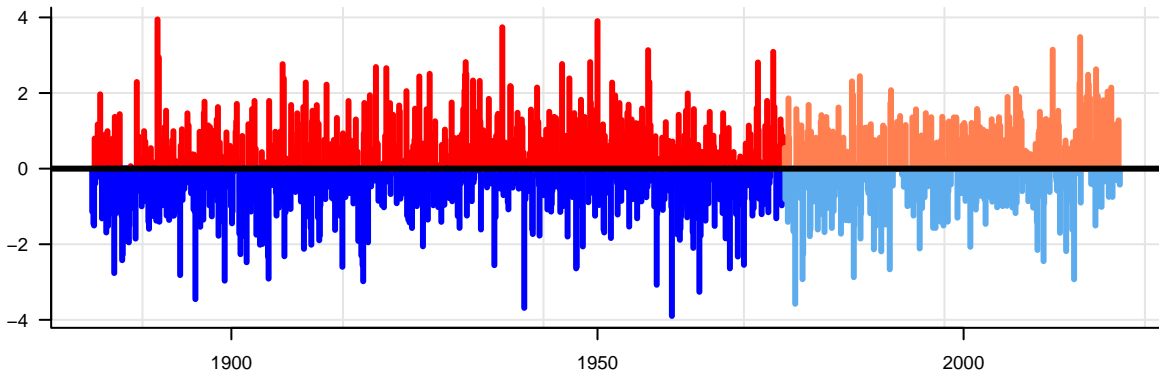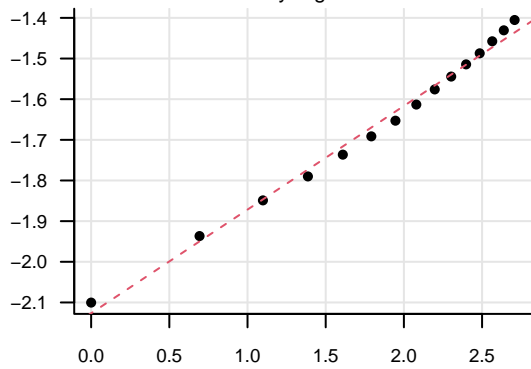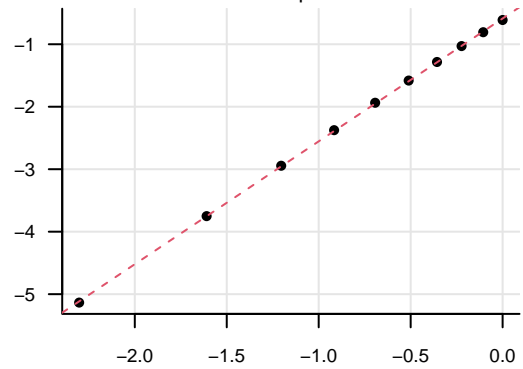
Kremsmunster

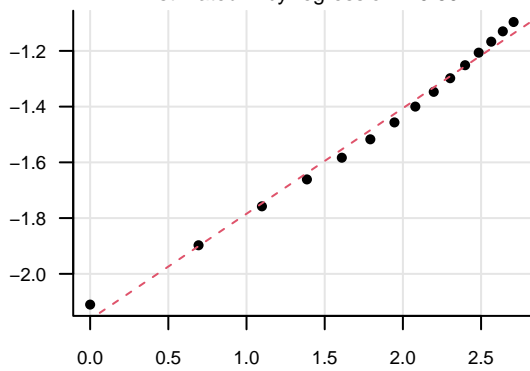### Autocorrelation
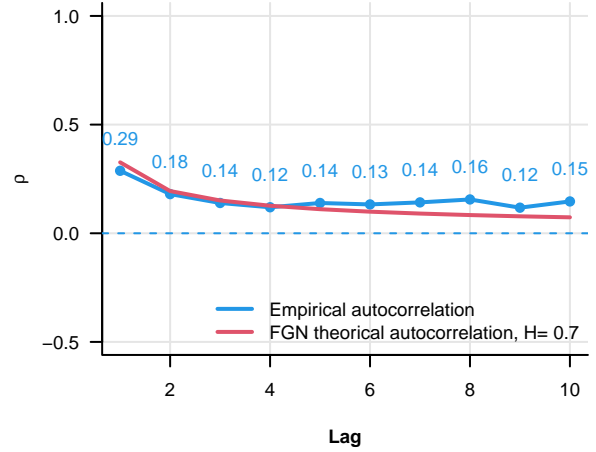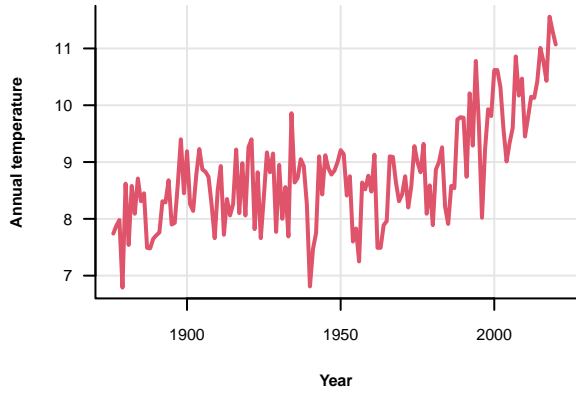
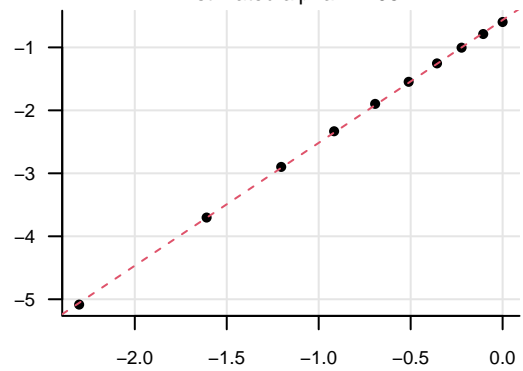### Deviation from the mean
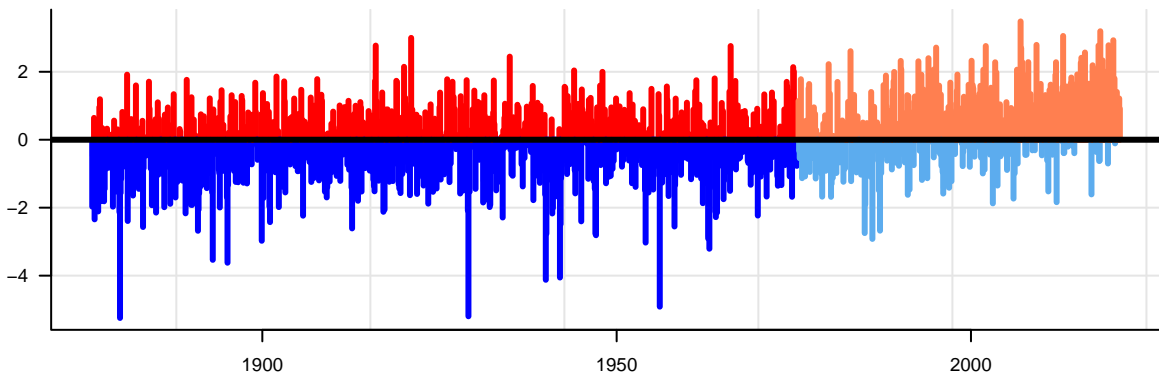
Self−similarity test
Estimated H by regression = 0.72
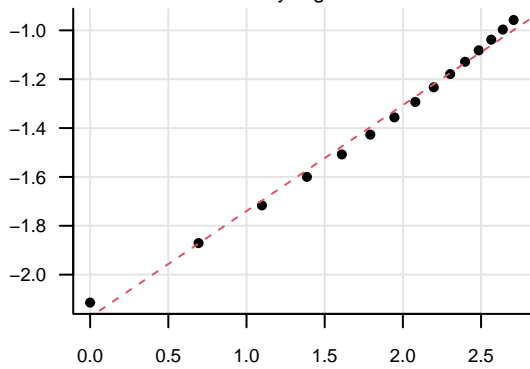
Normality test
Estimated alpha = 1.94
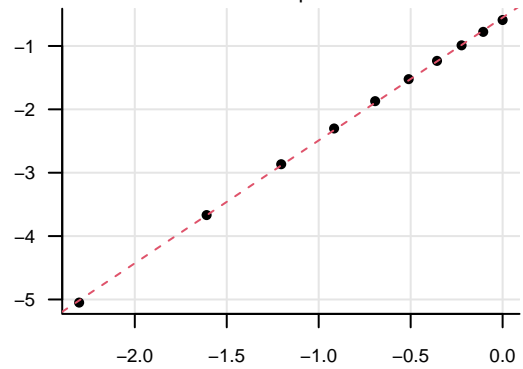
Lahore
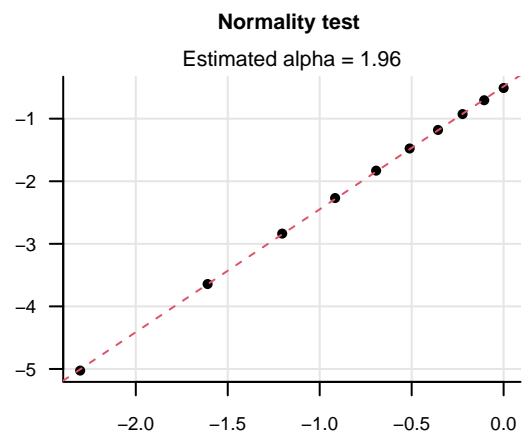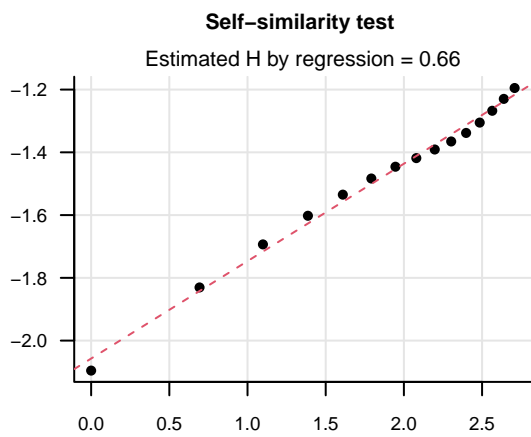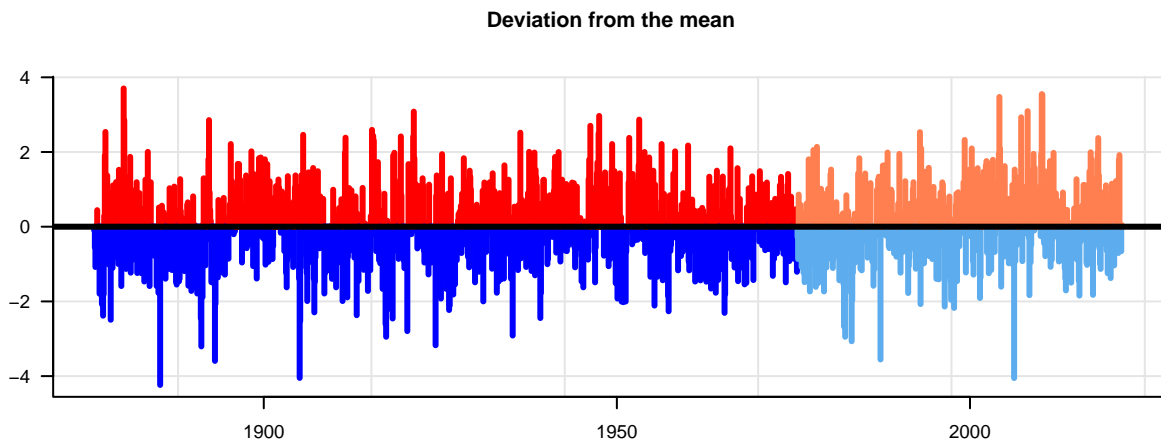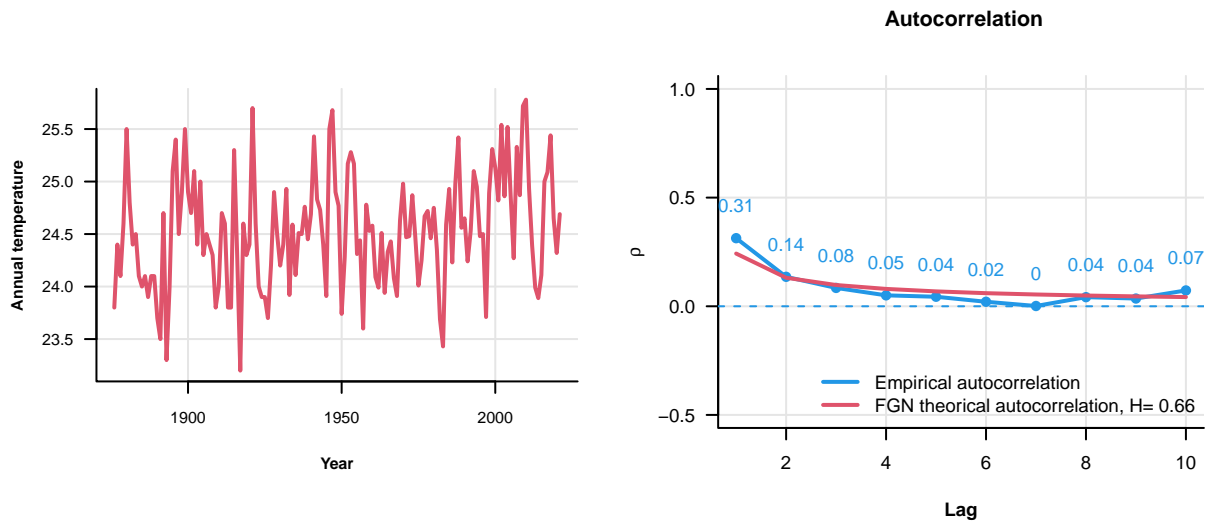
Lisbon

Autocorrelation
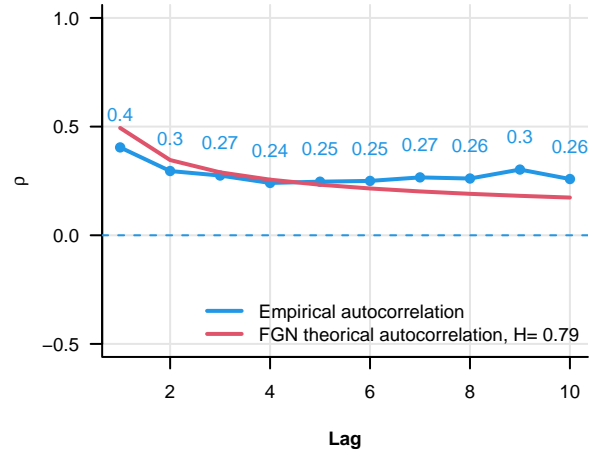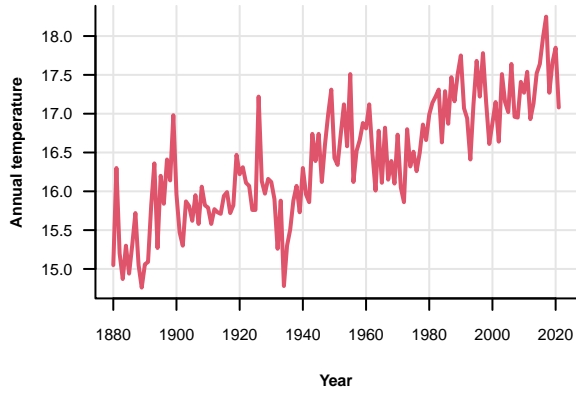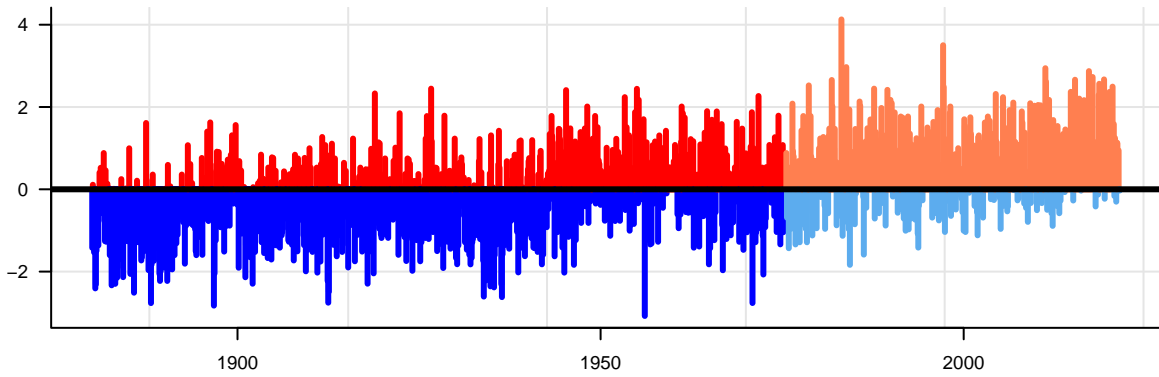
Deviation from the mean

Self-similarity test

Estimated H by regression = 0.81
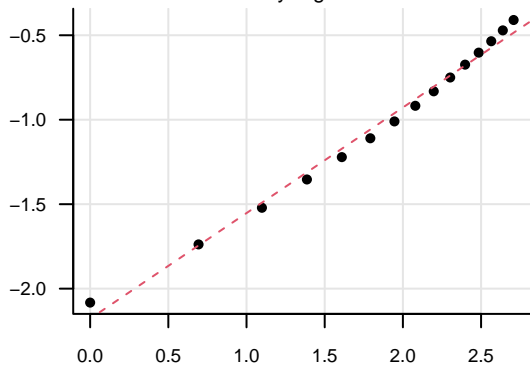
Normality test

Estimated alpha = 2

Madison

Autocorrelation
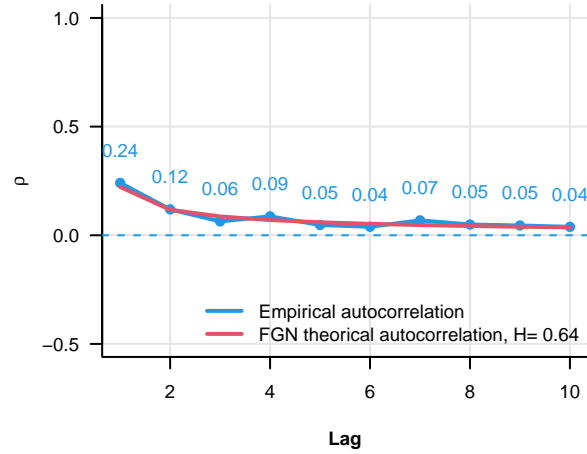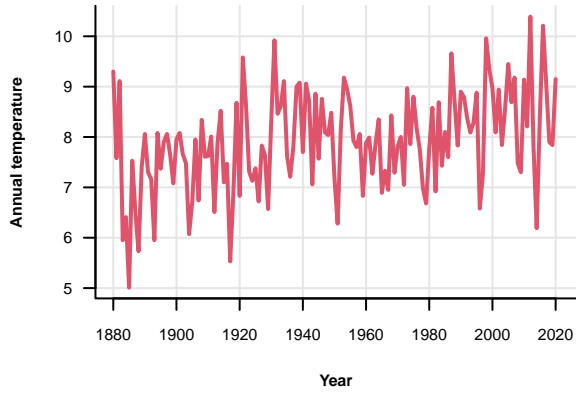
Empirical autocorrelation
FGN theorical autocorrelation, H= 0.64

Deviation from the mean
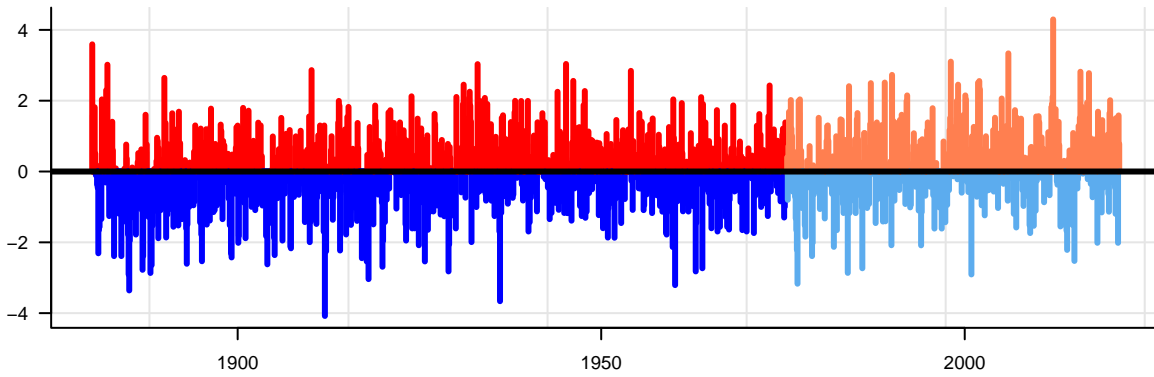
Self−similarity test
Estimated H by regression = 0.65
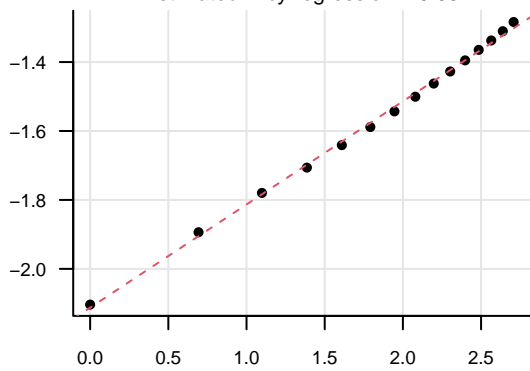
Normality test
Estimated alpha = 1.97

Madras

Autocorrelation

Deviation from the mean

Self−similarity test
Estimated H by regression = 0.77

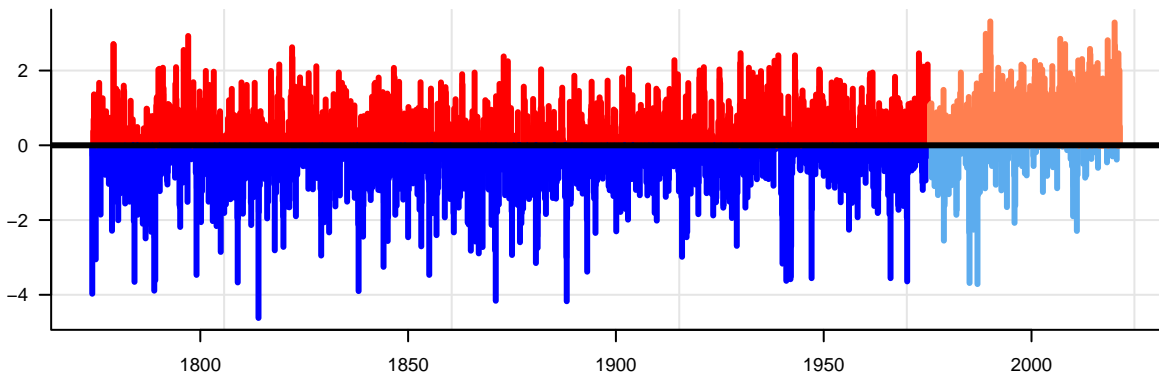## Normality test
Estimated alpha = 2.01
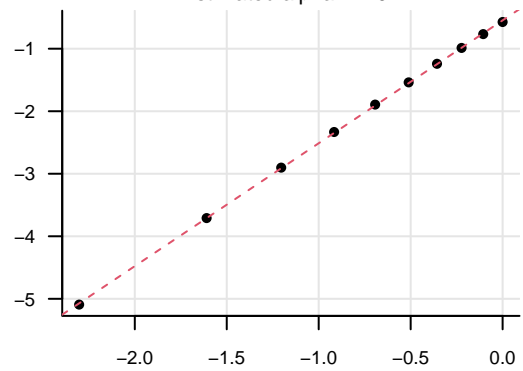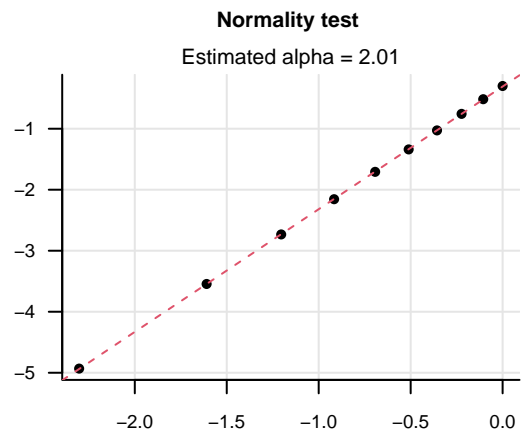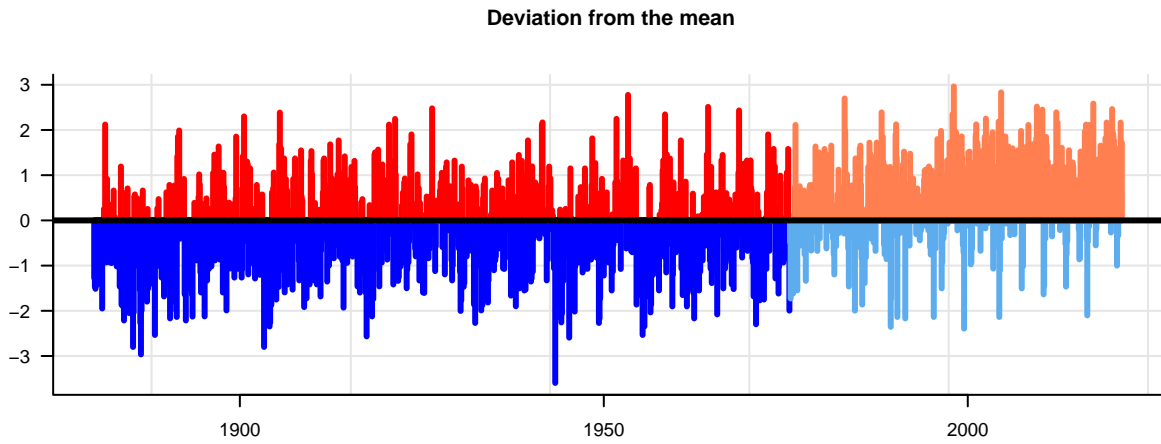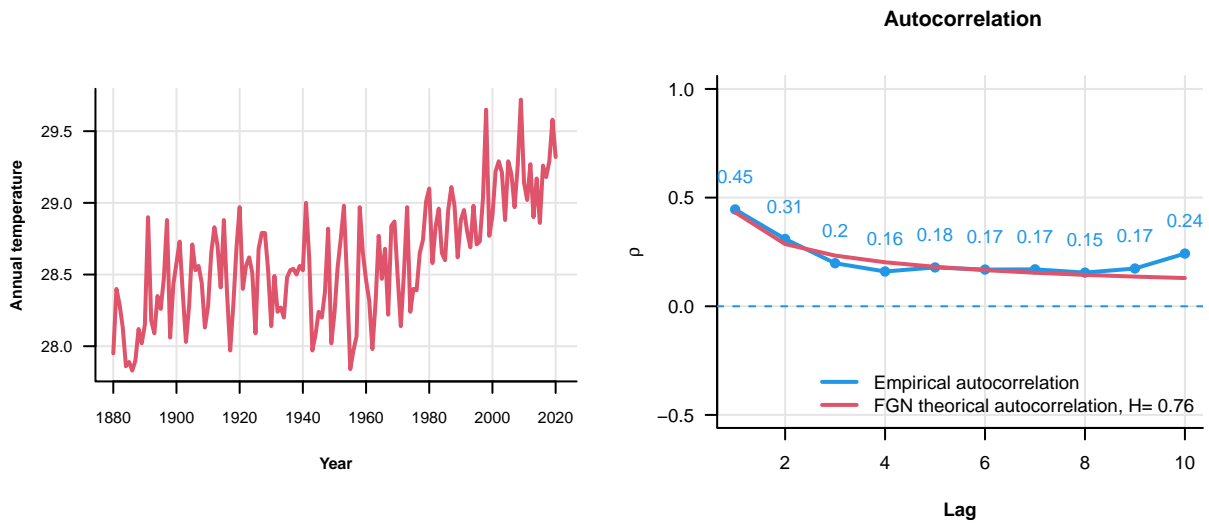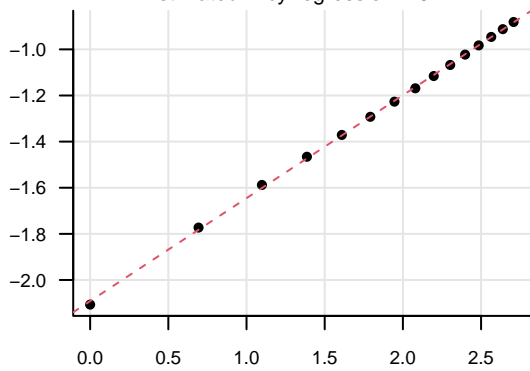
Marquette

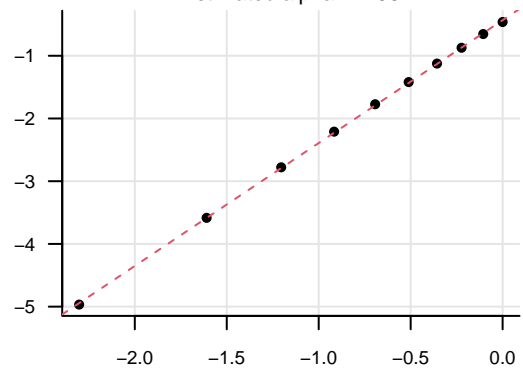## Autocorrelation

Deviation from the mean

Self−similarity test
Estimated H by regression = 0.73

Normality test
Estimated alpha = 1.97

Milwaukee
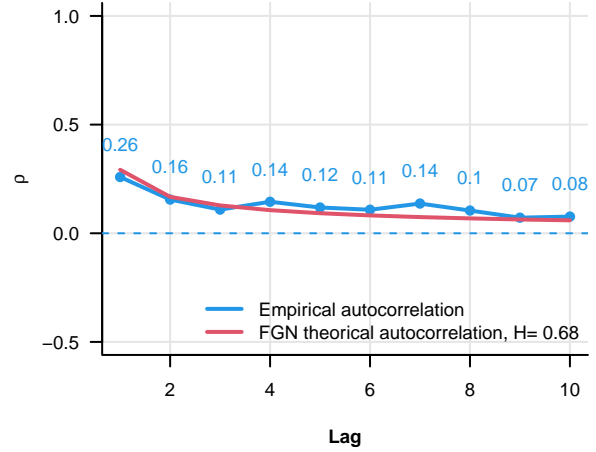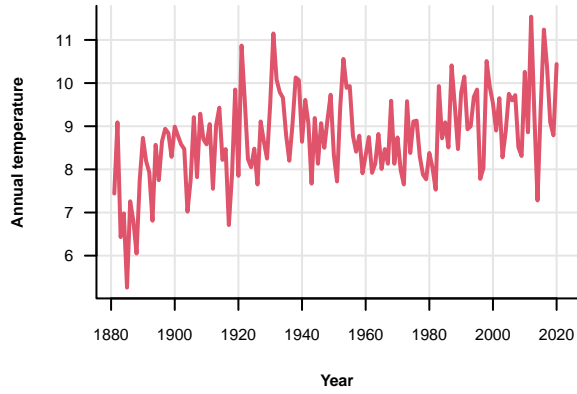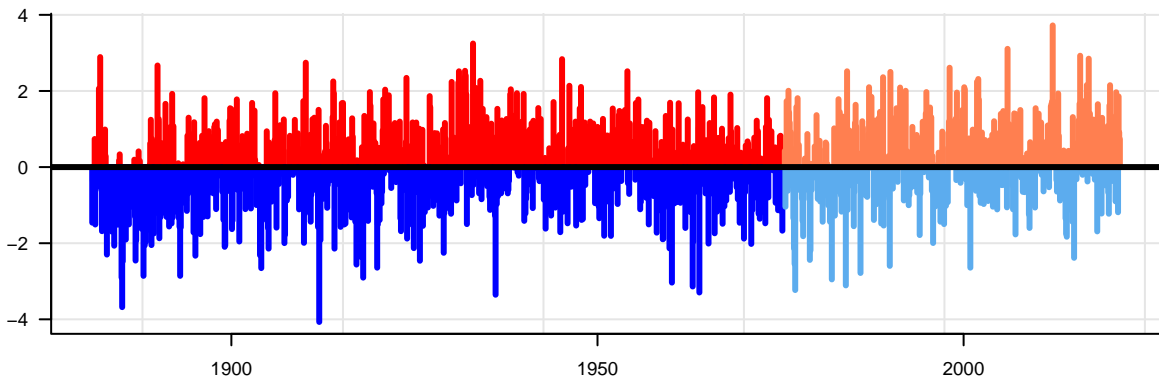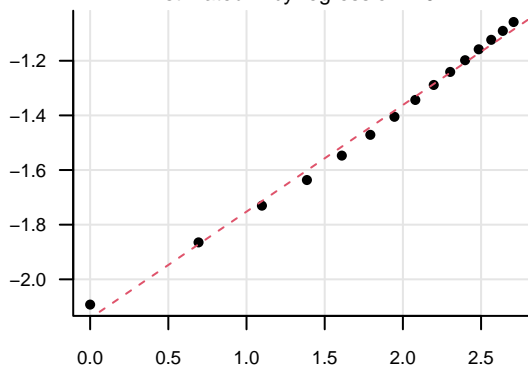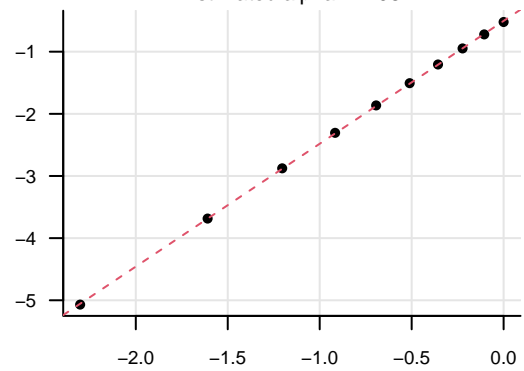
Mobile

Autocorrelation
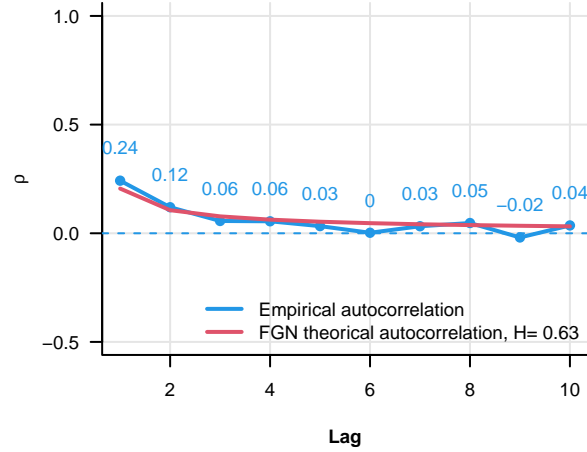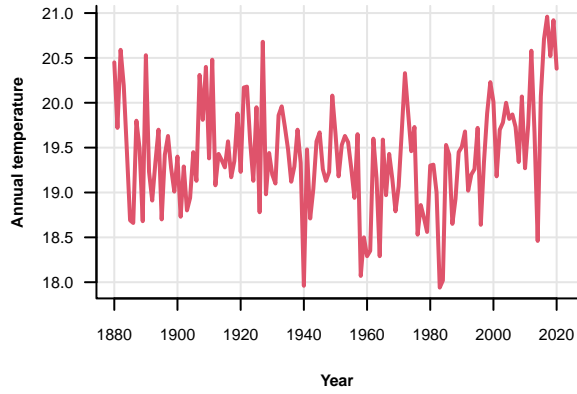
Deviation from the mean
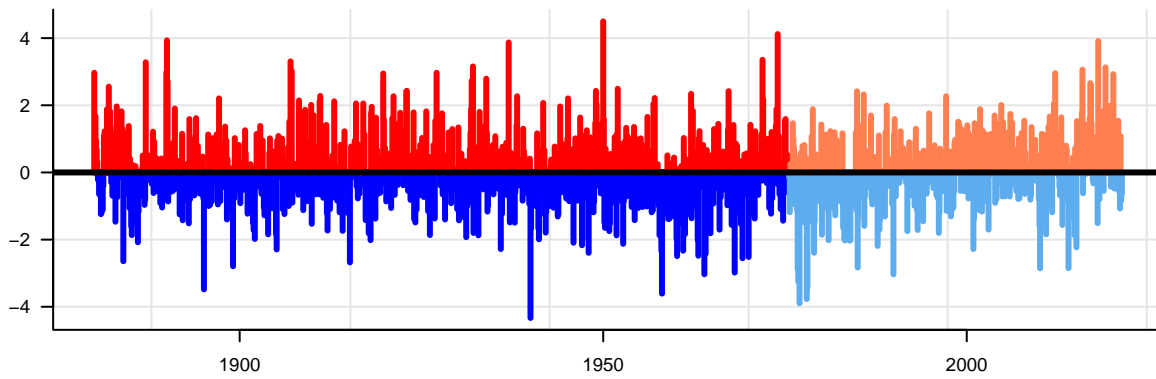
Self−similarity test
Estimated H by regression = 0.63
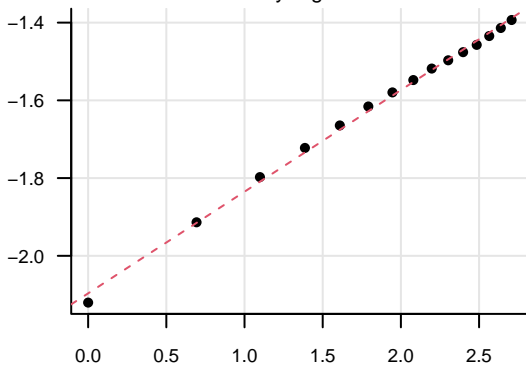
Normality test
Estimated alpha = 1.93
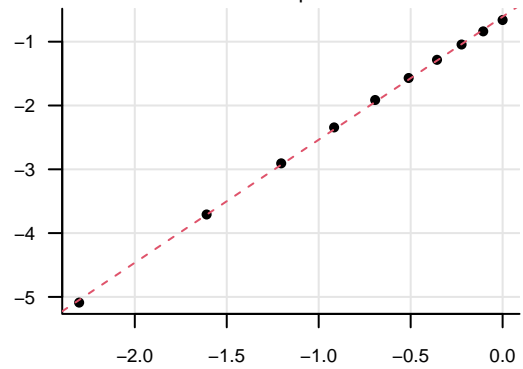
Nagasaki
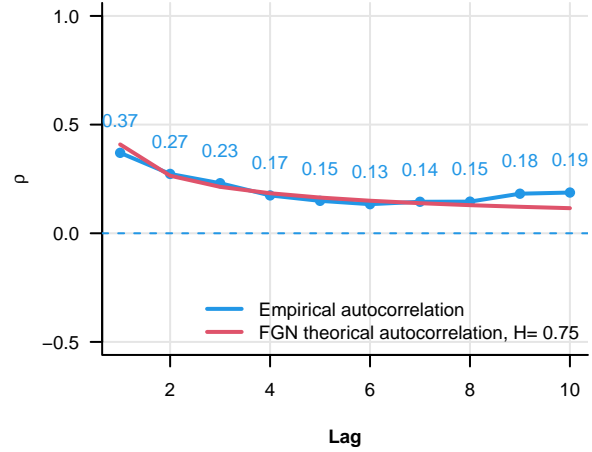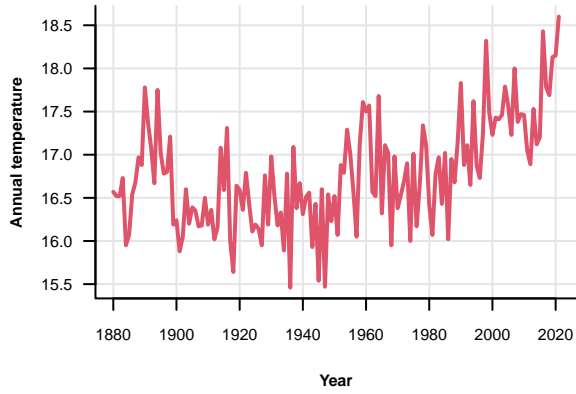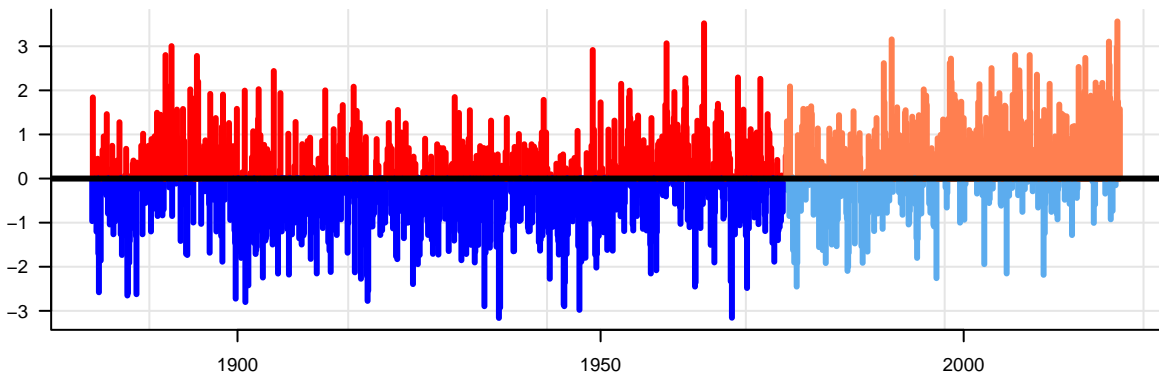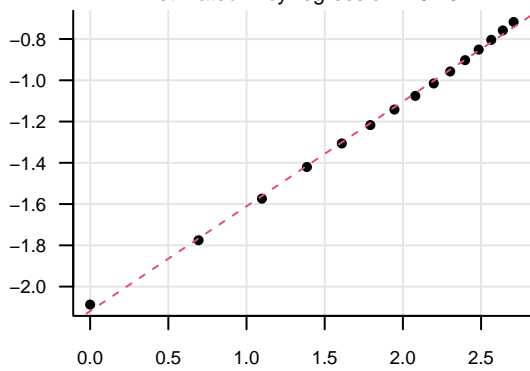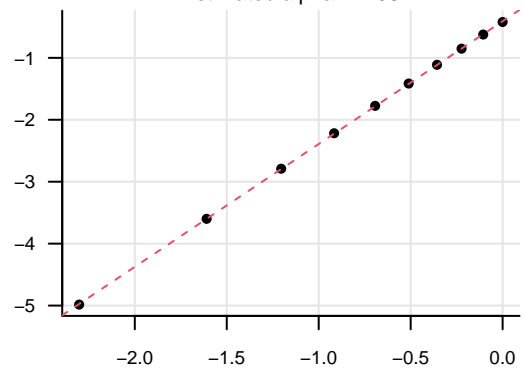
Nagpur

Autocorrelation

Deviation from the mean

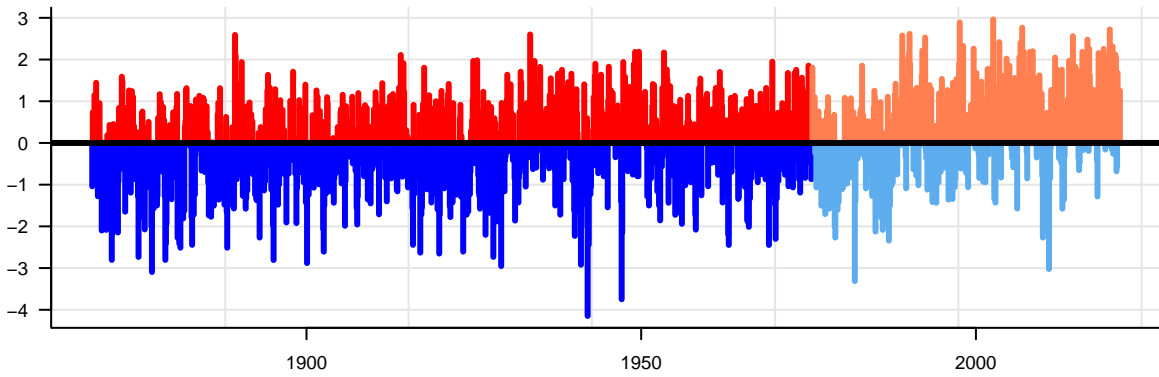## Self–similarity test
Estimated H by regression = 0.69

Normality test
Estimated alpha = 1.95

Nantes

Autocorrelation
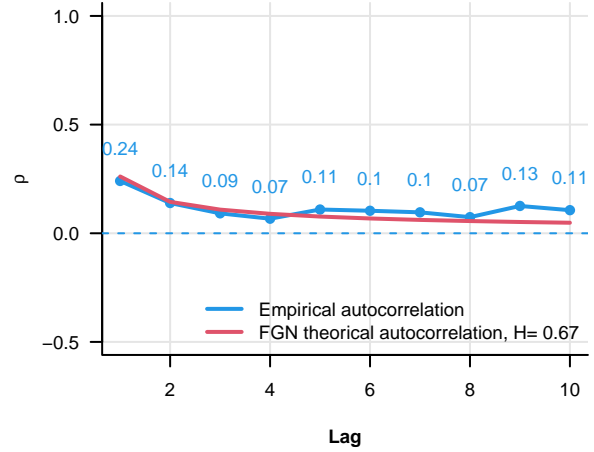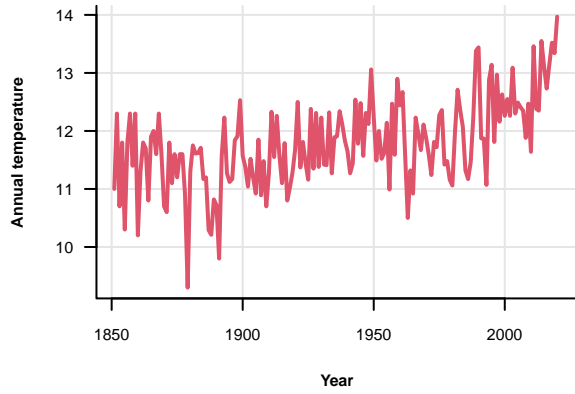
0.24 0.14 0.09 0.07 0.11 0.1 0.1 0.07 0.13 0.11

— Empirical autocorrelation
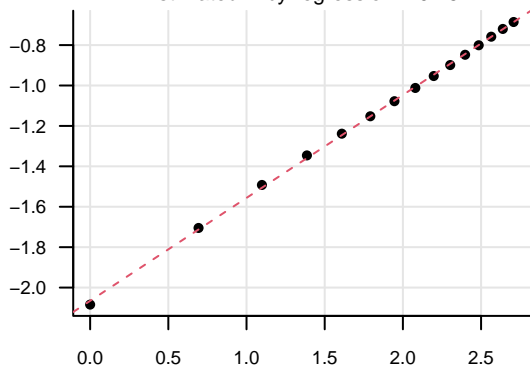— FGN theorical autocorrelation, H= 0.67

Deviation from the mean
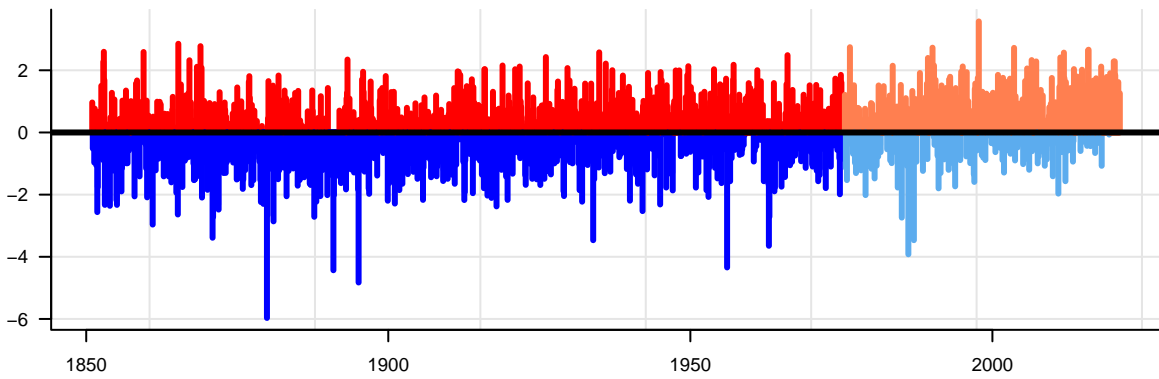
Self−similarity test

Estimated H by regression = 0.68
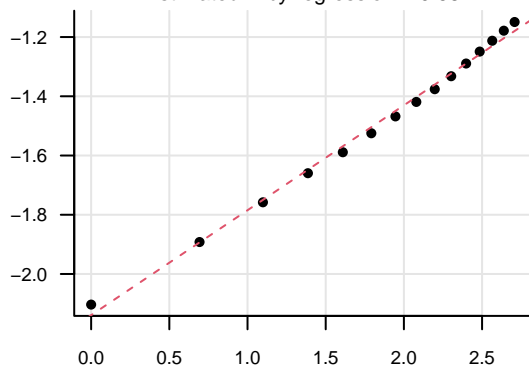
Normality test

Estimated alpha = 1.96
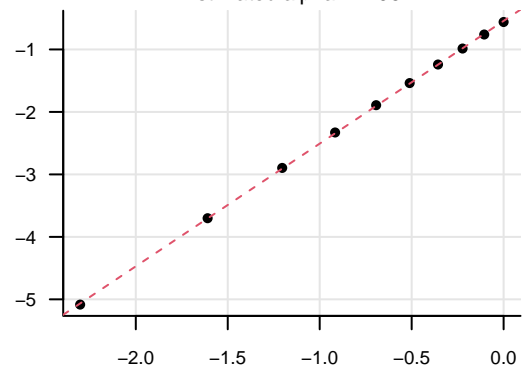
Nashville

Autocorrelation
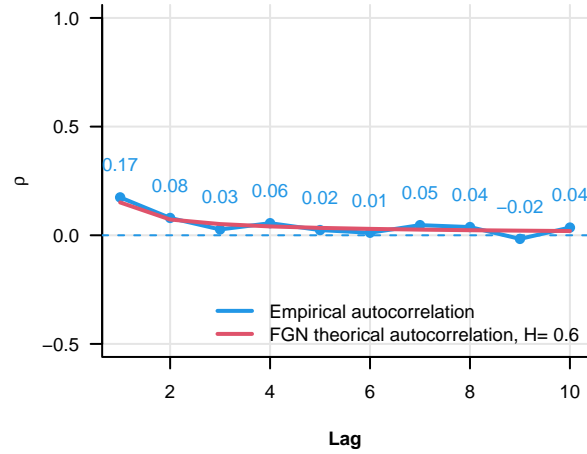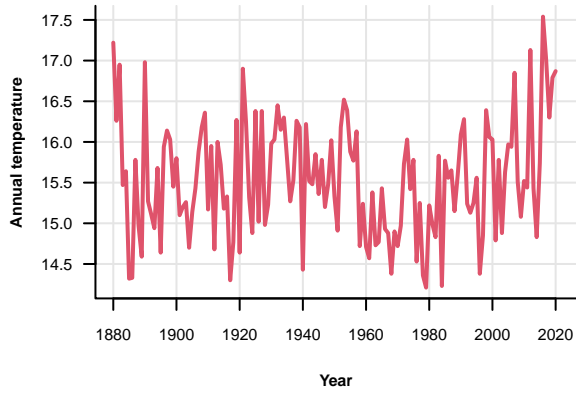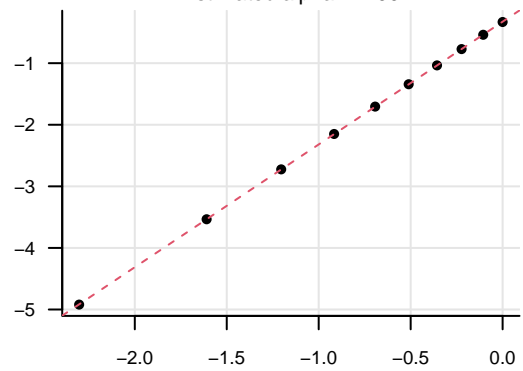

Deviation from the mean
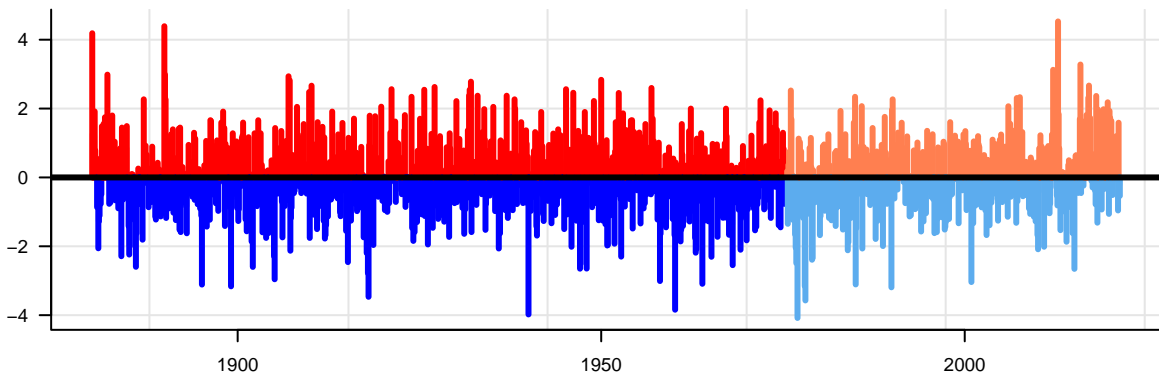
Self−similarity test
Estimated H by regression = 0.6
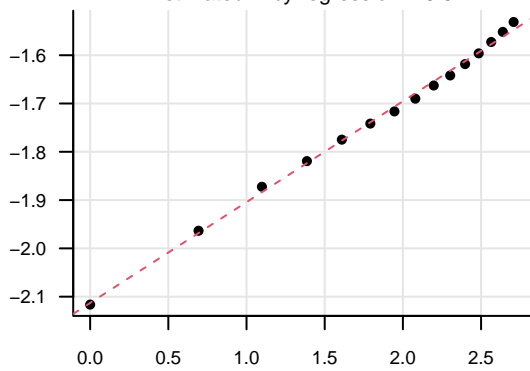
Normality test
Estimated alpha = 1.95

New Orleans

Autocorrelation

Deviation from the mean

Self−similarity test

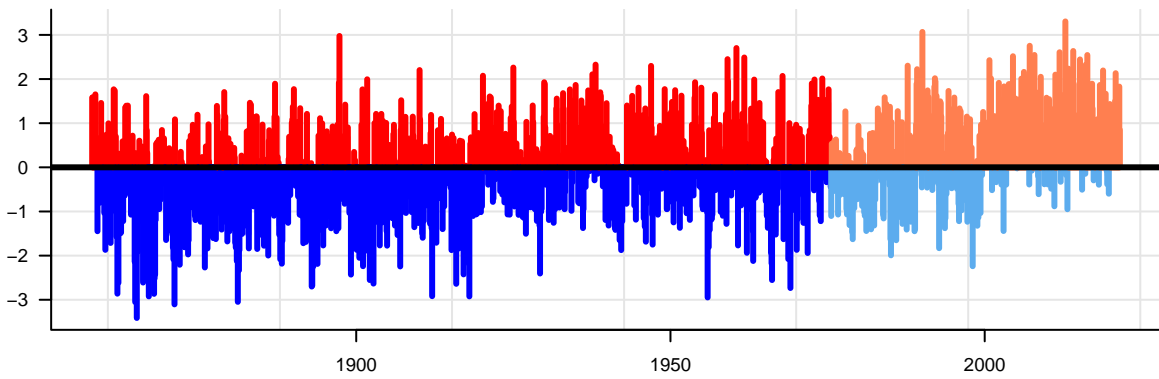Estimated H by regression = 0.72

Normality test

Estimated alpha = 1.94

New York

Autocorrelation

Deviation from the mean

Self−similarity test
Estimated H by regression = 0.76
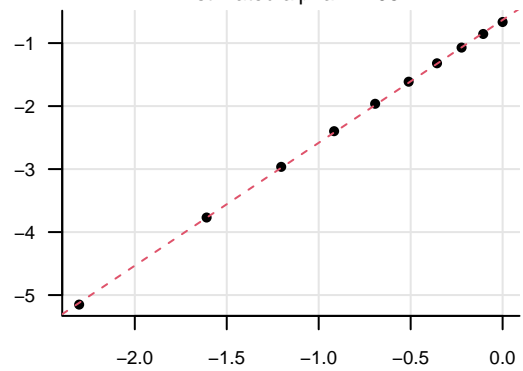
Normality test
Estimated alpha = 1.98
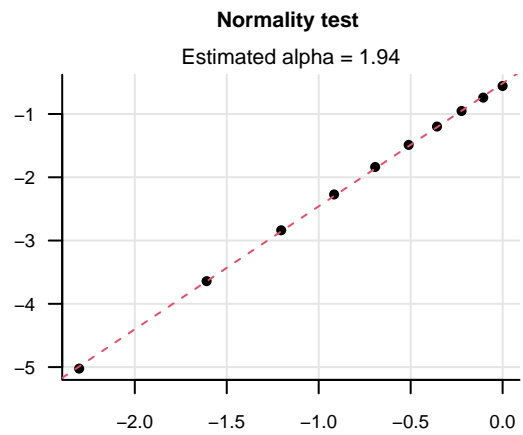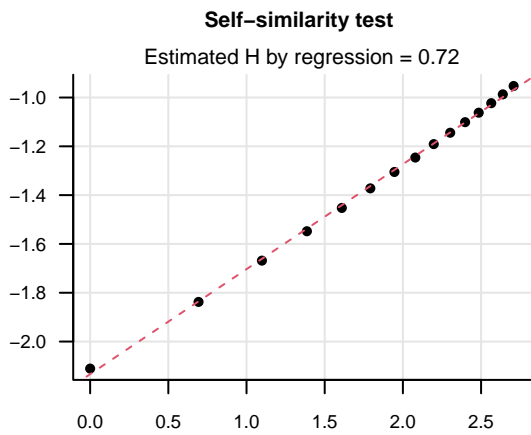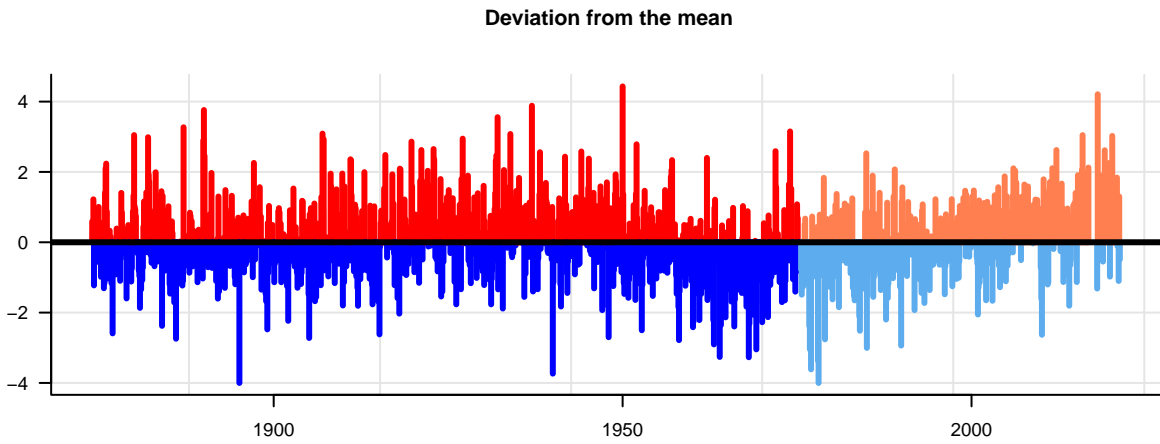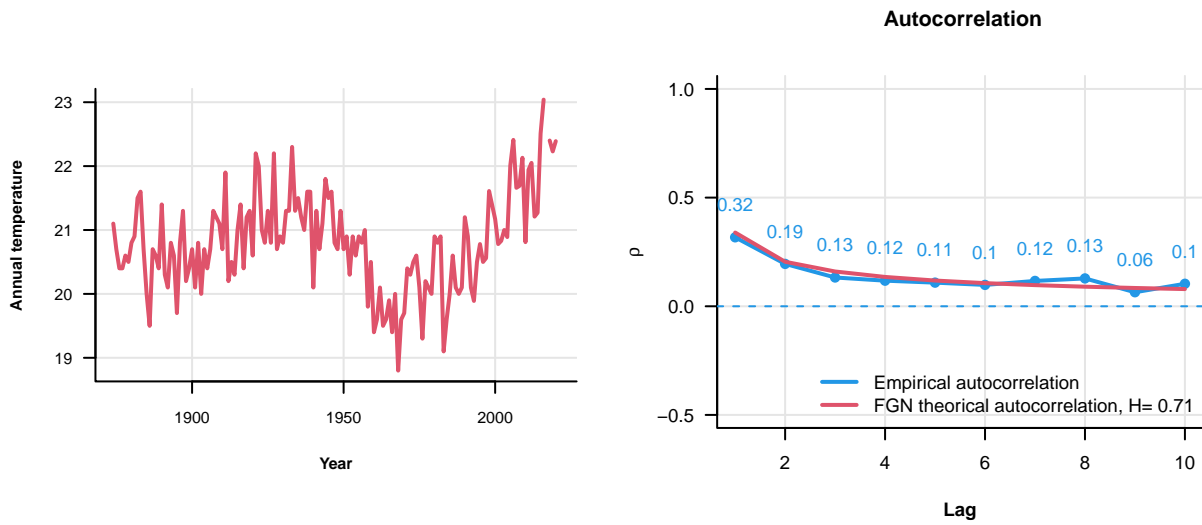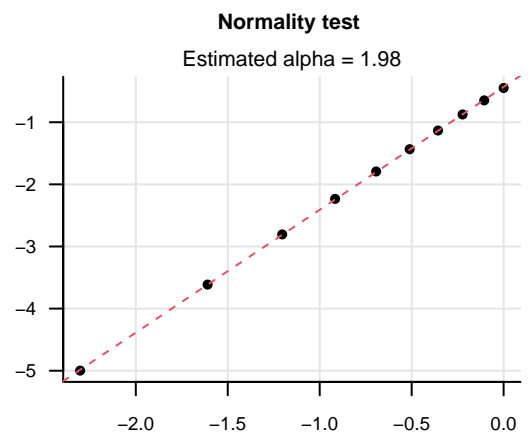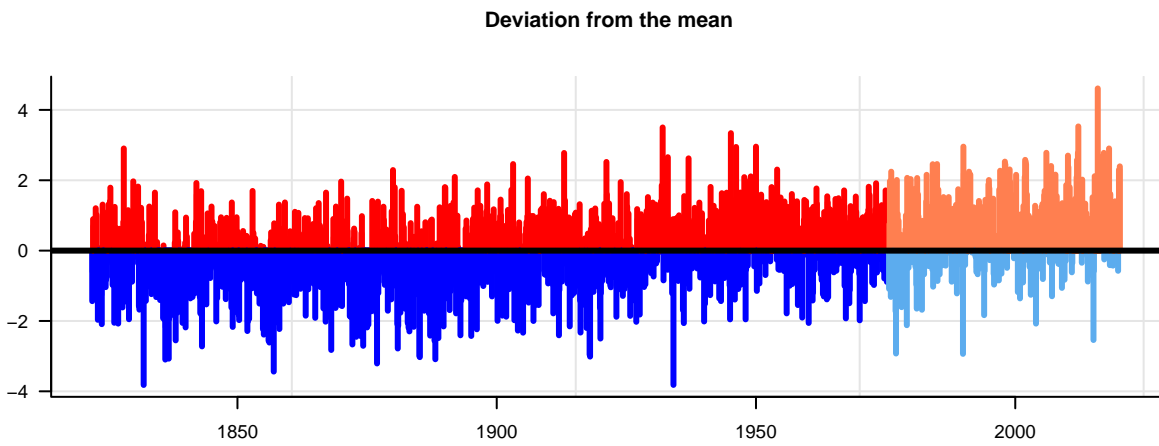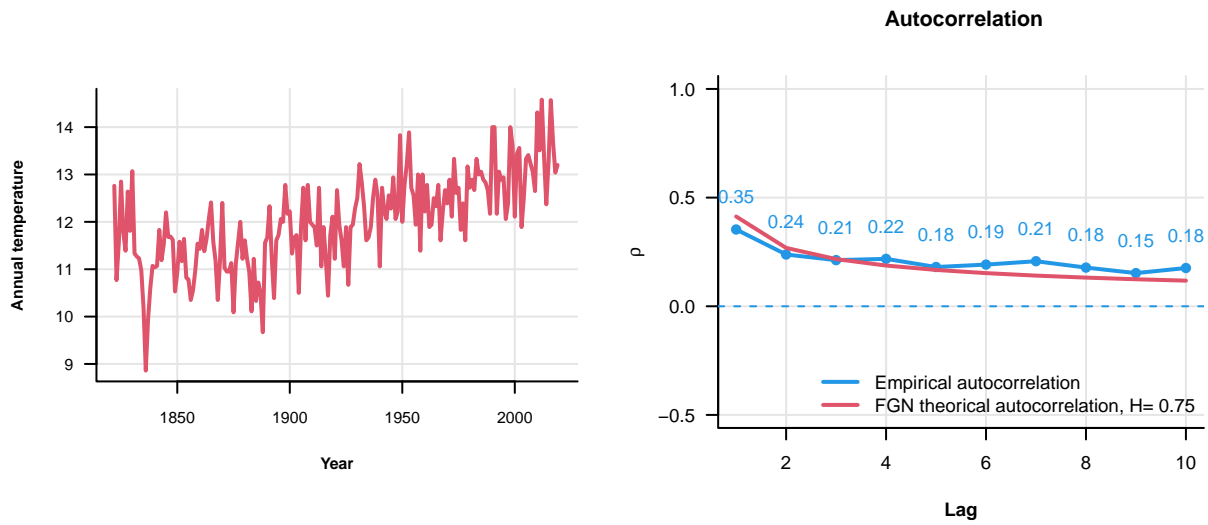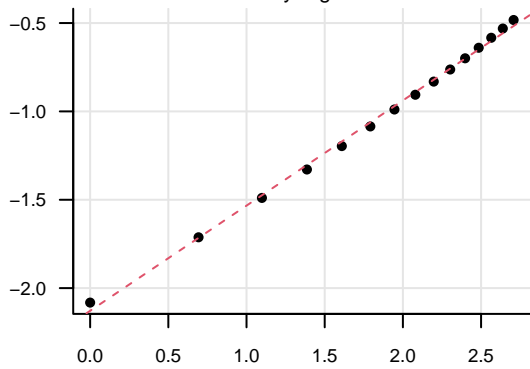
Oksoy Lighthouse

Autocorrelation
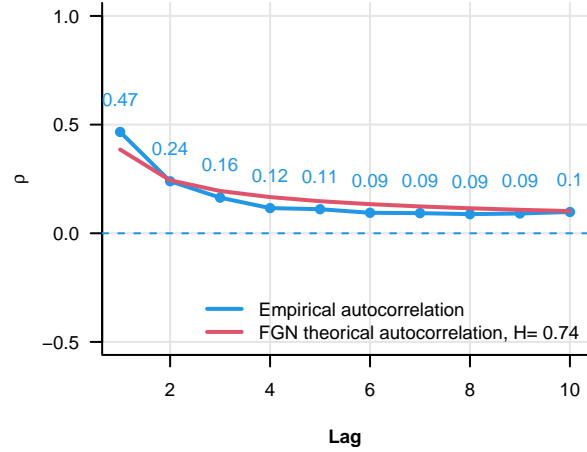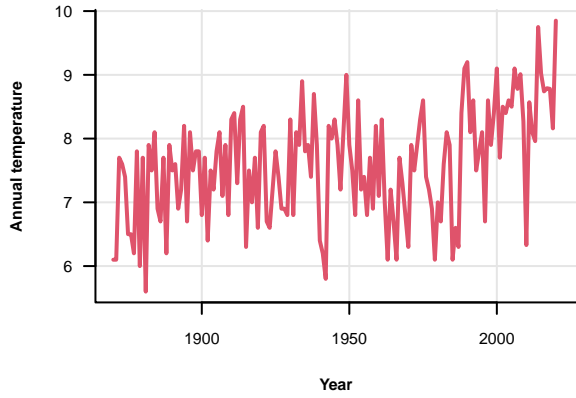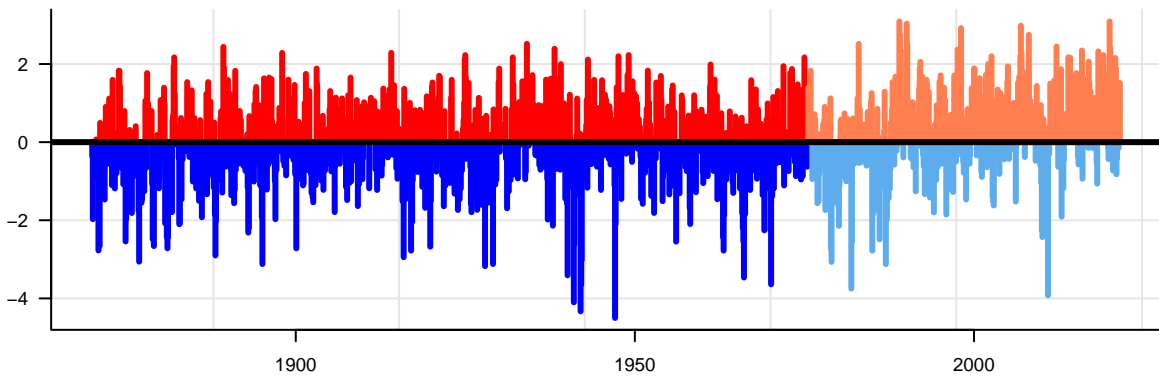
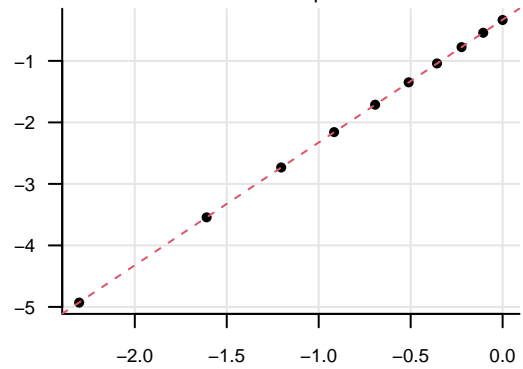### Deviation from the mean

Self–similarity test
Estimated H by regression = 0.73
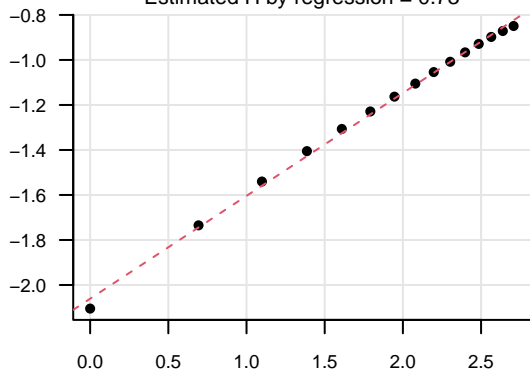
Normality test
Estimated alpha = 1.94
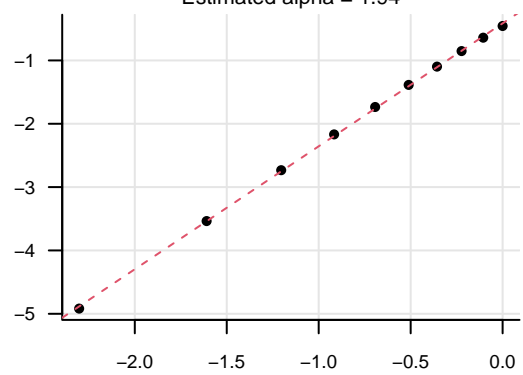
Ona

Autocorrelation
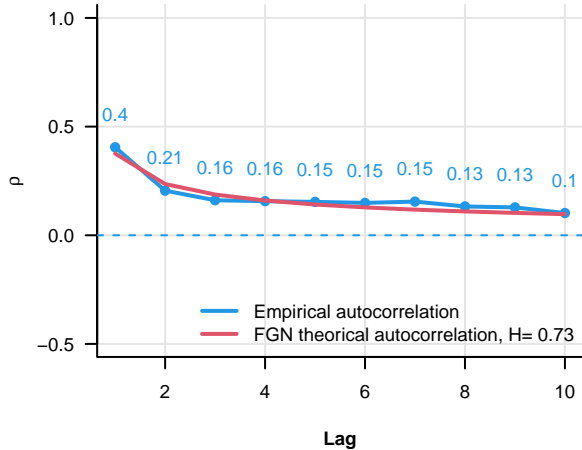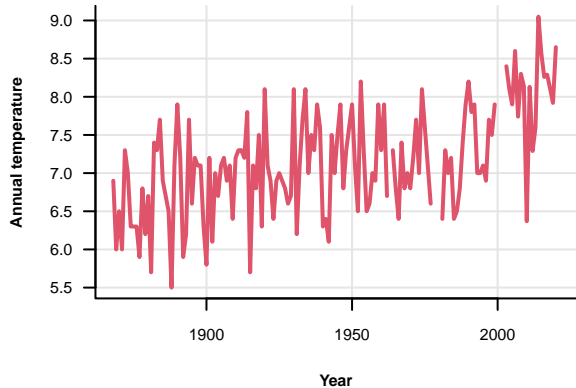
Deviation from the mean
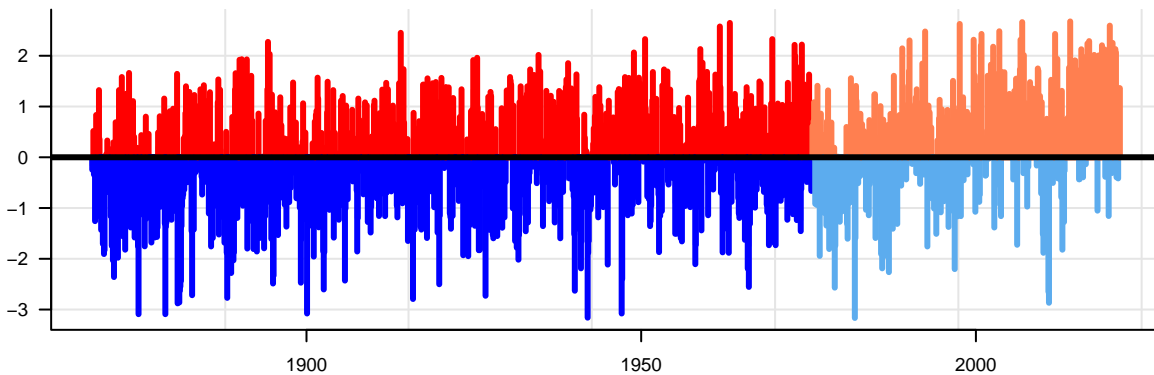
Self−similarity test
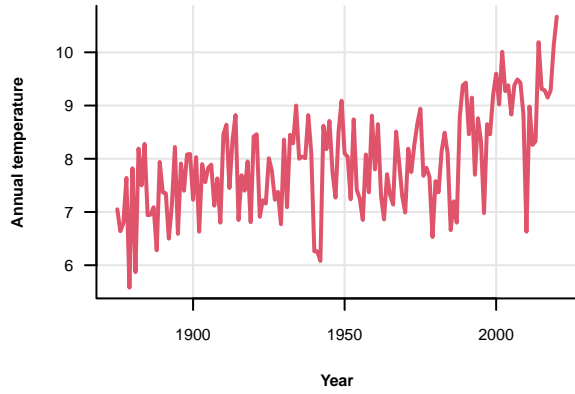Estimated H by regression = 0.74
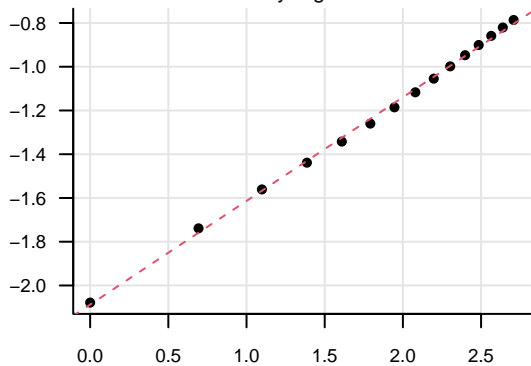
Normality test
Estimated alpha = 2
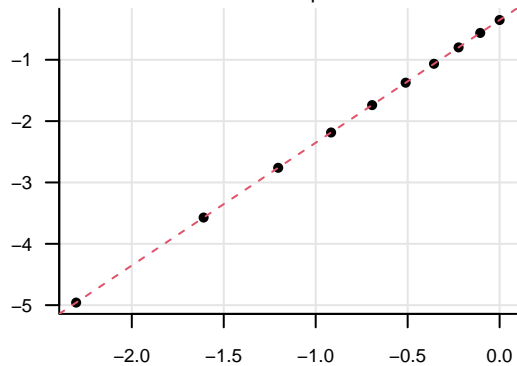
Oslo

Autocorrelation
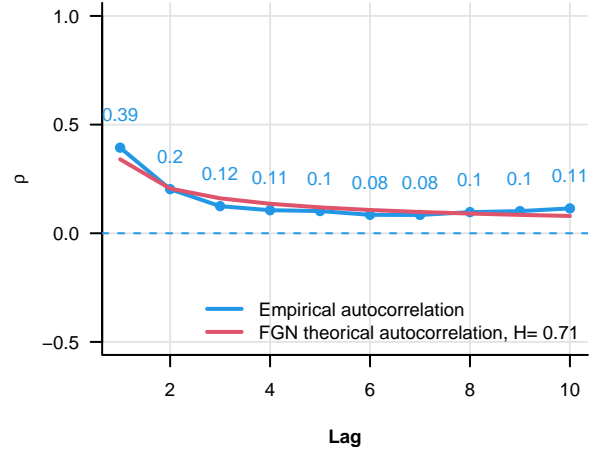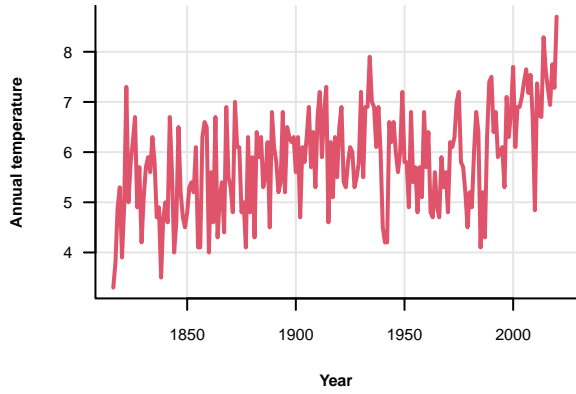
Deviation from the mean
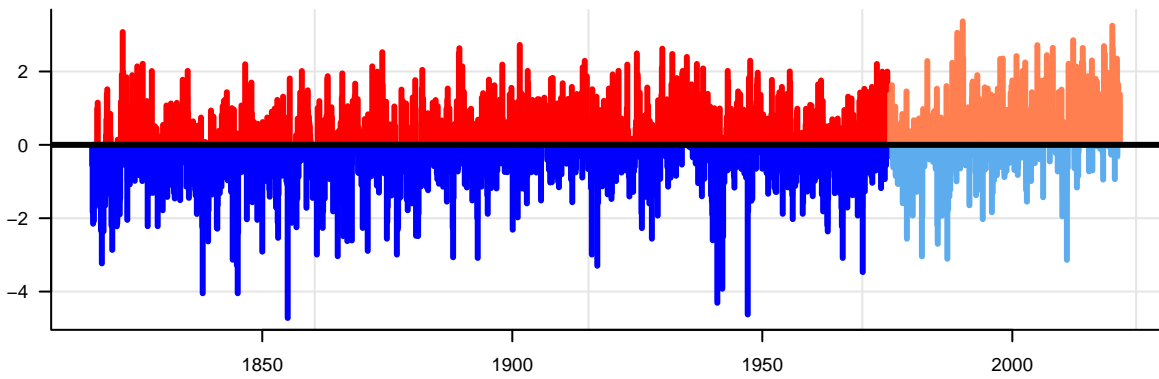
Self−similarity test

Estimated H by regression = 0.71
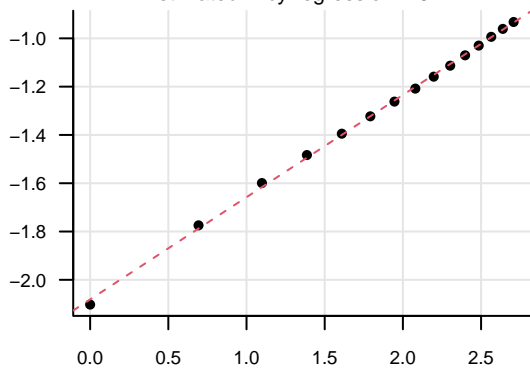
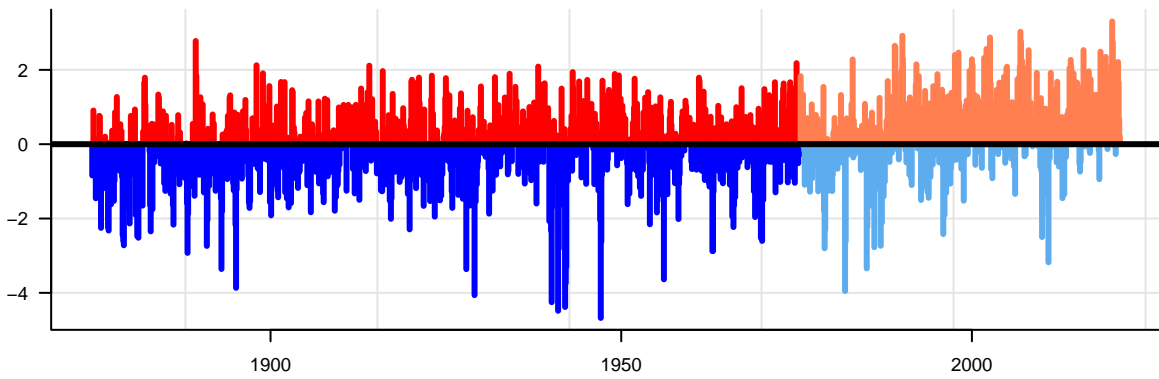

Normality test

Estimated alpha = 1.96
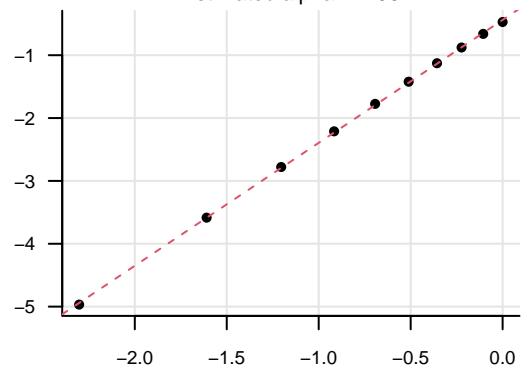
Paris

Autocorrelation
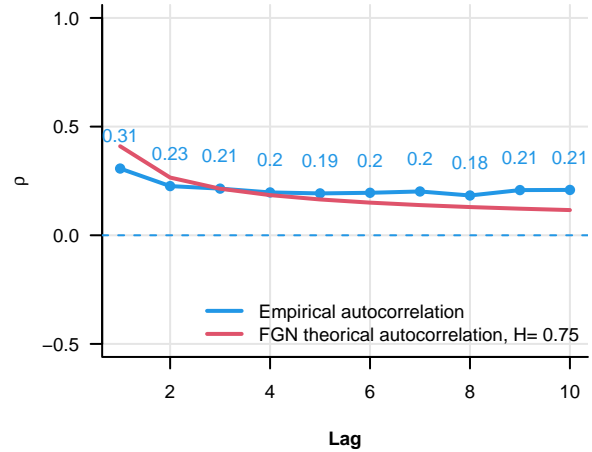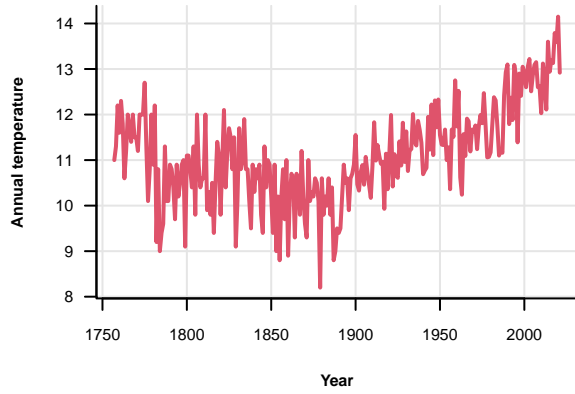
Deviation from the mean

Self–similarity test
Estimated H by regression = 0.77

Normality test
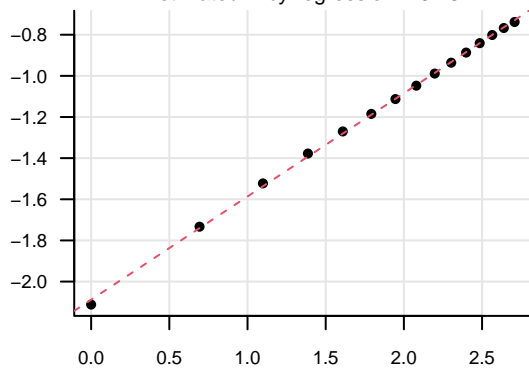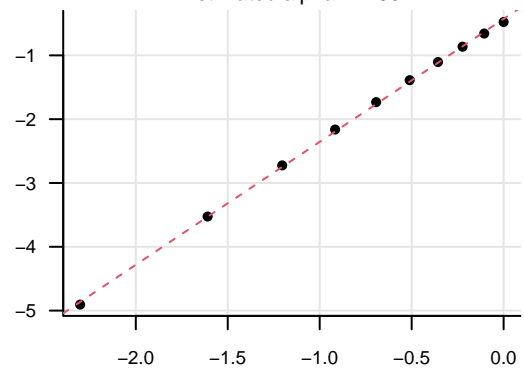Estimated alpha = 1.98
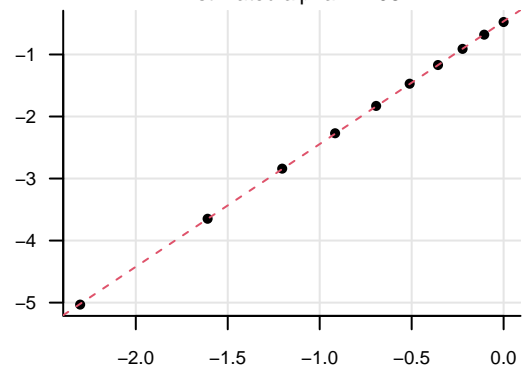
Prague

Autocorrelation
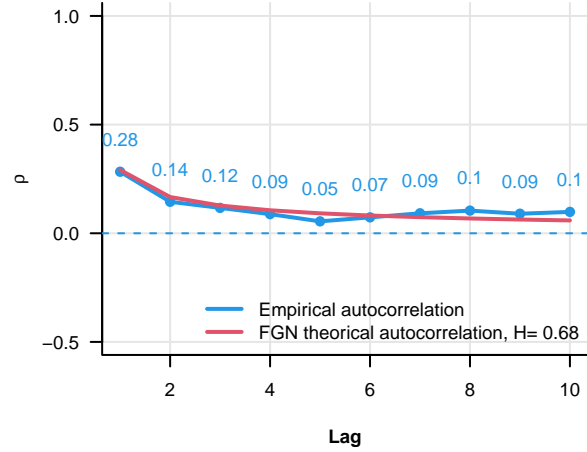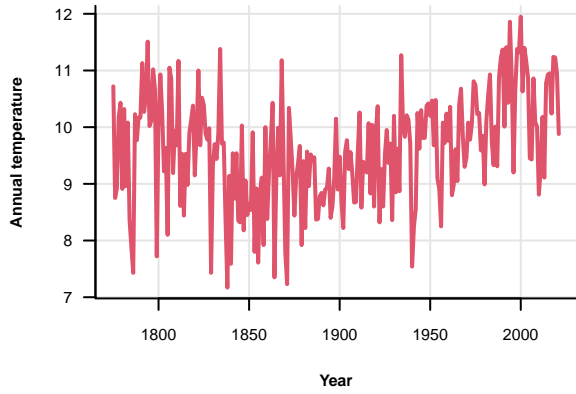
Deviation from the mean

Self–similarity test
Estimated H by regression = 0.69

Normality test
Estimated alpha = 1.94

Reykjavik

Roros

Autocorrelation

Deviation from the mean

Self−similarity test
Estimated H by regression = 0.68

Normality test
Estimated alpha = 1.94
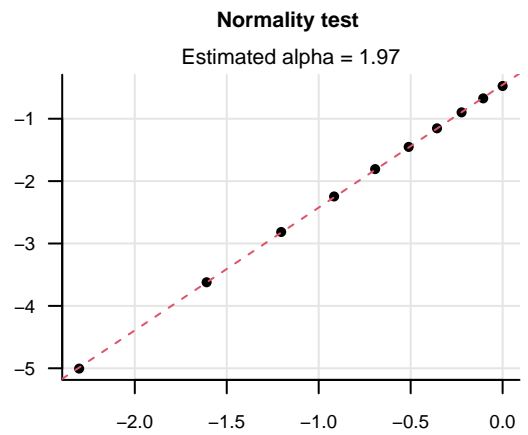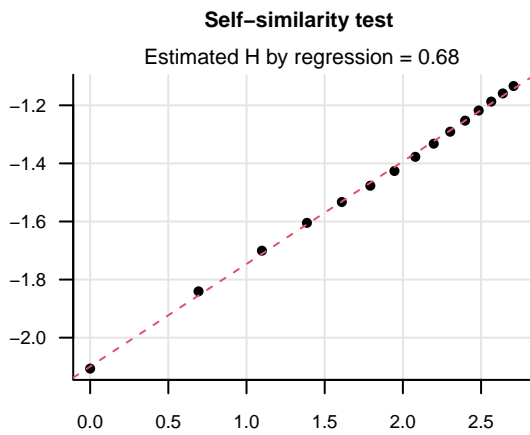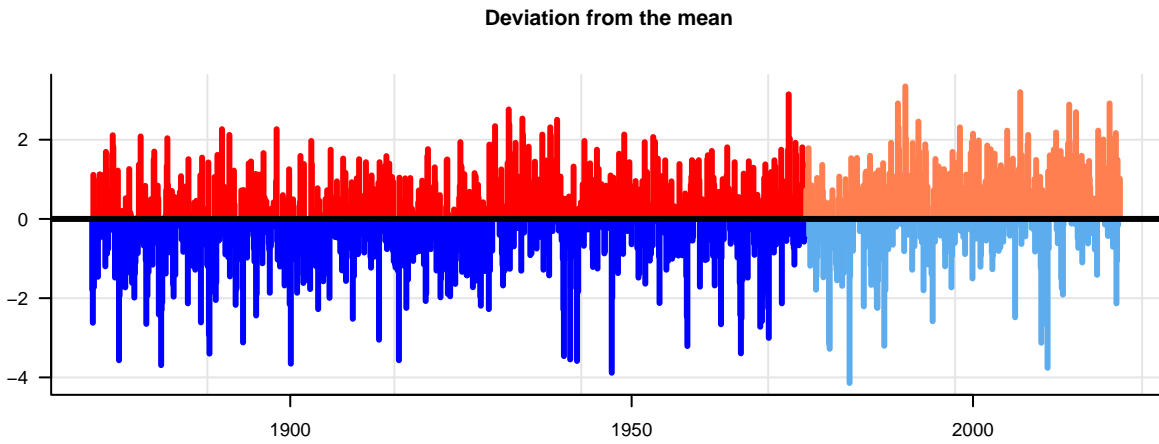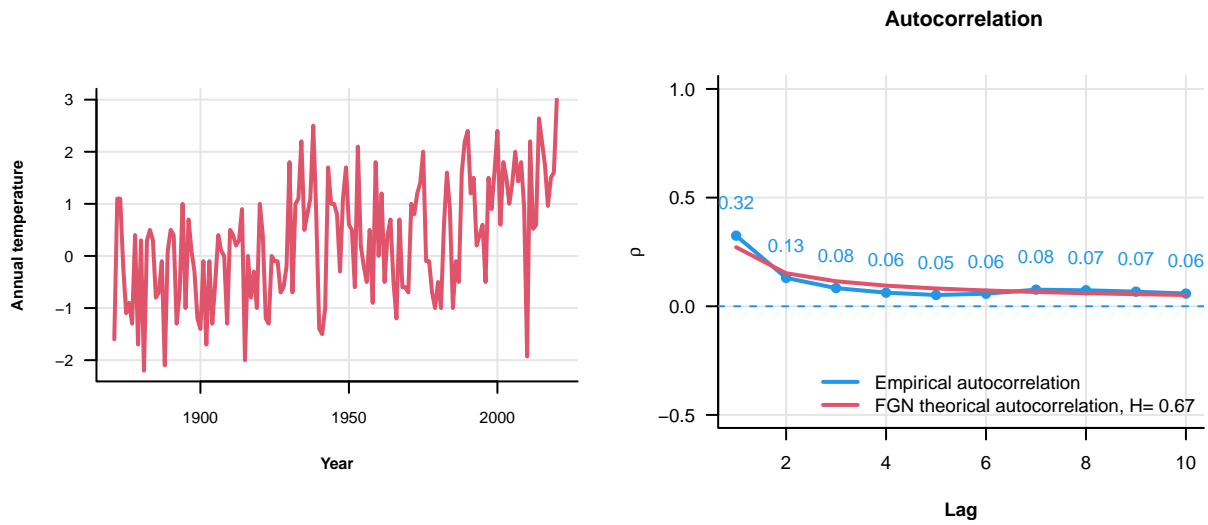
Sort

Autocorrelation

Deviation from the mean

Self−similarity test
Estimated H by regression = 0.64

Normality test
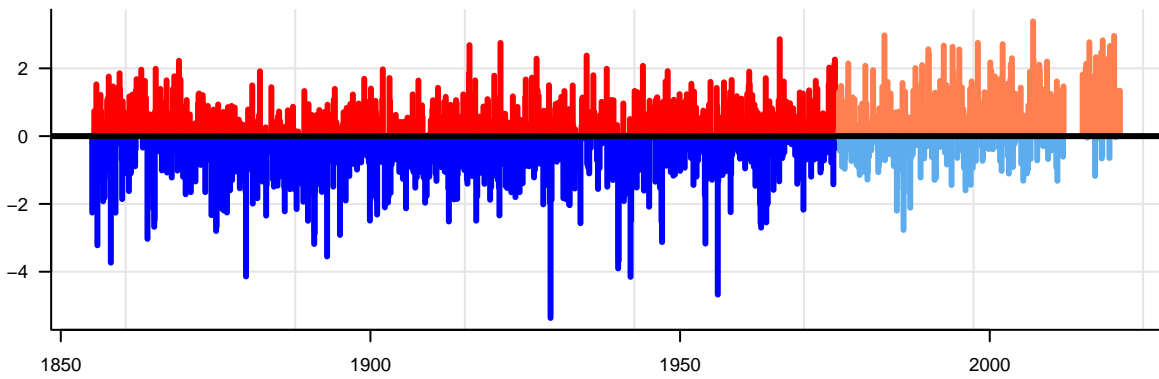Estimated alpha = 1.99

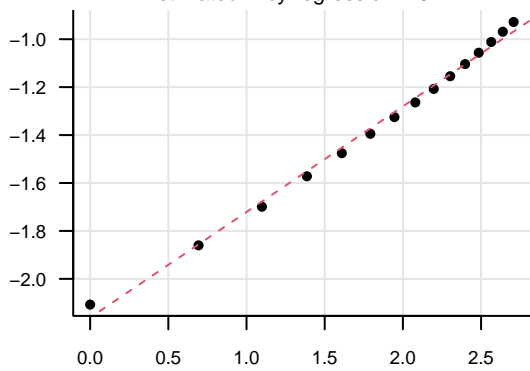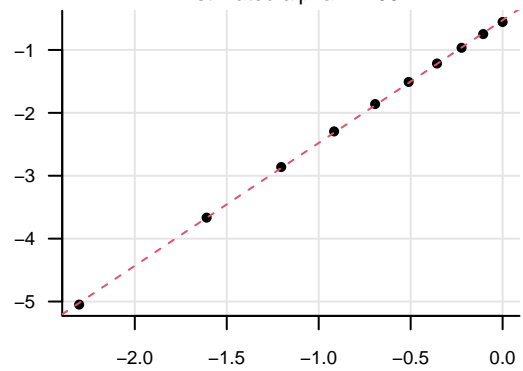# Sulina
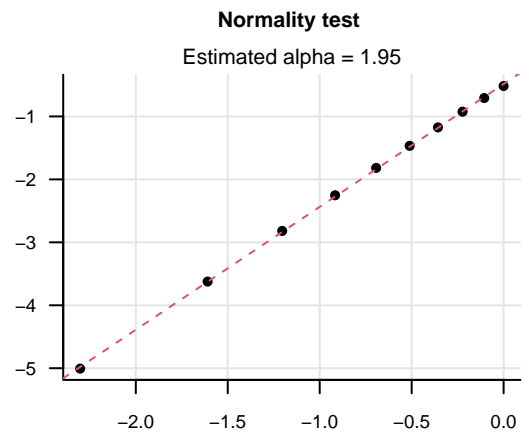
Tokyo
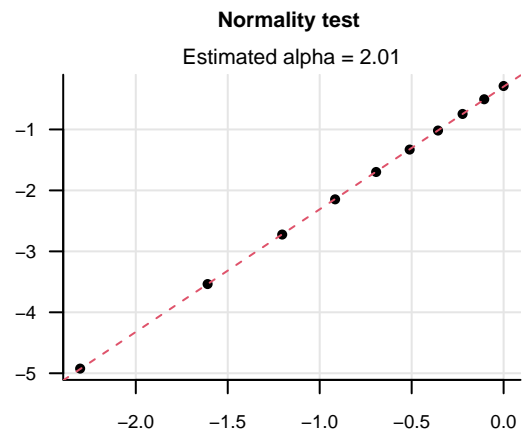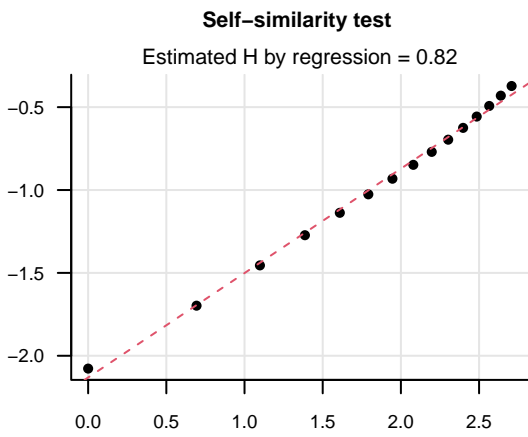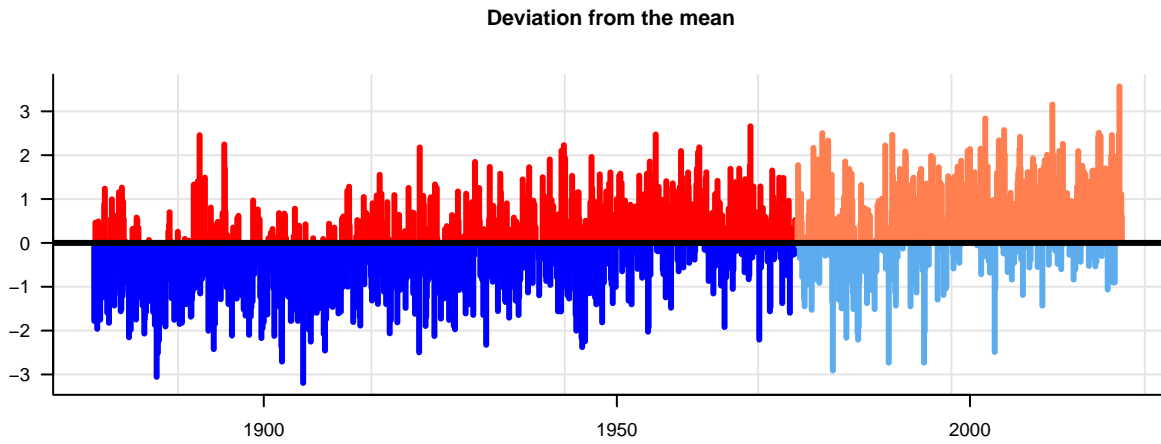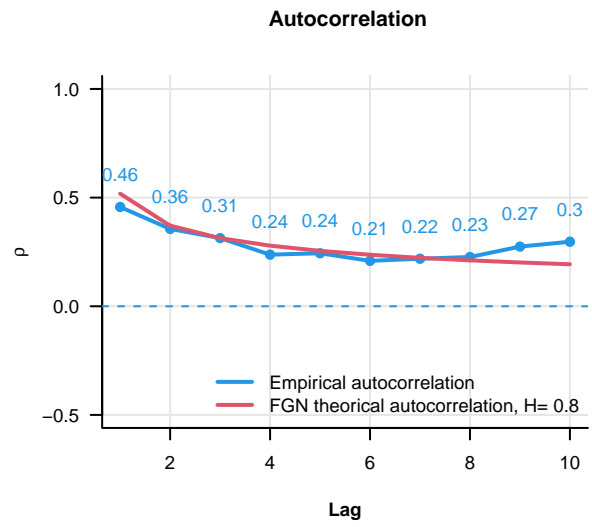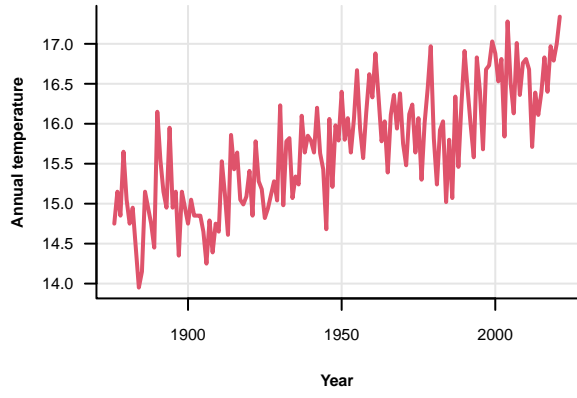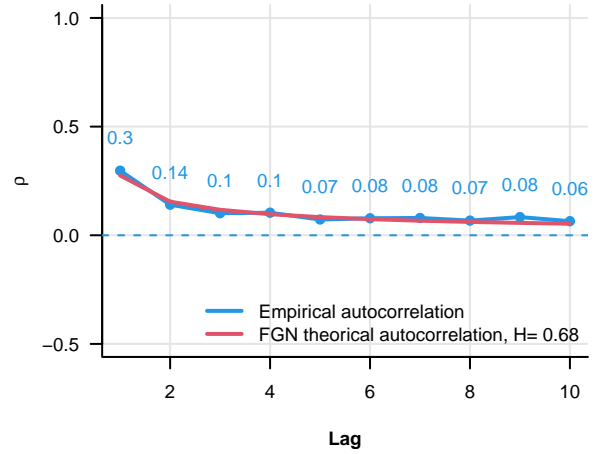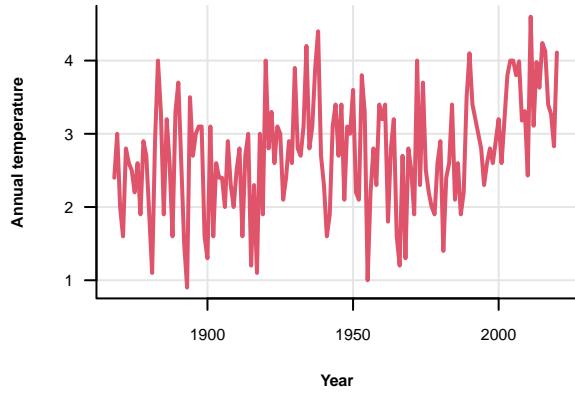
Autocorrelation

Deviation from the mean

Self−similarity test
Estimated H by regression = 0.82

Normality test
Estimated alpha = 2.01

Tromso

Uccle

Autocorrelation
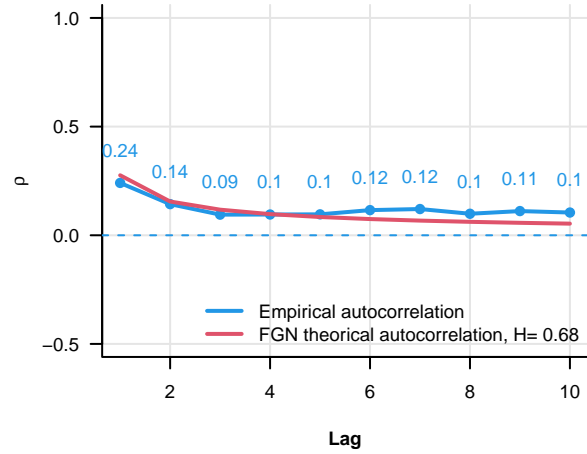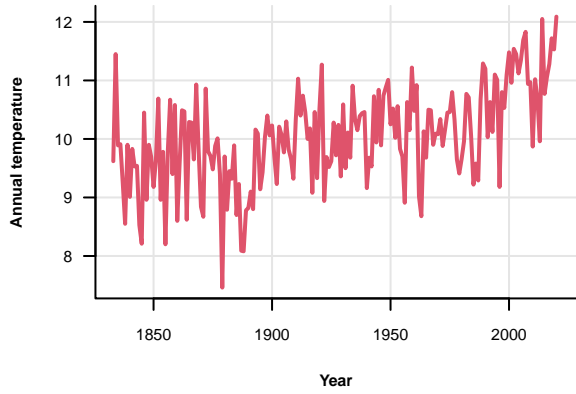
0.24 0.14 0.09 0.1 0.1 0.12 0.12 0.1 0.11 0.1

Empirical autocorrelation
FGN theorical autocorrelation, H= 0.68

Deviation from the mean
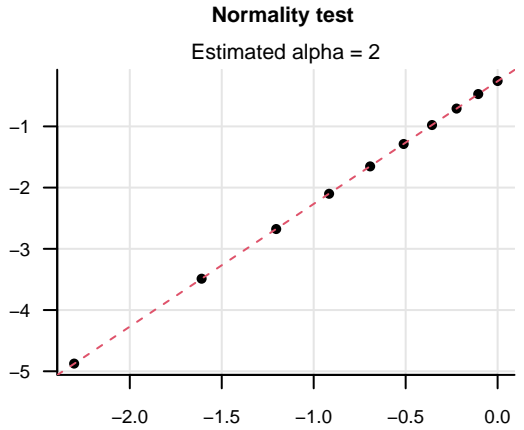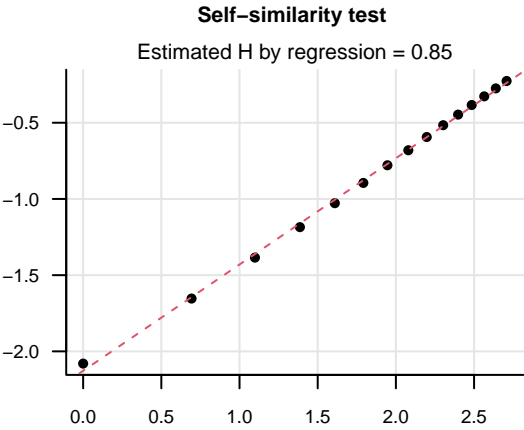

Self−similarity test

Estimated H by regression = 0.69

Normality test

Estimated alpha = 1.95

Uppsala

Autocorrelation
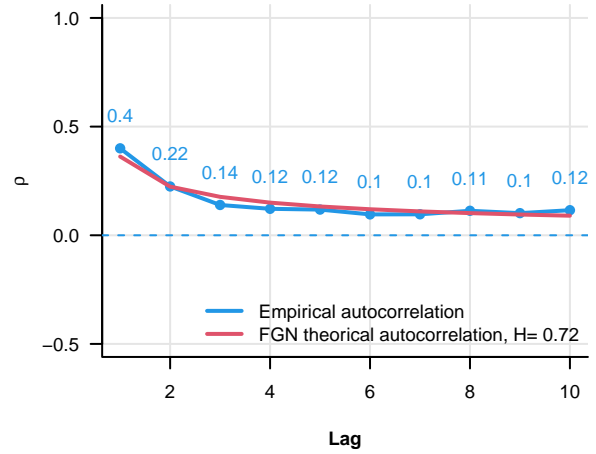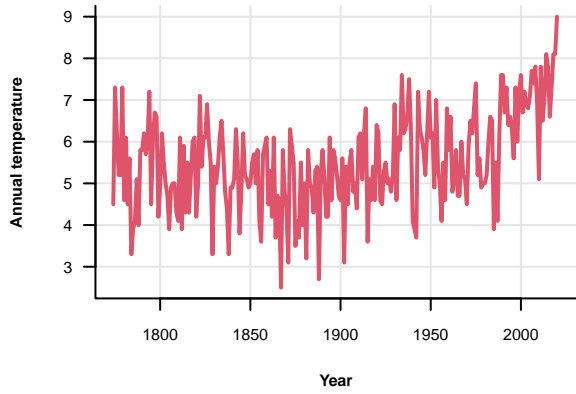
Deviation from the mean

Self−similarity test
Estimated H by regression = 0.72

Normality test
Estimated alpha = 1.96

Utsira

Autocorrelation
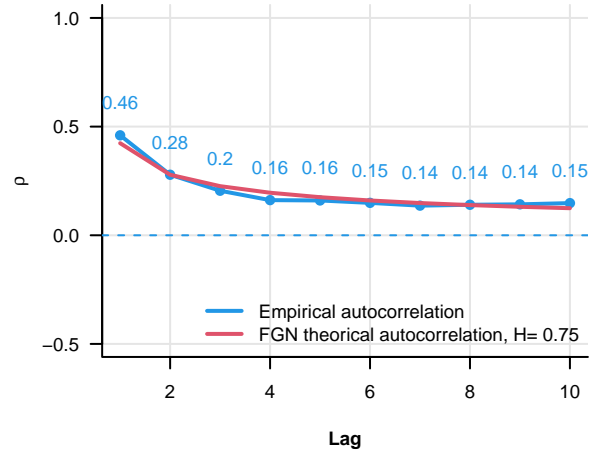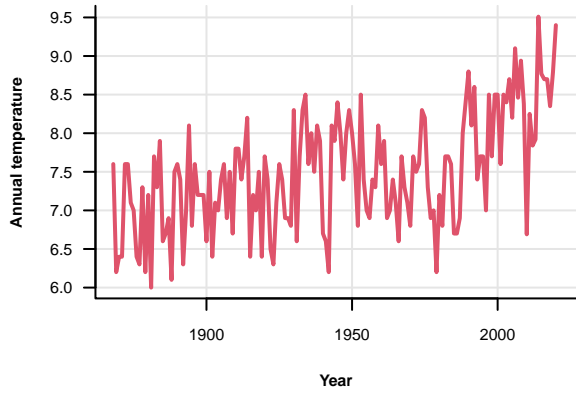
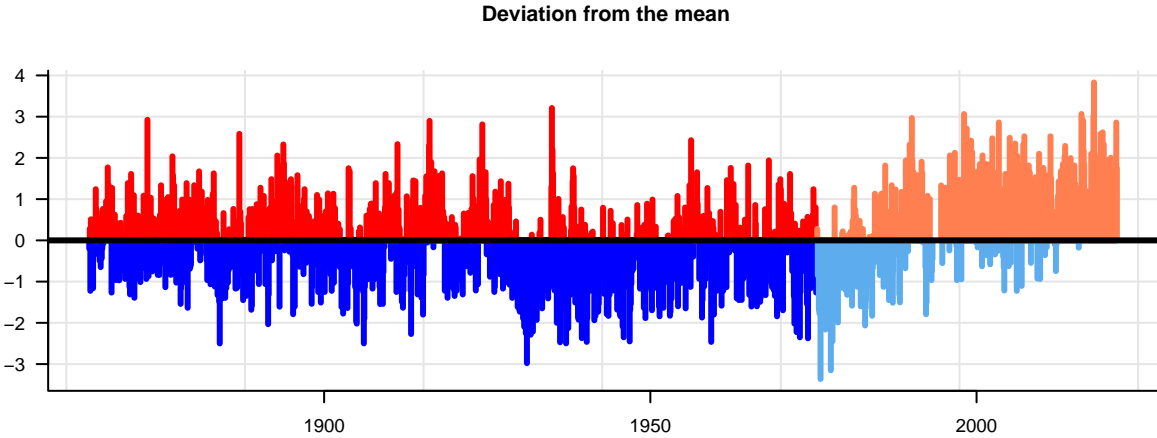## Deviation from the mean

Self-similarity test
Estimated H by regression = 0.75
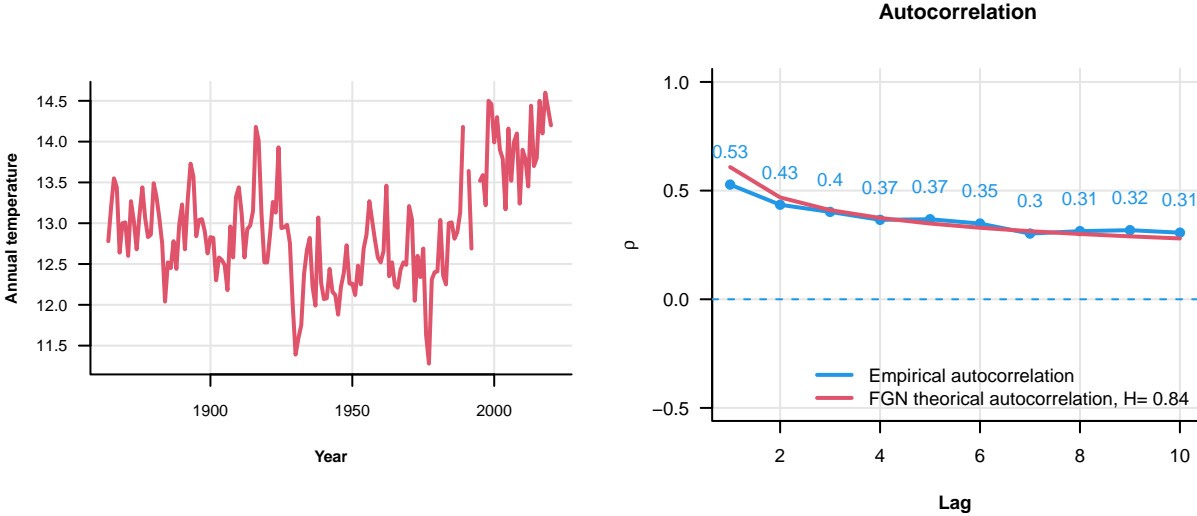
Normality test
Estimated alpha = 1.99

Vardo

Autocorrelation
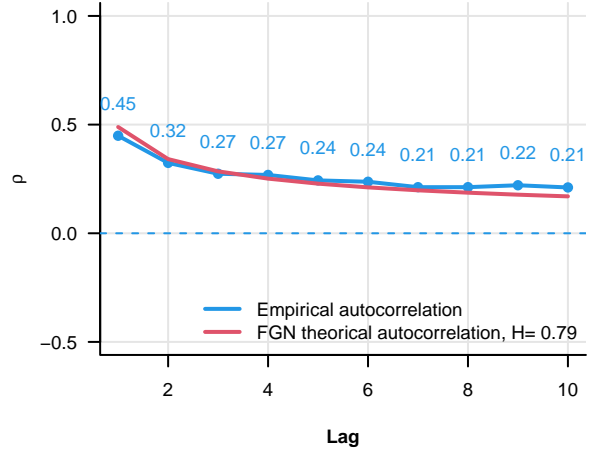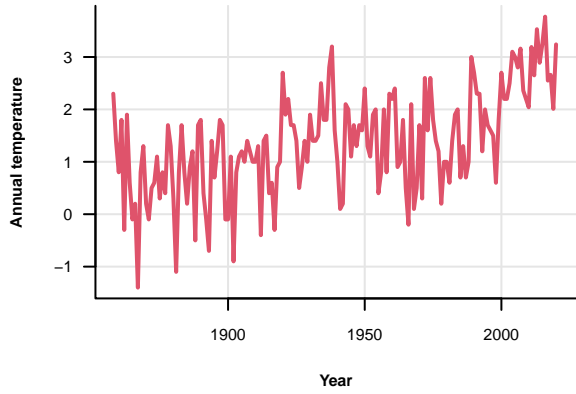
Deviation from the mean

Self–similarity test

Estimated H by regression = 0.8
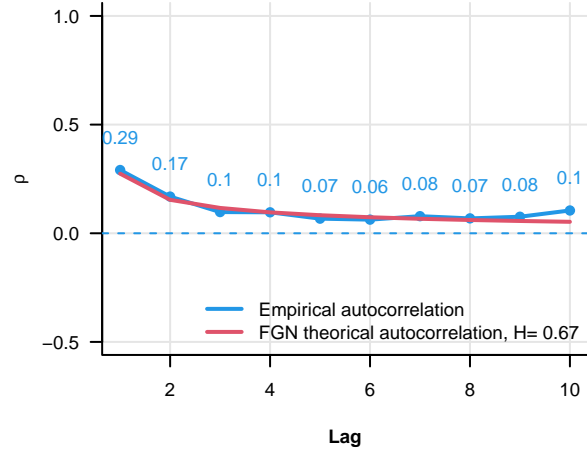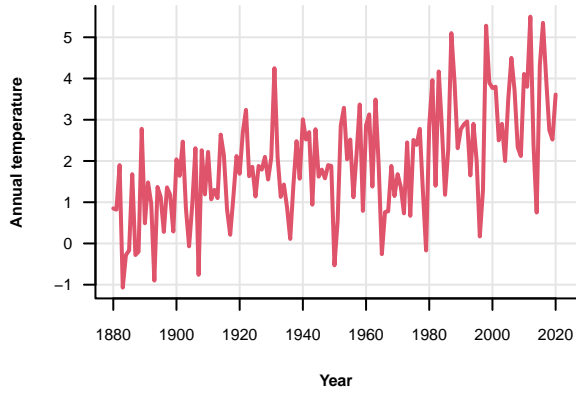
Normality test

Estimated alpha = 2
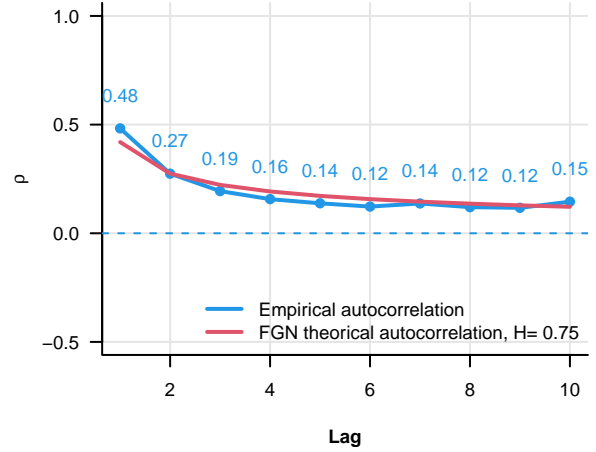
Vestervig

Vienna
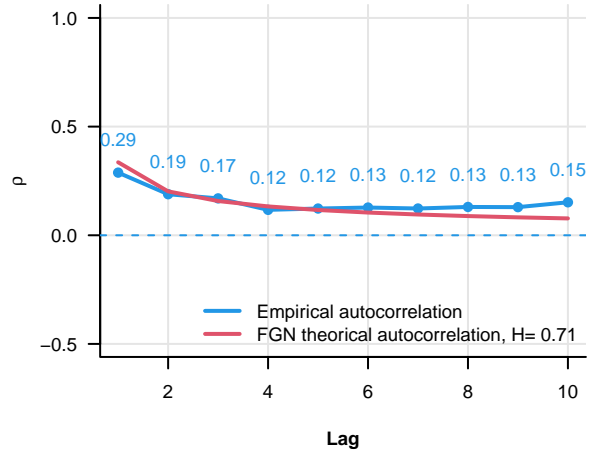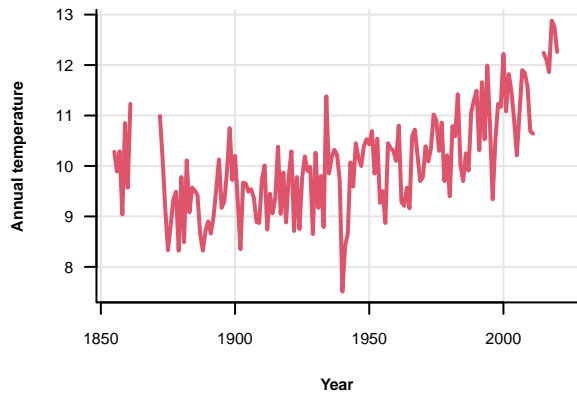
Wellington

Autocorrelation

Deviation from the mean

Self–similarity test

Estimated H by regression = 0.85

Normality test
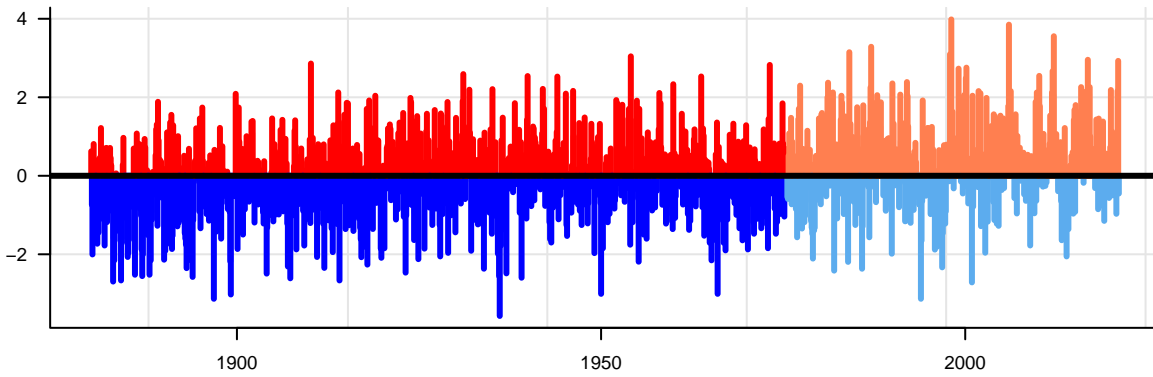
Estimated alpha = 2

Winnipeg

Autocorrelation

Deviation from the mean

Self−similarity test
Estimated H by regression = 0.68

Normality test
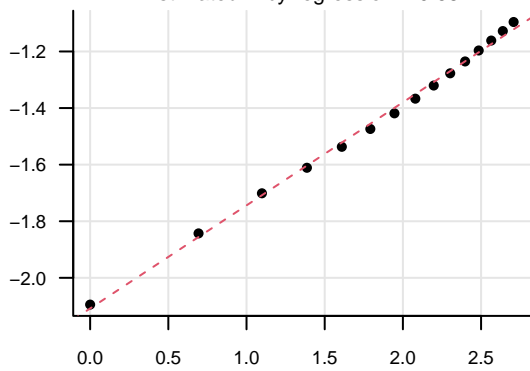Estimated alpha = 1.97

Zagreb

Autocorrelation

Deviation from the mean

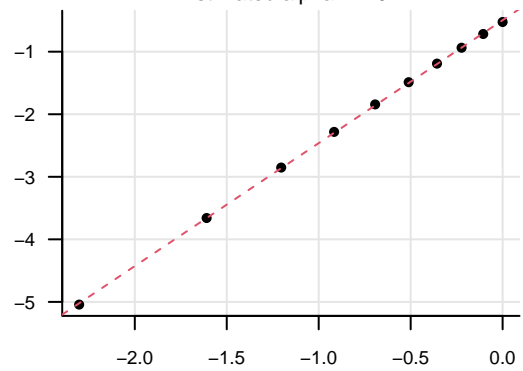## Self−similarity test
Estimated H by regression = 0.72

Normality test
Estimated alpha = 1.95